

**CHARACTERIZATION OF LIME-TREATED SOILS FOR  
ASSESSING SHORT-TERM STRENGTH BEHAVIOUR**

*A THESIS*

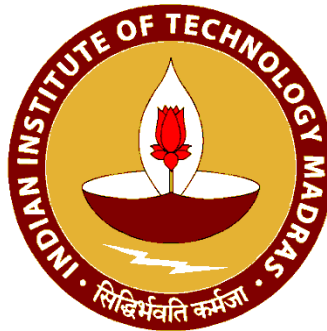
*Submitted by*

**SANDEEP BANDIPALLY**

*For the award of the degree*

*of*

**MASTER OF SCIENCE  
(By Research)**



**GEOTECHNICAL ENGINEERING DIVISION  
DEPARTMENT OF CIVIL ENGINEERING  
INDIAN INSTITUTE OF TECHNOLOGY MADRAS  
CHENNAI-600036**

**JUNE 2017**

**CHARACTERIZATION OF LIME-TREATED SOILS FOR  
ASSESSING SHORT-TERM STRENGTH BEHAVIOUR**

*A THESIS*

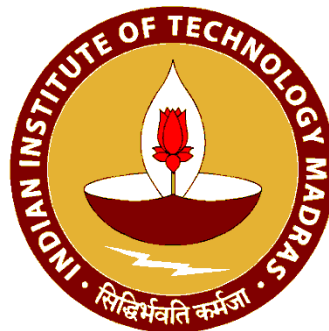
*Submitted by*

**SANDEEP BANDIPALLY**

*For the award of the degree*

*of*

**MASTER OF SCIENCE  
(By Research)**



**GEOTECHNICAL ENGINEERING DIVISION  
DEPARTMENT OF CIVIL ENGINEERING  
INDIAN INSTITUTE OF TECHNOLOGY MADRAS  
CHENNAI-600036**

**JUNE 2017**

## THESIS CERTIFICATE

This is to certify that the thesis entitled **Characterization of Lime-Treated Soils for Assessing Short-Term Strength Behaviour**, submitted by **Sandeep Bandipally**, to the Indian Institute of Technology Madras, Chennai for the award of the degree of *Master of Science*, is a bona fide record of the research work done by him under my supervision. The contents of this thesis, in full or in parts, have not been submitted to any other Institute or University for the award of any degree or diploma.

**Dr. D. N. Arnepalli**

(Research Supervisor)

Associate Professor

Department of Civil Engineering

Indian Institute of Technology Madras

Chennai - 600 036

Date: 12 June 2017

Place: Chennai

*Dedicated to  
Almighty and My parents*

## ACKNOWLEDGEMENTS

---

I would like to express my profound sense of gratitude to my thesis supervisor **Dr. D. N. Arnepalli** for his patient guidance, encouragement and support throughout my research work.

I wish to express my sincere thanks to **Prof. Ramamurthy K**, Head of the Civil Engineering Department. I am highly indebted to the General Test Committee members, **Prof. Manu Santhanam and Dr. Sankaran S**, for their valuable and constructive suggestions during my thesis work. It is my privilege to express my sincere thanks to the faculty **Prof. Gandhi S R, Prof. Boominathan A, Prof. Rajagopal K, Prof. Dodagoudar G R, Prof. Robinson R. G, Dr. Subhadeep Banerjee, Dr. Thyagaraj T** and **Dr. Vidya Bhushan Maji** of Geotechnical Engineering Division, IIT Madras for their constant encouragement during the course of my research programme.

I thank **Mrs. Chinchu Cherian** for mentoring and helping me throughout this research work. My association with **Mrs. Surya, Mr. Nikhil John, Ms. Surabhi** and **Ms. Anjana** is quite memorable and would like to thank for the moral support and friendly ambience created by them. I sincerely express my words of appreciation to **Mrs. Saranya, Mrs. Rejoice, Mrs. Rose, Mr. Leeban, Mrs. Arsha, Mrs. Jayalakshmi, Ms. Cherishma, Mr. Partha Narayan Mishra, Mr. Vinay Kumar, Mr. Biju, Ms. Treesa, Mr. K. S. R. Kumar, Mrs. Malavika** and all other research scholars and graduate students of the Geotechnical Engineering Division, Department of Civil Engineering, IIT Madras for their help at various stages of my research work.

I am grateful to **Ms. Pooja, Mr. Vijay, Mr. Rajesh** and **Ms. Priyusha** for their support during summer internship at IIT Madras.

I wish to acknowledge the employees of HOD office and stores & purchase of Civil Engineering Department, IIT Madras for their prompt help in procuring the equipment and consumables required for research work. I am obliged to **Mr. Murali, Mr. Thirupathi, Mr. Om Prakash, Mr. Suresh, Mr. Prince and Mr. Earnest** for their technical assistance during my experimental work. I extend my thanks to **Mrs. Malrrvizhi** for procuring her help towards my experimental work.

I take this opportunity to thank my friends *Abhinay, Ashwin, Krishna, Raviteja and Deepika* who provided support throughout the tough stages which made my life easy during this research work.

Words cannot express the affection, moral support and endurance shown by *my parents* and *my sister* throughout my research.

*Sandeep Bandipally*

## ABSTRACT

---

Keywords: Lime stabilization, Optimum lime content, Unconfined compressive strength, Curing conditions, Compaction state, Pozzolanic reactions, Hydration products.

The engineering properties of soil, along with associated economical and environmental aspects, are considered as the three main elements in geotechnical constructions such as embankments, structures and roads etc. In many cases, the engineering fraternity has to find solutions to deal with the problems associated with the in situ soils, arising from their unfavourable mechanical and chemical properties. During such instances, the engineering properties of such soils can be altered through chemical stabilization; hence, resulting in a better material appropriate for the construction activities. Soil stabilization using calcium-based admixtures such as lime, cement, and fly ash has been reported to enhance the geotechnical properties of problematic fine-grained soils.

Although lime stabilization is a widely practiced ground improvement method; yet, there is limited research carried out with regard to soil strength improvement, in terms of micro-structural variations of lime-treated soils. In view of this, the purpose of present study is to carry out an investigation on the role of lime in stabilization of fine-grained cohesive soils, and elucidate the possible underlying mechanisms of lime stabilization. A series of laboratory unconfined compressive strength (*UCS*) tests have been performed to determine the variation of 28-day strength with respect to lime content, compaction state and curing conditions. Further, advanced micro-analytical characterization has been conducted to assess the molecular-level changes, from micro-structural and chemico-mineralogical perspectives. This has been achieved by employing X-ray diffraction (*XRD*), energy dispersive X-ray spectroscopy (*EDS*), scanning electron microscopy (*SEM*), Fourier transform infrared spectroscopy (*FTIR*) and thermo gravimetric-differential thermal analysis (*TGA-DTA*), etc.

## TABLE OF CONTENTS

---

		Page No.
	<b>ABSTRACT</b>	i
	<b>List of Figures</b>	v
	<b>List of Tables</b>	viii
	<b>Nomenclature</b>	ix
<b>Chapter 1</b>	<b>INTRODUCTION</b>	1
1.1	General	1
1.2	Mechanism of lime stabilization	2
1.3	Scope and objective	6
1.4	Organization of the thesis	7
<b>Chapter 2</b>	<b>LITERATURE REVIEW</b>	9
2.1	General	9
2.2	Shallow stabilization	9
2.3	Deep stabilization	14
2.4	Characterization of stabilized soils	17
2.5	Transport properties of ionic species and their role in stabilization of soils	22
2.6	Summary and critical appraisal	27
<b>Chapter 3</b>	<b>EXPERIMENTAL INVESTIGATIONS AND TESTING METHODOLOGY</b>	30
3.1	General	30
3.2	Preliminary characterization	30
3.2.1	Specific gravity, gradational characteristics and consistency limits of geomaterials	30
3.2.2	Specific surface area of geomaterials	31
3.3	Chemical characterization	31
3.3.1	Cation exchange capacity of the selected materials	31
3.3.2	X-ray fluorescence spectroscopy	33
3.3.3	Simultaneous thermo gravimetric - differential thermal analysis	33



	3.3.4	Fourier transform infra-red spectroscopy	34
	3.4	Mineralogical characterization	36
	3.5	Microstructural characterization	37
	3.6	Geotechnical characterization	39
	3.6.1	Compaction characteristics of geomaterials	39
	3.6.2	Unconfined compressive strength of geomaterials	39
	3.7	Determination of optimum lime content	40
	3.8	Determination of buffering capacity	41
	3.9	Property evaluation of lime-treated soils	42
	3.9.1	Sample preparation for lime-treated soils	43
<b>Chapter 4</b>		<b>RESULTS AND DISCUSSIONS</b>	45
	4.1	General	45
	4.2	Preliminary characterization of geomaterials	45
	4.2.1	Specific gravity, gradational characteristics and consistency limits of geomaterials	45
	4.2.2	Specific surface area	47
	4.2.3	Cation exchange capacity	48
	4.2.4	Elemental composition of geomaterials	48
	4.2.5	Mineralogical properties of geomaterials	48
	4.2.6	Microstructural properties	51
	4.2.7	Geotechnical properties	53
		Compaction characteristics of geomaterials	53
		Unconfined compressive strength of geomaterials	53
	4.3	Influence of soil pH on the performance of lime-treated soils	54
	4.3.1	Optimum lime content of geomaterials	55
	4.3.2	Buffering capacity of geomaterials	57
	4.3.3	Effect of clay mineralogy on optimum lime content	60
	4.3.4	Effect of cations on the electro kinetic properties of geomaterials	61
	4.4	Strength evaluation of lime-treated soils	64
	4.4.1	Compaction characteristics of lime-treated soils	65

4.4.2	Compressive strength characteristics of lime-treated soils	67
4.4.3	Effect of placement moisture content and curing period on the lime-treated soils	72
4.5	Variations in chemical characteristics of lime-treated soils	76
4.5.1	Simultaneous thermo gravimetry-differential thermal analysis	76
4.5.2	Fourier transform-infra red spectroscopy	82
4.6	Variations in mineralogical characteristics of lime-treated soils	86
4.6.1	X-Ray diffraction	86
4.6.2	Energy dispersive spectroscopy	90
4.7	Variations in microstructural characteristics of lime-treated soils	91
4.7.1	Scanning electron microscopy	91
<b>Chapter 5</b>	<b>CONCLUSIONS</b>	93
5.1	General	93
5.2	Influence of inherent soil properties on <i>OLC</i>	93
5.3	Compressive strength behaviour of lime-treated soils	94
5.4	Characterization of lime-treated soils	95
	<b>FUTURE SCOPE OF RESEARCH WORK</b>	97
	<b>APPENDIX</b>	98
	<b>REFERENCES</b>	107
	<b>PUBLICATIONS FROM THE STUDY</b>	119

## List of Figures

Figure	Caption	Page No.
1.1	Schematic of the mechanism of lime stabilization	4
1.2	Chemical and pozzolanic soil-lime interactions	4
3.1	Photographic view of atomic absorption spectrometer used in this study	32
3.2	Photographic view of X-ray analytical microscope used in this study	33
3.3	Photographic view of thermo gravimetric analyzer used in this study	34
3.4	Photographic view of Fourier transform-infrared spectrometer used in this study	35
3.5	Photographic view of X-ray powder diffractometer used in this study	36
3.6	Photographic view of scanning electron microscope used in this study	37
3.7	Photographic view of lyophilizer used in this study	38
3.8	Photographic view of unconfined compressive strength test conducted in this study	40
3.9	Photographic view of humidity chambers used in this study	43
4.1	Particle size distribution characteristics of the selected geomaterials	46
4.2	Plasticity chart	46
4.3	Variation of ethylene glycol monoethyl ether weight with time	47
4.4	X-ray diffractograms of selected geomaterials	50
4.5	X-ray diffractograms of clay-size fraction of selected geomaterials	51
4.6	Scanning electron microscope & energy dispersive spectroscopy of selected geomaterials	52
4.7	Variation of <i>pH</i> of the soil suspension with lime content for various geomaterials corresponding to (a) 1-hour; (b) 24 hours equilibration	56
4.8	Variation of <i>pH</i> of the soil suspension with acid titration for determining buffer capacity of virgin geomaterials	58
4.9	Variation of <i>pH</i> of the soil suspension with alkali titration concentration for determining buffer capacity of virgin geomaterials	59
4.10	Variation of optimum lime content with soil <i>pH</i> for different soils	61
4.11	Variation of electrical conductivity of soil suspension with NaOH titration	62
4.12	Variation of electrical conductivity of soil suspension with Ca(OH) <sub>2</sub> titration	63
4.13	Variation of electrical conductivity of soil suspension with HNO <sub>3</sub> titration	64
4.14	Compaction curves for different soil-lime mixtures of white clay and	66

	sodium bentonite	
4.15	Unconfined compressive strength of 28-day cured lime-treated white clay and sodium bentonite at 25 °C	67
4.16	Unconfined compressive strength of 28-day cured lime-treated white clay and sodium bentonite at 40 °C	68
4.17	<i>pH</i> and electrical conductivity of lime-treated white clay and sodium bentonite at 25 °C and 40 °C	70
4.18	Determination of optimum lime content using Eades and Grim <i>pH</i> test	71
4.19	Effect of compaction and curing conditions on <i>UCS</i> of (a) virgin; (b) lime-treated white clay	74
4.20	Effect of compaction and curing conditions on <i>UCS</i> of (a) virgin; and (b) lime-treated sodium bentonite	75
4.21	Comparison of thermo gravimetric curves obtained for virgin and lime-treated sodium bentonite	77
4.22	Comparison of derivative thermo gravimetric curves obtained for virgin and lime-treated sodium bentonite	77
4.23	Thermo gravimetric weight loss of various phases present in 28-day cured lime-treated sodium bentonite at 25 °C	78
4.24	Derivative thermo gravimetric curves of lime-treated sodium bentonite over different temperature ranges	81
4.25	Infra-red spectra for lime-treated sodium bentonite after 28-day curing at 25 °C	84
4.26	Major bands identified in the infra-red spectra for virgin sodium bentonite after 28-day curing at 25 °C	85
4.27	Major bands identified in the infra-red spectra for lime-treated sodium bentonite soil after 28-day curing (a) <i>O-H</i> bond of inner hydroxyl groups; (b) <i>H-O-H</i> bond of water and <i>Ca-O</i> bond of lime; (c) <i>Si-O</i> and <i>Al-O</i> bonds in clay minerals	85
4.28	X-ray diffractogram of hydrated lime	87
4.29	X-ray diffractogram of virgin sodium bentonite	88
4.30	X-ray diffractograms of lime-treated sodium bentonite with varying lime content	89
4.31	Major sections of X-ray diffractograms of lime-treated sodium bentonite with varying lime content	89
4.32	Scanning electron micrograph of lime-treated sodium bentonite cured for 28-day at 25 °C with (a) 0 % lime; (b) 6 % lime; (c) 12 % lime; (d) 20 % lime	92
A- 1	Standard proctor compaction curves for selected geomaterials	98

A- 2	Stress-strain curves of lime-treated white clay cured at 25 °C for 28 days	99
A- 3	Stress-strain curves of lime-treated white clay cured at 40 °C for 28 days	100
A- 4	Stress-strain curves of lime-treated sodium bentonite cured at 25 °C for 28 days	101
A- 5	Stress-strain curves of lime-treated sodium bentonite cured at 40 °C for 28 days	102
A- 6	Energy dispersive spectroscopy of untreated sodium bentonite cured for 28-days at 25 °C	103
A- 7	Energy dispersive spectroscopy of sodium bentonite treated with 6 % lime and cured for 28-days at 25 °C	104
A- 8	Energy dispersive spectroscopy of sodium bentonite treated with 12 % lime and cured for 28-days at 25 °C	105
A- 9	Energy dispersive spectroscopy of sodium bentonite treated with 20 % lime and cured for 28-days at 25 °C	106

## List of Tables

<b>Table</b>	<b>Caption</b>	<b>Page No.</b>
4.1	Physical characteristics of geomaterials	45
4.2	Elemental compositions of selected geomaterials	49
4.3	Major minerals present in the selected geomaterials	49
4.4	Compaction characteristics of geomaterials	53
4.5	Unconfined compressive strength of geomaterials	53
4.6	Optimum lime content values of selected geomaterials	56
4.7	Buffer capacity values of selected geomaterials	60
4.8	Variation of compaction characteristics of geomaterials with lime content	66
4.9	Comparison of optimum lime content of geomaterials	72
4.10	Elemental composition of lime-treated sodium bentonite cured for 28-day at 25 °C	90

## Nomenclature

### Abbreviations

<i>AAS</i>	atomic absorption spectroscopy
<i>ATR</i>	attenuated total reflectance
<i>CAH</i>	calcium aluminate hydrate
<i>CASH</i>	calcium aluminate silicate hydrate
<i>CBR</i>	California bearing ratio
<i>CEC</i>	cation exchange capacity
<i>CECRI</i>	central electro chemical research institute
<i>CSH</i>	calcium silicate hydrate
<i>DMC</i>	dry of optimum moisture content
<i>DTA</i>	differential thermal analysis
<i>DTG</i>	derivative thermogravimetry
<i>EC</i>	electrical conductivity
<i>EDS</i>	energy dispersive spectroscopy
<i>EGME</i>	ethylene glycol mono ethyl ether
<i>FTIR</i>	Fourier-transform infrared spectroscopy
<i>FWHM</i>	full width at half-maximum
<i>GSD</i>	grain size distribution
<i>HL</i>	hydrated lime
<i>ICDD</i>	International centre for diffraction data
<i>ICL</i>	initial consumption of lime
<i>IR</i>	infra-red
<i>LC</i>	lime column
<i>LOI</i>	loss on ignition

<i>LP</i>	lime pile
<i>LSPI</i>	lime slurry pressure injection
<i>MDD</i>	maximum dry density
<i>MIP</i>	mercury intrusion porosimetry
<i>MIR</i>	middle infra-red
<i>NMR</i>	nuclear magnetic resonance
<i>OLC</i>	optimum lime content
<i>OMC</i>	optimum moisture content
<i>OPC</i>	ordinary portland cement
<i>PI</i>	plasticity index
<i>PSD</i>	pore size distribution
<i>RH</i>	relative humidity
<i>SEM</i>	scanning electron microscopy
<i>SSA</i>	specific surface area
<i>SWCC</i>	soil water characteristic curve
<i>TGA</i>	thermo gravimetry analysis
<i>TG</i>	thermo gravimetry
<i>TLM</i>	triple layer model
<i>UATR</i>	universal attenuated total reflectance
<i>UCS</i>	unconfined compressive strength
<i>USCS</i>	unified soil classification system
<i>UU</i>	unconsolidated unconfined
<i>WMC</i>	wet of optimum moisture content
<i>XRD</i>	X-ray diffraction
<i>XRF</i>	X-ray fluorescence
<i>ZAV</i>	zero air void



## Notations

<i>Al</i>	alumina
<i>BT</i>	sodium bentonite soil
<i>Ca</i>	calcium
$\text{Ca(OH)}_2$	hydrated lime
$\text{Ca}^{2+}$	calcium ion
$\text{CaCl}_2$	calcium chloride/calcium hydroxide
$\text{CaCO}_3$	calcium carbonate
$\text{CaO}$	quick lime/calcium oxide
<i>CH</i>	high compressible clay
<i>CI</i>	medium compressible clay
<i>CL</i>	low compressible clay
<i>G</i>	specific gravity
$\text{H}^+$	hydrogen ion
$\text{H}_2\text{O}_2$	hydrogen peroxide
$\text{HNO}_3$	nitric acid
<i>k</i>	coefficient of permeability
$\text{KBr}$	potassium bromide
<i>L/S</i>	liquid to solid ratio
$\text{NaCl}$	sodium chloride
$\text{NaOH}$	sodium hydroxide
<i>O</i>	oxygen
<i>OH</i>	hydroxyl ion
$\text{OLC}_{pH}$	optimum lime content as per Eades and Grim (1966) pH test
$\text{OLC}_{UCS}$	optimum lime content as per 28-day unconfined compressive strength
<i>SC</i>	sandy clay soil

$S_i$	silica
$UCS_{28\text{-day}}$	28-day unconfined compressive strength
$W_c$	weight of <i>EGME</i> sorbed by the soil
$WC$	white clay soil
$w_L$	liquid limit
$w_P$	plastic limit
$W_s$	air-dried weight of the soil

## **1.1 GENERAL**

The geotechnical properties of problematic fine-grained soils such as soft and expansive clays have been modified by adopting numerous ground improvement techniques, depending upon the soil type, site-specific conditions, and degree of improvement desired. The simplest non-scientific approach is either removal or replacement of in-situ problematic soil by a non-problematic superior-quality material. However, the application of this technique becomes limited due to constraints such as scarcity of natural material, non-affordability of high-quality material, and inaccessibility of sites. Hence, it becomes uneconomical due to the expenses associated with the disposal of excavated material as well as the inherent high transportation costs (Gillot, 1987). In such instances, alternative scientifically proven methods such as mechanical and chemical ground improvement techniques are employed for shallow as well as deep stabilization of fine-grained cohesive soils. These treatments include densification either by compaction or preloading, pore-water pressure reduction techniques such as consolidation or electro-osmosis, bonding of soil particles by ground freezing, grouting, and chemical treatment, as well as the use of reinforcing elements such as geosynthetics and stone columns (Powrie, 1987). Upon stabilization, the soil will be transformed into a superior grade and more durable material with enhanced strength, stiffness, permeability and volume change properties, which makes the material suitable for various construction activities.

The chemical stabilization of problematic fine-grained soils entails amalgamating chemical binder with virgin soils to enhance hydraulic and mechanical properties of the in-situ soil. In general, the task of stabilizer/binding agent in the chemical treatment method is to either encourage the physical and chemical bonds among the soil particles or filling of the inter- and intra-particle pore spaces (Jayakumar and Sing, 2012). This method is apposite for many geotechnical engineering applications such as pavement subgrades and subbases, building foundations, embankments and slopes to prevent the damages that might occur due to the excessive settlement and swelling behaviour of soft and expansive in-situ soils (Ismail, 2006). Depending on the depth of the problematic soil layer to be improved, chemical stabilization can be classified as (a) surface/shallow stabilization; and (b) deep stabilization.

As per the codal procedures and various field records, shallow stabilization techniques are chosen for improving pavement subgrades and shallow building foundations, for up to a depth of 1.5 m to 2.5 m below the natural ground surface. The conventional shallow stabilization begins with the aid of excavation and removal of top soil, pulverization of sub-soil accompanied by dry/wet mixing of chemical stabilizers (viz., lime, cement, fly ash, etc.) in appropriate weight proportions. Ensuing uniform mixing of soil and stabilizer, the mixture is compacted to attain the corresponding maximum field dry unit weight at its optimum moisture content. The depth of stabilized zone may be further increased up to additional few meters by adopting the deep stabilization techniques such as chemical grouting as well as dry lime/cement pile & column and lime slurry pressure injection (*LSPI*). In the lime pile (*LP*) & lime column (*LC*) method, the predominant mechanism of improvement involves diffusive transport of calcium ( $Ca^{2+}$ ) and hydroxyl ( $OH$ ) ions from the installed *LP* or *LC* into surrounding in-situ soil. Following, immediate hydration and long-term pozzolanic reactions between available free calcium ions and reactive clay minerals lead to cementation of the soil in the influential zone. In the due course of time, the central lime pile and modified in-situ soil form a strong and stable mass with increased bearing capacity as well as total and differential settlement properties (Rogers and Glendinning, 1996). Further, grouting and pressure injection techniques involve pressurized pumping of slurried chemical admixture into the in-situ soil to augment the physico-hydro-mechanical properties of the treated soil matrix (Rao and Rajasekaran, 1994).

## **1.2 MECHANISM OF LIME STABILIZATION**

Lime stabilization is one of the oldest forms of chemical stabilization being popularly practiced around the world, particularly in the arid and semi-arid regions. Further, lime proves to be the most effective stabilizing agent for problematic soils with a higher clay-size fraction in them, by reducing their plasticity properties and increasing load bearing capacity. When quicklime ( $CaO$ ) is added to the soil, it undergoes rapid hydration reaction by absorbing soil moisture (32 % of the initial weight of quicklime combines with water molecules to form hydrated lime ( $Ca[OH]_2$ ), as illustrated in Equation 1.1 (Beetham *et al.*, 2014).



As indicated above, a large amount of heat energy is generated during this exothermic hydration process and the total volume of lime doubles. Further, the moisture content of the soil is reduced through chemical absorption and exothermal effects accompanied by a slight improvement in its shear strength (Schifano and Hadlow, 2007). With the existence of adequate moisture in soil pores (i.e., pore-solution), so formed hydrated lime dissolves into the pore solution, and thereby increases the calcium and hydroxyl ion concentration in it. During this instant, cation exchange reactions are stimulated by exchanging the divalent calcium cations in the pore-solution with the of monovalent existing cations on the surface of negatively charged clay minerals present in the soil. This phenomenon continues until the charge deficiency of the clay minerals is completely satisfied, and results in flocculation-agglomeration of soil particles by the contraction of diffused double layer on clay mineral surface (Kavak and Baykal, 2012). Subsequently, the moisture-holding ability of the soil is reduced which in turn leads to improved plasticity properties. Furthermore, the flocculation-agglomeration of clay particles modify particle-size distribution into a more coarse graded nature, and hence, improves its workability (Croft, 1968).

In addition, a high concentration of hydroxyl ions furnished with the aid of lime raises soil *pH* to form a highly alkaline medium (equivalent to *pH* of saturated lime solution). This, in turn facilitates the dissociation of clay mineral structure and dissolution of reactive silica (*Si*) and alumina(*Al*) into pore-solution (Cherian and Arnepalli, 2015). Further, these reactive clay minerals chemical and pozzolanic reactions with excess free calcium ions leading to the formation and deposition of cementitious products such as calcium-silicate-hydrates (*CSH*) and/or calcium-aluminate-hydrates (*CAH*) (Jung and Bobet, 2008). These reactions proceed as long as the high *pH*, adequate supply of free calcium and reactive clay minerals as well as sufficient moisture in the system is maintained. As a result, the treated soil matrix is cemented into a hard mass by the strong binding action of *CSH* and *CAH* gels on clay particles, which consequently enhance the strength and durability characteristics. The basic mechanism of lime stabilization of clayey soils and its chemical, as well as pozzolanic interactions, are shown schematically in Figure 1.1 and Figure 1.2.

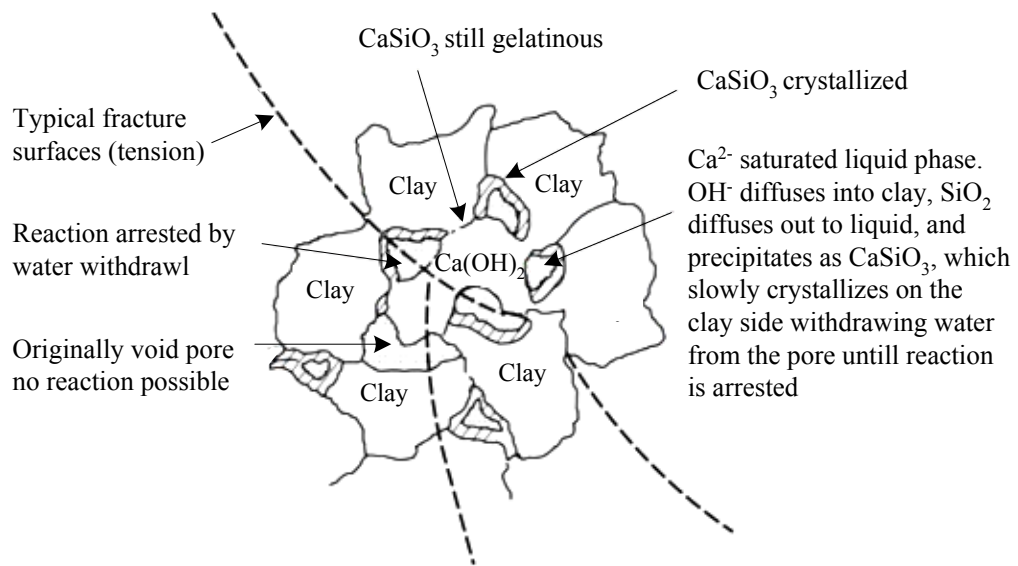


Figure 1.1 Schematic of the mechanism of lime stabilization  
(adapted from Ingles and Metcalf, 1972)

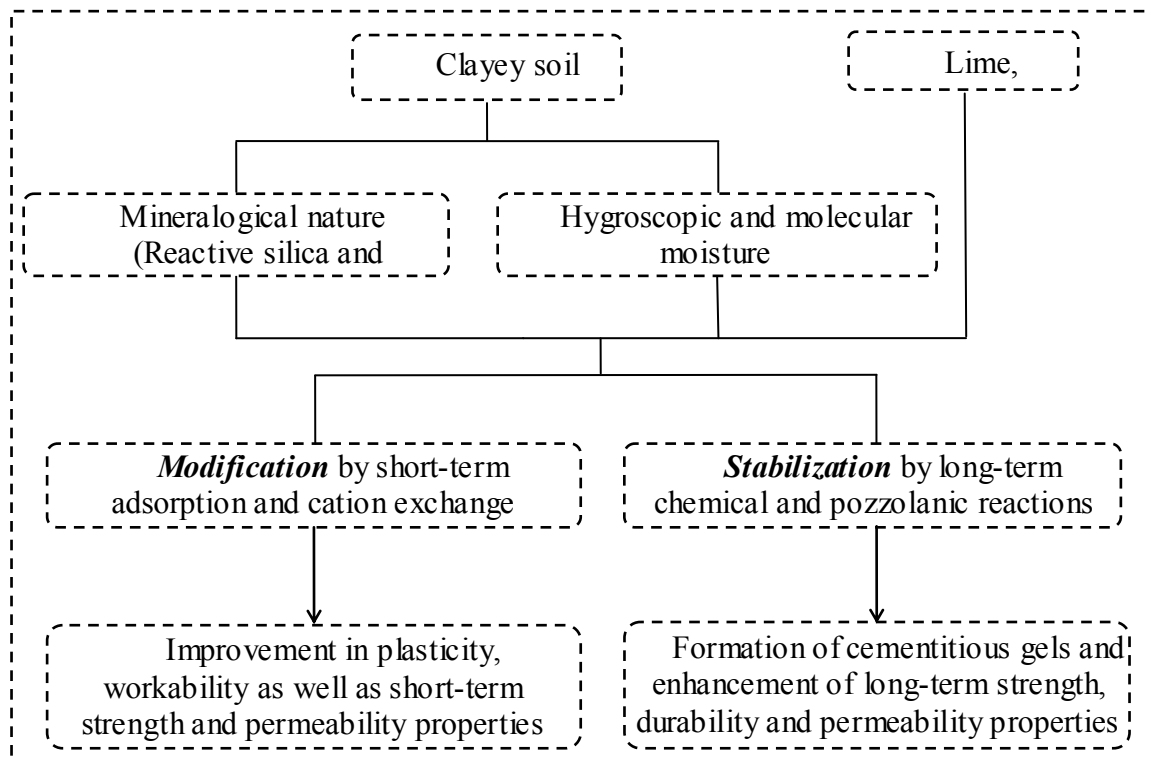


Figure 1.2 Chemical and pozzolanic soil-lime interactions

When compared to quick lime, hydrated lime ( $\text{Ca}[\text{OH}]_2$ ) is more preferred for the majority of the field applications pertaining to soil stabilization, owing to the difficulty associated with storage and handling of the former. When hydrated lime is added to a clayey soil, the free calcium ions supplied from lime should primarily satisfy the inherent sorption affinity of the soil, the extent of which depend up on the chemico-mineralogical properties of the treated soil. These calcium ions are not readily available for pozzolanic reactions; therefore, an additional amount of lime is required for fully mobilizing permanent stabilization of the soil rather than only short-term modification. Since lime itself does not have significant shear strength, the presence of excess residual lime content in the soil system might impart adverse effects on the stabilization process. Therefore, optimum lime content (*OLC*) is an important parameter associated with lime treatment, which is very crucial for efficacious and cost-effective stabilization of soils. The *OLC* is defined as the quantity of hydrated lime required for fulfilling the short-term soil-lime interactions, and still provide ample amount of free calcium ions and high residual pH necessary to offer apposite conditions for long-term pozzolanic reactions (Eades and Grim, 1962; Little, 1987; Cherian and Arnepalli, 2015). Previous researchers have proposed empirical correlations and experimental methodologies for determining *OLC* of the fine-grained soils, in terms of their clay-size fraction and plasticity characteristics (Eades and Grim, 1962; Little, 1987; Ingles and Metcalf, 1972; Nelson and Miller, 1992; *ASTM D6276*). Among the available methods popularly used Eades and Grim test (Eades and Grim, 1962 & 1966) measures the *pH* of different soil-lime suspensions at liquid to solid ratio of four and the lime content which raises the *pH* of soil suspension to 12.3 (incidentally equals to *pH* of saturated lime solution) is reported as *OLC*.

The *pH* buffering capacity of soil plays a predominant role in determining its *OLC* for lime stabilization, as it is a measure of resistance to *pH* change. It is defined as the amount of soil acidity or alkalinity that must be neutralized so as to respectively increase or decrease the soil *pH* by one unit (Kissel *et al.*, 2005). Titration method is usually followed to determine the *pH* buffering capacity of the soil, in which various molar concentrations of an acid or base are added to the soil. The titration curves of soil *pH* versus acid/alkali concentration are plotted and the negative slope of the curve is considered as *pH* buffering capacity of the soil (Yong *et al.*, 1990 & 2009).

The efficiency of lime stabilization for improving the chemico-mechanical properties of problematic in-situ soils has been extensively researched by the scientific community for past many decades (Rajasekaran and Rao, 2002 & 2004; Rao and Mathew, 1995). From the vast literature review, it is understood that the chemical kinetics of the pozzolanic reaction mechanisms involved with short-term and long-term soil-lime reactions are complex, and not yet understood at the fundamental level. Most of the studies focused primarily on the evaluation of the macro-level variations in the lime-treated soil; however, not many efforts have been made to assess the key changes occurring within the soil microstructure as well as clay mineralogy coupled with the macro-level variations. Further, very few researchers made serious attempts to assess the degree of lime treatment in terms of the qualitative and semi-quantitative estimation of the rate of clay mineral dissociation as well as the advanced characterization of pozzolanic reaction products formation, by employing sophisticated microscopic and spectroscopic techniques (Saeed *et al.*, 2013 & 2015; Eisazadeh *et al.*, 2010).

Moreover, the reliability and accuracy of conventional methods used for determining the *OLC* are observed to be highly influenced by the various parameters such as inherent soil mineralogy as well as testing conditions (Cherian and Arnepalli, 2015). Hence, it becomes essential to evaluate the effects of these factors on *OLC* value, which otherwise plays a pivotal role in governing the maximum performance of lime-treated soil in the long run. As a whole, it can be stated that a better understanding of chemical interactions between the lime and clay minerals present in soil as well as estimating the role of various influencing parameters becomes indispensable for the development of the design guidelines for the most efficient lime stabilization of fine-grained cohesive soils.

### **1.3 SCOPE AND OBJECTIVE**

In view of the limitations of available literature as discussed above, the primary aim of the present study is to investigate the key influences of inherent soil properties (*viz.*, soil *pH* and buffering capacity) upon the determination of *OLC* using conventional methods. As an offshoot, the study also attempts to understand and account for the major limitations of conventional Eades and Grim test used for *OLC* determination, by considering the



significance of interaction period (or equilibration time) as well as temperature effects. Studies are also conducted to determine the chief role played by the pore-fluid chemistry (type of ions present in the pore solution) in governing the inherent properties of virgin soil (viz., *pH* and mineralogy), which in turn influence the rate of pozzolanic reactions during lime stabilization and its efficacy.

The secondary aim of the study is to determine the significant variations of the macro-level compressive strength properties of the fine-grained cohesive soil treated with varying lime content, placement moisture and curing conditions (time and temperature), using laboratory unconfined compressive strength (*UCS*) tests. Furthermore, in order to predict the underlying micro-level mechanisms which may be responsible for macro-level engineering behaviour changes, the qualitative and semi-quantitative estimation of new reaction products as well as alterations of virgin clay minerals are evaluated by employing the sophisticated techniques such as X-ray diffraction (*XRD*), simultaneous thermo-gravimetry-differential thermal analysis (*TGA-DTA*), scanning electron microscopy-energy dispersive spectroscopy (*SEM-EDS*), Fourier transform-infra red (*FTIR*) spectroscopy, atomic absorption spectroscopy (*AAS*), etc. The obtained results are compared vis-à-vis virgin soil properties in order to identify the predominant mechanisms involved in stabilization process and to quantify the degree of improvement achieved.

#### **1.4 ORGANIZATION OF THE THESIS**

**Chapter 1:** This chapter describes the introduction, scope, and objectives of the present study.

**Chapter 2:** This chapter presents the review of literature pertaining to the qualitative and semi-quantitative evaluation of lime-treated fine-grained soils, in terms of the physicochemical, mineralogical, microstructural and geotechnical properties. The important fundamental literature pertaining to the principles and data interpretation methods for advanced characterization techniques employed in the qualitative and quantitative analysis of lime-treated soils are also discussed.

Based on the reviewed literature, the critical appraisal of the literature is also reported.

**Chapter 3:** This chapter describes the methodologies employed to obtain physicochemical, mineralogical, microstructural and geotechnical properties of the virgin and lime-treated soils. The experimental works carried out to evaluate the influence of virgin soil *pH* and *pH* buffering capacity properties as well as the effects of testing conditions upon the determination of *OLC* is also presented. Moreover, the laboratory tests carried out to determine the role of pore-fluid chemistry in governing the geotechnical properties of virgin soil are discussed. The methods followed for sample preparation, testing and evaluation of obtained results regarding the compaction and *UCS* tests as well as, *XRD*, *TGA-DTA*, *SEM-EDS*, *FTIR*, *AAS*, etc. are discussed in this chapter. This chapter also reports the fundamental properties of selected soils for the present study.

**Chapter 4:** This chapter describes the results and discussions pertaining to the variations of physicochemical, mineralogical, microstructural and geotechnical properties of soil upon lime treatment. Further, the results obtained from the evaluation of the influence of virgin soil *pH* and buffer capacity properties as well as the effects of testing conditions upon the determination of *OLC* are also presented. Moreover, the observations from the laboratory tests carried out to determine the role of pore fluid chemistry in governing the inherent properties of virgin soil are presented. The experimental observations pertaining to compaction and *UCS* studies of lime-treated soil with varying lime content, placement moisture content, and curing temperature are presented. Following, the results of advanced, *XRD*, *TGA-DTA*, *SEM-EDS*, *FTIR*, *AAS*, etc., are also discussed in this section.

**Chapter 5:** This chapter summarizes the findings and major conclusions of the present study.

## **2.1 GENERAL**

This chapter describes literature pertaining to the lime stabilization ground improvement technique which has been widely employed for enhancing the geotechnical properties of problematic fine-grained soils. This chapter also presents a brief review of studies which highlighted the influence of various parameters such as clay-size fraction and its mineralogy, soil *pH*, optimum lime content and curing conditions on long-term chemical and pozzolanic reactions. Further summary of mechanisms of lime column/pile and lime slurry injection employed by the previous researchers to assess the long-term performance of the deep stabilization is also reported in this chapter. In order to understand the migration phenomena of calcium and hydroxyl ions in deep stabilization by employing lime pile/column and lime slurry techniques, the knowledge of migration properties of ionic species in terms of diffusion as well as sorption & desorption characteristics of in-situ soil is essential. In addition, the literature pertaining to characterization tools like *XRD*, *TGA-DTA*, *FTIR*, and *SEM-EDS* is also discussed briefly.

In view of this, the reviewed literature has been categorized into four major groups and named as shallow stabilization, deep stabilization, characterization of stabilized soils, transport properties of ionic species and their role in stabilization of soils. For the sake of brevity, the essence of these studies is presented briefly in the following sections.

## **2.2 SHALLOW STABILIZATION**

Lav and Lav (2000) conducted research on the microstructural advancement of stabilized fly ash in view of its utilization as a base material for pavement construction. Fly ash used in this study was procured from an Eraring thermal power station in New South Wales, Australia. The fly ash was stabilized with cement as well as lime by 10 % of its mass and allowed for curing of 7, 14, 28, 90, 180 and 360 days. Further, unconfined compressive strength (*UCS*), microstructural (*SEM*), chemical (*XRF*), mineralogical (*XRD*) and *TGA-DTA* analyses were carried out on the treated samples cured over a range of curing periods. Micro structural

studies revealed that the fly ash particles acted as nucleation centres for hydration or pozzolanic reactions. The voids among the soil particles were filled by the growing hydrates with time. From the obtained results it was observed that the rate of formation of cementitious products which are responsible for the increase in *UCS* is practically same in the case of lime- and cement- treated soils.

Sakr *et al.*, (2009) conducted experimental investigations on lime-treated soft clay, which comprises of 14 % organic matter, collected from Idku city, Egypt. The various lime fractions such as 1, 3, 5 and 7 percent by weight of dry soil were added to the soil and cured for a wide range of curing periods (*viz.*, 7, 15, 30 and 60 days). Following, the conventional laboratory tests such as grain size distribution (*GSD*) analysis, consistency limits, *UCS*, vane shear test and odometer tests were conducted on cured soil samples, in addition to the mineralogical and microstructural examinations. The results also showed that the changes in the mineralogical contents and soil fabric of lime-treated high organic soft clay improved soil plasticity, strength and compressibility properties. Hence, this study reported that the lime stabilization is effective in stabilizing soft clay soil with high organic content.

Al-Mukhtar *et al.*, (2010) performed experimental investigations on an expansive Impersol clay to quantify the effect of elevated temperature on pozzolanic reactions between soil and lime. The obtained results indicated that curing at an elevated temperature such as 50 °C accelerates the pozzolanic reactions and leads to the rapid development of shear strength. The lime consumption was observed to be more during the initial days of accelerated curing. Almost 20 % of the lime was consumed during the first few months of curing and resulted in the reduction of soil *pH*; however, the change in soil *pH* diminished with the increase of initial lime content. The electrical conductivity (*EC*) of the soil-lime solution decreased at a slower rate on the first day followed by a higher rate during the first week and reached constant value subsequently. The shear wave velocity of the treated soil increased with increasing the lime content but it was stabilized within initial 7 days of curing. On the other hand, the *UCS* value of treated soil showed an increment with lime content as well as curing period. The *XRD* studies on the soil treated with lime content 6 percent or higher revealed the formation of pozzolanic products *viz.* calcium aluminate hydrate (*CAH*) and calcium silicate hydrate (*CSH*) corresponding to curing period of 1 day and 7 days. The rate at which these

cementitious products formed by pozzolanic reactions were further correlated to curing period as well as percent lime added.

Nasrizar *et al.*, (2010) examined the role of percent lime on the shear strength characteristics of a Chennai black cotton soil. The soil was mixed with different percentages of lime (i.e., 3 %, 5 %, 7 % and 9 %) and cylindrical samples were cast for assessing their unconfined compressive strength. These samples were incubated at three different temperatures of 5 °C, 30 °C and 50 °C for different curing periods of 7, 14, 28 and 90 days, respectively. The obtained results indicated that the *UCS* increased proportionally up to certain lime content beyond which the *UCS* reduced. The optimum lime content in terms of *UCS* was highly depended on the curing temperature. The addition of lime upto the initial consumption of lime (*ICL*) was observed to be not very effective in enhancing the *UCS* with curing temperature. Moreover, It was observed that the significant portion of strength gain was achieved within the initial 7 days curing period.

Al-Kiki *et al.*, (2011) studied the durability and strength characteristics of clayey soil stabilized with lime. The tests carried out included *UCS* analysis of samples stabilized with the optimum lime percent of 4 % as well as durability tests on samples subjected to various cycles of wet-dry, dry-wet and freeze-thaw, long-term soaking and slake tests, etc. The results obtained indicated that the efficiency of lime in achieving the higher *UCS* of clayey soil impart a negative effect on the long-term durability. The wetting-drying cycles showed a greater reduction in the *UCS* compared to the drying-wetting cycles; on the contrary, the volume change of samples which were initially subjected to drying was greater than those subjected to initial wetting. On the other hand, freeze-thaw cycles caused a decrement in the *UCS* values, and moreover, the percentage loss in *UCS* was greater than wetting and drying cases. During soaking tests, it was found that lime-treated samples exhibit continuous strength gain up to a soaking period of 5 days, beyond this period, the *UCS* of the treated samples decreased proportionately with a soaking period. As a whole, the stabilized samples with 4 % and 6 % lime proved to have higher durability towards the cycles of wetting and drying as well as freeze-thaw.

Kavak and Baykal (2012) studied the strength behaviour and micro-structural characteristics of kaolinite clay stabilized with lime and cured for a long period. Kaolinite was mixed with various lime contents varying from 0 to 12 % and *OLC* was found to be 4 percent as per Eades and Grim *pH* test (1962). Further, the soil was mixed at optimum moisture content using 4 % and 12 % of lime by dry weight and cured under control conditions for a period up to 10 years. At the end of specified curing periods, the samples were evaluated for *UCS* so as to monitor the strength variations with curing period. The *UCS* of the lime-treated kaolinite was increased by 8 and 21 times as that of its virgin value corresponding to the curing period of 28 days and 10 years, respectively. The long-term strength of kaolinite treated either with 4 % or 12 % was found to be comparable. This is due to the facts that, no significant increase in the long-term strength occurred when the soil was treated with lime content beyond the *OLC* value. The *XRD* and *SEM* studies on long-term cured samples for 10 years revealed the presence of both highly crystalline and amorphous calcium aluminate silicate (*CASH*) hydrates in them, which indicated the occurrence of uninterrupted pozzolanic reactions under the prevalence of sustained conducive environmental conditions.

Thyagaraj *et al.*, (2012) have attempted to understand the stabilization of an expansive soil via precipitation mechanism in the laboratory by sequential mixing of  $\text{CaCl}_2$  and  $\text{NaOH}$  solutions with soil. The experimental results indicated an increase in the *UCS* with the increasing percentage of lime precipitation as well as with curing period. During the early period of lime precipitation (i.e., within 24 hours), the nominal strength increase was attributed to the poorly developed cementation products, which may be effective in controlling the swell potential of the soil. The enhancement in strength for a curing period of 7 to 21 days was primarily due to the short-term lime reactions as well as cementitious products formed by pozzolanic reactions. It was concluded that the mixing of expansive soil with  $\text{CaCl}_2$  first followed by  $\text{NaOH}$  solution is more effective than the vice à versa.

Tran *et al.*, (2014) studied the effect of lime treatment on the microstructure and hydraulic conductivity of compacted expansive clay. For this purpose, the dry soil was mixed with 5 % quick lime and compacted statically in an odometer cell at its optimal moisture content. The hydraulic conductivity of the virgin, as well as treated samples cured up to 7 days, were

assessed upon complete saturation. It was observed that hydration of lime, as well as altered fabric structure due to the modification of soil, did not affect the fraction of intra-aggregate pores. However, these phenomena caused the alteration of inter-aggregate pores in the specimen, which in turn is responsible for the enhanced hydraulic conductivity of treated soil. Precisely, the hydraulic conductivity of lime-treated specimen increased progressively during the initial three days of modification phase and attained the constant value during the subsequent four days, which corresponds to a lag period prior to the stabilization phase. The microstructure observation showed that stabilization reactions initiated during the early phase. However, commendable changes were observed only after 7 days of curing. The study also hypothesised that the hydraulic conductivity of long-term (i.e., beyond 7 days of curing) cured lime-treated sample may decrease owing to the formation of well matured cementitious compounds.

Muhmed and Wanatowski (2013) conducted experiments to investigate the microstructure and strength behaviour of kaolin clay treated with lime. The soil was treated with 5 % hydrated lime and assessed for its engineering behaviour in terms of Atterberg limits, compaction properties, *UCS*, and morphological characteristics. Based on the obtained results, it was reported that the lime-treated kaolin clay showed a nominal reduction in its plasticity by 3 % and an increment in its optimum moisture content by 3.4 %. The *UCS* value of the lime-treated soil increased from the virgin strength of 183 kPa to 390 kPa corresponding to 28 days of curing. From the morphological analysis using *SEM-EDS*, the presence of cementitious products in the lime-treated kaolin clay was observed, which might have resulted due to pozzolanic interactions between lime and reactive fraction of clay.

Magdy and Mostafa (2012) quantified the changes in the engineering properties of clayey soils upon stabilization with a traditional stabilizer lime and non-traditional stabilizer Homra. The selected soils were stabilized with 1 % - 11 % of lime, 5 % - 15 % of Homra, independently and assessed for their engineering properties as per the codal provisions. The results obtained indicated that both the stabilizers were effective in reducing the plasticity as well as swelling potential. It was also observed that there was an enhancement in shear strength as well as California bearing ratio by five times of the virgin soil. Stabilization of soil with the combination of lime and Homra altered the compaction properties in terms of

optimum moisture content and dry unit weight. From this study, it was summarized that lime and Homra combination has the potential for enhancing the engineering properties of clayey soils.

Bekki *et al.*, (2015) carried out durability studies on lime-, cement-, and mixture of lime & cement-treated silty soil in view of its application in road construction. The obtained results indicated a substantial improvement in the workability and bearing capacity of the treated soil. It was reported that the soil treated with either 5 % cement or a combination of 1 % lime & 4 % cement yielded identical superior California bearing ratio (*CBR*) value. However, the durability of the soil treated with a mixture of 1 % lime & 4 % cement was found to be superior, which signified the efficiency of the hybrid treatment method.

### **2.3 DEEP STABILIZATION**

Rao and Mathew (1995) made an attempt to study the effect of lime stabilization on permeability characteristics of marine clay obtained from East Coast of India by employing lime column technique. The experimental program was conducted in two phases. In the first phase, a single lime column was installed in the centre of a cylindrical soil specimen of diameter 600 mm and depth 550 mm. After establishing the diffusion profile of lime from a lime column based on the isolated unit lime column set up, the investigations were extended to a group of lime columns. Thus, the study evaluated the interaction among the lime columns in a lime column group using a rectangular tank of 1000×1000×750 mm. Further, a number of soil samples were exhumed from the test setup at a different radial distance and varying experimental duration. Based on the *pH* measurements performed using these samples, it was inferred that the enhancement in *pH* value with time was owing to the diffusion of lime from *LC* into the surrounding soil medium. From the X-ray diffraction analysis on the exhumed samples, the formation of new cementitious products due to the interactions between lime and surrounding soil was established. Furthermore, the permeability measurements made using the exhumed specimens in an odometer cell indicated an increase of *k*-value up to twenty-three times that of virgin soil.



Rajasekaran and Rao (2002) investigated the changes in the compressibility and permeability properties of treated marine clay using lime column, in view of predicting the engineering behaviour of lime-treated cohesive soils. The treated marine clay showed an increase  $k$ -value up to a maximum of 15 to 18 times its virgin value. Similarly, the shear strength of the treated soil increased up to 8-10 times as that of untreated soil within 30 to 45 days of curing. In the case of lime injection systems, the  $k$ -value and  $UCS$  value increased up to 10 to 15 and 8 to 10 times, respectively, as that of virgin soil. In addition, the consolidation behaviour of treated soil indicated reduction in its compressibility as low as half to one-third as that of virgin soil.

Rajasekaran and Rao (2004) conducted an investigation to evaluate the usage of falling cone technique to determine the shear strength of lime-treated soils. Marine clay procured from East Coast of India near Chennai was used for this study. In view of selecting the suitable improvement technique to enhance the strength characteristics of soft marine clays, lime column, and lime injection techniques were assessed. The migration of lime from  $LC$  into the soil system was estimated with respect to time. Laboratory vane shear, as well as falling cone experiments, were carried out to monitor the strength variations. The  $XRD$  analysis was used to establish the rate of formation of cementitious compounds as well as alteration of clay mineralogy upon treatment with lime. The obtained results indicated that the shear strength of lime-treated soil increased by 8 to 10 times as that of untreated soil. It was also reported that both  $LC$  and lime injection techniques could be employed to enhance engineering behaviour of marine clays. Further, the obtained results revealed a linear relationship between shear strength values obtained from the falling cone and laboratory vane shear tests.

Barker *et al.*, (2006) attempted to understand the mechanisms of ion migration from lime piles. Experiments were conducted using London clay and quick lime of 96 % purity. A lime pile of 10 mm diameter and 100 mm long in the form of slurry was placed in the centre of soil column; the soil was moulded at a water content of 1.2 times the liquidity index in a plastic tube of 150 mm diameter and 200 mm long. Lime slurry was also placed at the same water content as that of surrounding soil, to avoid the transport of ions by advection phenomena. The entire setup was incubated in a temperature control room for curing and

samples were collected from it at different radial distances over a range of curing periods 2-49 days. Shear strength by the cone penetration, plasticity and water content measurements were carried out to quantify the consequent changes in clay properties. Furthermore,  $pH$ , electrical conductivity ( $EC$ ), and measurement of ion concentration using atomic absorption spectroscopy indicated the process of cation ion exchange and clay mineral dissolution. The variation in properties of the soil surrounding the lime pile is mainly attributed to ion migration under a combination of chemical, electrical, and hydraulic gradients.

Wilkinson *et al.*, (2010) conducted field as well as laboratory lime slurry pressure injection (*LSP*) studies on in-situ soil at a site in Australia. Following, investigations on stabilized soil were carried out by excavating a trench, and the variations of geotechnical properties were determined by conducting field and laboratory tests. From the observations made on the surface of the excavated trench, it was inferred that slurry was well distributed within the shrinkage cracks in the desiccated portion of the upper soil region. Whereas, the slurry was conveyed through the planes of hydraulic fractures in the soils beyond the desiccated upper soil region. Laboratory swell tests on the exhumed specimens from stabilized soils confirmed the reduction of the intrinsic swell properties in the upper soil regions. The cone penetration tests on stabilized soils indicated an increase in the soil strength. Furthermore, morphological features obtained using *SEM* and *XRD* studies confirmed the physicochemical and cementitious processes in stabilized soils. The aggregation of clay platelets was observed with the outward diffusion of calcium cations within the proximity of slurry seams, and hence, resulted in a subdued shrink/swell propensity.

Shen *et al.*, (2010) identified six major phenomena such as soil thixotropy, soil fracturing; cement penetration and diffusion, cementation, consolidation, and heating which are responsible for enhancement in engineering properties of the soil surrounding deep mixing cement columns. The laboratory tests were performed to investigate the effects of the above-mentioned phenomenon on engineering behaviour of treated soft marine Ariake clay. The test results showed that an influential zone of property changes existed in surrounding clay ranging from the edge of the cement column to the distance of about twice of its radius. Within this influential zone, decrease in water content as well as increase in  $pH$  and electric

conductivity were noticed and was found to be varying proportionately with distance towards the boundary of the cement column. It was also reported that the undrained shear strengths of the surrounding clays decreased substantially soon after mixing, however the shear strength reached its original value within 7 days of column installation and continued to increase up to the curing period of 28 days.

Muntohar and Juin-Liao (2006) studied the radial and vertical strength distributions around a *LC* installed in expansive soft clay. The dimensions of *LC* used in this study were 50 mm diameter and 200 mm length. The strength of the soil surrounding the *LC* was assessed in terms of *UCS* as well as cone penetration resistance using static cone penetrometer. The test results showed that the installed *LC* enhanced the surrounding soil strength up to a radial distance of four times its diameter (i.e., influence zone). The degree of improvement in the strength near the surface of the *LC* was high and decreased linearly with the distance away from it. It was also reported that the degree of improvement in strength of the soil in the zone of influence enhanced with curing period. The cone penetration resistance values inferred that the installation of *LC* influenced soil strength up to a depth of four times the diameter of *LC* beneath its bottom. Further, the outcome of the study confirmed that the installation of *LC* resulted in the lower water content of the surrounding soil adjacent to the column and increased proportionately towards its virgin value (prior to the installation of *LC*) up to the farthest boundary of the influence zone and remained constant thereafter.

## **2.4 CHARACTERIZATION OF STABILIZED SOILS**

Ghosh and Subbarao (2001) studied the physicochemical and microstructural modifications of a class-F fly ash stabilized with 6 and 10 % lime as well as in combination with 1 % gypsum. The treated specimens were cured at 30 °C up to a curing period of 10 months. The treated soil was characterized using *XRD*, *TGA-DTA*, *SEM-EDS* to understand the interactions between fly ash, lime and gypsum. The obtained X-ray diffractograms showed the emergence of new peaks; also, certain peaks were observed to have lower peak intensities which might be due to the amorphous nature of newly formed phases. From the *SEM* images, the development of pozzolanic reaction products could be clearly observed after curing period of 3 months, which further got densified with increasing curing period. Moreover, the

increment in strength and durability along with decreasing permeability of the stabilized specimens was correlated with this development of new reaction products. Hence, this study concluded that fly ash modified with lime and gypsum can be used potentially in the civil engineering applications.

Chew *et al.*, (2004) examined the micro-structural development of cement-treated marine clay in relation to the engineering properties. The soil microstructure was investigated using *SEM* and mercury intrusion porosimetry (*MIP*) analyses, and laser diffraction measurement was employed for determining the particle size distribution of cement-treated clay. Further, the mineralogical properties were evaluated using *XRD* analysis in order to identify the characteristic variations caused by soil-cement interactions. The index and engineering properties such as hygroscopic moisture content, void ratio, consistency limits, permeability, and *UCS* were determined by following the guidelines provided in *ASTM* standards. The results indicated that significantly large scale changes occurred in the properties and behaviour of cement-treated marine clay when compared to their untreated counterparts. This can be explained in terms of the combined interactions of four underlying microstructural mechanisms. These mechanisms are hydration reactions which form the hydrated lime leading to flocculation of clay particles, sorption of calcium ions, deposition and filling by cementitious products on clay particles and pores, as well as the presence of water trapped within the clay clusters.

Nontananandh *et al.*, (2005) made an attempt to correlate the strength enhancement of cement stabilized soils with the formation of reaction products by conducting *XRD* analysis. In addition, conventional laboratory *UCS* tests were also performed. For this purpose, a clayey soil was treated with Type I ordinary Portland cement at a mix proportion of 200 kg/m<sup>3</sup>. Further, specimens for *UCS* tests were casted and cured for different periods of 3, 7, 14, 28 and 90 days. Following, *XRD* analysis was performed on the fragments collected from the failed samples of *UCS* tests. The experimental results showed significant gain of short-term strength during the initial periods of curing (before 28 days), while the change in strength was observed to be insignificant with curing period during long-term curing. This investigation elucidated that the formation of reaction products as can be seen from *XRD* primarily attributed to the significant strength gain.

Lasledj and Al-Mukthar (2008) studied the influence of lime stabilization on the engineering behaviour and microstructure of expansive clayey soil with the help of laboratory-based experiments. The tests were conducted on soil treated with 0-20 % of hydrated lime. *XRD* studies were performed to ascertain the mineralogical changes in the lime-treated soil in terms of the reaction products formed by soil-lime interactions. Based on the experimental results, it was observed that lime stabilization led to the control of swelling and surface charge properties. It was also observed that with the addition of 8 % lime, swelling pressure and swell potential reduced to zero after a curing period of three days, whereas no significant change in plasticity index of the soil is reported even with high lime content (6 % and beyond) and curing period. The X-ray diffractograms indicated that the evolution of new reflections corresponded to the formation of *CAH* in soil samples treated with lime content beyond 8 %.

Vazquez *et al.*, (2010) assessed the multifractal characteristics of pore size distributions measured using *MIP* technique. The geomaterials used in this study were collected from two different topographic positions and soil use. These two different types of soil samples were distinguished by different proportions of fines fraction and organic matter contents. The soil samples characterized by higher clay and organic matter content were observed to have higher macro pore volume. The main characteristics of the pore size distributions (*PSD*) measured from *MIP* could be fitted well with the Multi-fractal models. Therefore, it was inferred that the different patterns of *PSD* would be distinguished clearly by multi-fractal analysis.

Eisazadeh *et al.*, (2010) made an attempt to comprehend the key mechanisms responsible for the strength enhancement and changes in the molecular structure of phosphoric acid stabilization with respect to curing period. The geomaterials considered in this study were bentonite and lateritic soils. Nuclear magnetic resonance (*NMR*) and *FTIR* were employed to investigate the molecular level changes in the structure of bentonite and lateritic soil stabilized with phosphoric acid. From the obtained results, it was inferred that the primary factor responsible for the enhancement of stabilized soils was surface alteration mechanism. Furthermore, the results indicated that the reactive alumina was also accountable for the formation of new cementitious products to a certain extent.

Horpibulsuk *et al.*, (2010) attempted to understand the development of strength in cement-stabilized silty clay from the microstructural and chemico-mineralogical analyses. *SEM*, *MIP*, and *TGA-DTA* tests were employed to estimate the qualitative and quantitative changes in the microstructure and mineralogy of cement treated soils. The effect of moulding moisture content, curing period and cement content on the strength gain was evaluated. The structure of cement treated specimens was modified significantly due to the inter-cluster cementation bonding by newly formed pozzolanic reaction products which led to the reduction of pore space. Moreover, maximum strength was observed at a moisture content of 1.2 times optimum moisture content. This might be endorsed to the formation of a higher quantity of cementitious products because of the availability of higher moisture for pozzolanic reactions. It was inferred from the *MIP* studies that during short-term stabilization period, the macro pore volume (larger than 0.1  $\mu\text{m}$ ) increased and micro pore volume (smaller than 0.1  $\mu\text{m}$ ) decreased due to the deposition of cement gel into the pores. Whereas, long-term stabilized samples showed a decrement in the total pore volume, which might be the potential reason for long-term strength development.

Stoltz *et al.*, (2012) studied the swelling/shrinkage behaviour of lime-treated expansive clayey soil at macro and micro level by conducting wetting and drying tests. The soil specimens were mixed with lime contents of 0 %, 2 %, and 5 %. Further the samples were compacted and cured for a period of 0, 28, and 180 days. Later, the soil-water characteristic curves (*SWCC*) of these compacted specimens were determined after their respective curing periods. The micro-structural modification was assessed by employing *MIP* technique. The obtained results showed that volumetric swelling upon wetting was controlled by lime treatment from the initial state. The hydro-mechanical behaviour of lime-treated soils was significantly altered upon drying by increasing the compacted shrinkage limit suction. As a whole, it can be inferred from the *MIP* tests that both the macro- and micro-porosity fabric of the lime-treated soils was altered upon drying.

Saeed *et al.*, (2013) attempted to study the micro-structural characteristics of lime-treated brown kaolin clay samples. The laboratory *UCS* test was conducted on the stabilized specimens along with microstructural studies using *XRD*, *SEM*, and *FTIR*. From the microstructural analyses, it was observed that kaolinite mineral was rapidly exhausted by the

pozzolanic reactions to produce the gismondine (a form of *CASH* gel), which was in turn responsible for the strength gains in the lime-treated samples with progressing curing time. On the other hand, it was noticed that the illite mineral did not show any reactions with advancing time.

Sasanian and Newson (2013) employed the *MIP* technique to study the pore size distribution effects of two clays with varying moisture content. The moisture contents employed in this study were of liquidity indices ranging from 0 to 3. Further, *MIP* was carried out on the air-dried specimens. The obtained results from *MIP* indicated the distribution of pores in two different ranges referred as intra- and inter-cluster pores. It was found that the volume of inter-cluster pores increased with the addition of water to air-dried soil whereas the volume of intra-cluster pores remained same. However, further addition of water to the wet material resulted in the variation of inter-cluster pore volume. It can be inferred from this study that *MIP* probably underestimated the void ratio of specimens with higher moisture content. This can be attributed to the limitation of *MIP* test to detect the large pores.

Quang and Chai (2015) examined the permeability characteristics of lime and cement-stabilized soils, in terms of permeability coefficient,  $k$ -value. The obtained results indicated that under same void ratio conditions, the  $k$ -value of cement treated soil was almost same as that of virgin soils up to 8 % and decreased beyond. Similarly, the threshold lime content for lime-treated soils was determined to be 4 %. Further, the micro-structural analysis was carried out by *MIP* and *SEM* tests. The results indicated that same  $k$ -value of treated and virgin samples during the initial stages might be due to the filling of intra-aggregate pores by the newly formed cementitious products. Further, the decrement in the  $k$ -value might be attributed to filling of the inter-aggregate pores by cementitious products.

Saeed *et al.*, (2015) assessed the typical changes imparted in the fabric and structure of tropical kaolin clays due to mineralogical influences with respect to different curing conditions and lime contents. The microstructural characterizations were made using *XRD*, and *SEM*. Additionally, *UCS* tests were also carried out to illustrate the effect of lime on the strength of treated soil matrix. The results indicated that increasing lime content resulted in

an improvement in the compaction properties, in terms of decreasing maximum dry unit weight and increasing optimum moisture content. Besides, the *UCS* of stabilized clay increased with the addition of lime. Further, the development of strength of lime-treated samples was also observed to increase with curing time. The formation of calcium aluminate silicate hydrate (*CASH*) was observed from the *XRD* analysis after 200 days of curing, and the presence of the cementitious products was further verified by *SEM* analysis.

Aravind and Sivapulliah (2016) conducted a series of oedometer, swell, compressibility, permeability tests and micro-analytical studies (viz., *XRD*, *SEM*, and *EDS*) to understand the volume change behaviour of lime-treated the gypseous soil with respect to various curing periods. The geomaterial used in this study was montmorillonitic soil. The compacted specimens started swelling immediately upon inundation with water. Further, with the increasing gypsum content, the swelling also increased. However, the curing period does not seem to have any significant effect on the percentage swelling. This might be attributed to the formation and growth of ettringite crystals as well as cementitious compounds which were confirmed through detailed micro-analytical studies. Also, the formation of new cementitious reaction products was found to have a significant influence on the compressibility and permeability behaviour of treated soil.

## **2.5 TRANSPORT PROPERTIES OF IONIC SPECIES AND THEIR ROLE IN STABILIZATION OF SOILS**

Kenneth *et al.*, (1991) have evaluated diffusion coefficient ( $D_m$ ) in soil sediments by various laboratory techniques. For this purpose, the soil sediments collected from the fresh water Okeechobee lake were used in this study. The different methods used for evaluating the diffusion coefficients were: diffusion of tritium tracer into the sediment from an overlying water column spiked with the known concentration of the tracer (referred as method-1), solute diffusion from a spiked sediment column into an overlying water column (referred as method-2), solute diffusing from a spiked sediment column to a tracer-free sediment column (referred as method-3). The method-1 consumed very less time and was more efficient. Even though, the obtained  $D_m$  values from method-1 were found to be in a similar way as that of methods-2 and -3. Among all the methods,  $D_m$  values from method-3 were slightly lower than



the other two methods. This might be due to the improper sediment extrusion and sectioning which affects the concentration profiles. Therefore, it can be inferred from this study that method-1 is ideally suitable for estimation of diffusion coefficients in the laboratory as well as in marine and fresh water sediments.

Shackelford and Daniel (1991) studied the effect of placement moisture content and method of compaction on the diffusion of ionic species in a compacted clay soil. The ionic species employed in this study for measuring effective diffusion coefficients ( $D^*$ ) included three anions ( $Br^-$ ,  $Cl^-$ , and  $I^-$ ) and three cations ( $Cd^{2+}$ ,  $K^+$ , and  $Zn^{2+}$ ). The kaolinite and Lufkin clay were selected for the study, and the compacted soils were allowed to interact with a simulated waste leachate containing the above-mentioned ionic species. The calculated  $D^*$  values for Lufkin clay varied between  $4 \times 10^{-10}$  to  $2 \times 10^{-9}$  m<sup>2</sup>/s for various ions. It was also observed that placement moisture content and method of compaction had no significant effect on the measured  $D^*$  values. The calculated  $D^*$  values for  $Cl^-$  and  $Br^-$  in kaolinite were found to be in good agreement with values reported in the literature. However, the obtained  $D^*$  values pertaining to cations were comparatively high. This might be endorsed to nonlinear adsorption behaviour at relatively high concentrations and also the possibility of chemical precipitation of the heavy metal species, particularly for  $Cd^{2+}$  and  $Zn^{2+}$  cations.

Sato *et al.*, (1996) determined the diffusion coefficients of various ions i.e.,  $Cs^+$ ,  $Pb^{2+}$ ,  $Sm^{3+}$ ,  $Ni^{2+}$ ,  $SeO_4^{2-}$ , and  $TcO_4^-$  through water ( $D_o$ ) based on Nernst-Einstein equation ( $D_o = RT/F^2|Z|$ ). The Kohlrauschs square-root law was used for determining the limiting ionic equivalent conductivity ( $\lambda_0$ ) of  $Cs^+$ ,  $Pb^{2+}$ ,  $Sm^{3+}$ ,  $Ni^{2+}$ ,  $SeO_4^{2-}$  whereas for  $TcO_4^-$  it was derived from the relation between the concentration of in the solution and the  $\lambda_0$  because of its weak electrolyte. The obtained  $D_o$  values were in a range of  $1.4-2.2 \times 10^{-9}$  which were also in good agreement with the literature. Further, the activation energy needed for diffusion was found to be less than a factor of two.

Zhang and Gjorv (1996) performed an experimental investigation of the diffusion behaviour of chloride ( $Cl^-$ ) ions through concrete. In the natural salt solutions such as seawater as well as laboratory grade concentrated electrolytic aqueous solutions, the diffusion phenomenon may be influenced by the reduced chemical potential of ionic interactions. From

the study, it was noticed that the diffusion of chloride ions was intervened by the electrical double layer formed on the solid surface and the chemical binding, as well as, the lagging motion of the cations present in the solution. On a whole, it can be inferred that the diffusion behaviour of the chloride ions in concrete is not simple as described by Fick's law of diffusion; rather a complex and intricate transport process.

Zhang *et al.*, (1998) modelled the diffusion of chlorine in the surface treated concrete. The model was proposed for all types of surface treatment. The obtained results indicated that diffusion of chloride is controlled by both the surface treatment and the substrate. It was observed that surface treatment led to the significant reduction of chloride concentration at the concrete surface. However, the interfacial concentration was increasing with time. Hence, Fick's law is not valid for the chloride profile in the concrete substrate. However, the diffusion coefficients were reported to be less than the actual diffusion coefficients when Fick's law was used for this chloride profiles.

Tsai *et al.*, (2001) conducted the batch and through-diffusion experiments on Jih-Hsing for evaluating the sorption and diffusion behaviour of  $Cs^+$  and  $Sr^+$ . The batch sorption results indicated that the Freundlich isotherm represents the sorption behaviour of  $Cs^+$  and  $Sr^+$  in a better way and distribution coefficients ( $K_d$ ) were determined to be 1200 ml/g and 800 ml/g respectively. Further, the retardation factors ( $R$ ) were calculated for samples at different densities. The value of  $R$  for cesium and strontium at densities of 1.8 g/cm<sup>3</sup>, 2.0 g/cm<sup>3</sup>, 2.2 g/cm<sup>3</sup> were calculated as 5685, 7744, 11000 and 3790, 5162, and 7334 respectively. Following, the diffusion experiments were conducted on samples compacted at same densities as mentioned above. The diffusion coefficients for  $Cs^+$  were determined as  $(2.83 \pm 0.75) \times 10^{-13}$  m<sup>2</sup>/s,  $(1.97 \pm 0.02) \times 10^{-13}$  m<sup>2</sup>/s and  $(1.91 \pm 0.12) \times 10^{-13}$  m<sup>2</sup>/s, respectively. Similarly, the diffusion coefficients for  $Sr^+$  were reported to be  $(1.33 \pm 0.13) \times 10^{-13}$  m<sup>2</sup>/s,  $(1.51 \pm 0.15) \times 10^{-13}$  m<sup>2</sup>/s, and  $(1.34 \pm 0.1) \times 10^{-13}$  m<sup>2</sup>/s. Further, the  $R$  values were calculated for diffusion experiments at the obtained sample densities of 1.8 g/cm<sup>3</sup>, 2.0 g/cm<sup>3</sup> and 2.2 g/cm<sup>3</sup>. The obtained values were reported to be 1166±355, 2113±123, 2796±171 for cesium and 713±258, 510±68, 846±158 for strontium. From these observations, it was inferred that the retardation factors obtained from batch experiments were one order of magnitude higher than values obtained from the diffusion experiments.

Zawawi *et al.*, (2004) conducted the chloride permeability tests in normal and blended concrete by the application of electric field at different voltages. For this purpose, the concrete specimens of 100 mm diameter and 25 mm thick were fabricated and cured for 28 days. The tests were conducted in a two compartment cell with specimen being sandwiched between them. One cell was filled with NaCl solution and another cell was filled with NaOH solution. Further, they were subjected to different voltages of 12, 30 and 60 volts for 24 hours. The obtained results for different voltages showed that the chloride permeability index at 12 volts after 24 hours was similar to that of values obtained for 30 and 60 volts after 6 hours. The fly ash blended cement concrete showed a relatively higher resistance of 75 % to 110 %, against the chloride movement in concrete as compared to that in ordinary Portland cement (*OPC*) concrete.

Leroy *et al.*, (2005) modelled the diffusion of ions in bentonite under the influence of hydraulic, electrical, and chemical gradients. The modified Donnan model was used for modelling the concentrations of the ions in the pore water of the bentonite which accounts for the partition of the counter ions between the Stern and Gouy-Chapman layers. An explicit complexation model combined with electric triple layer model (*TLM*) was used at the mineral/water interface. In the determination of formation factor of the medium, the effective porosity was obtained by removing the fraction of hydration water covering the surface of the clay minerals. The studies were carried out in two phases. In the first phase, a salinity gradient was considered between the two reservoirs in contact with the cylindrical bentonite sample. The obtained results indicated that the diffusion of salt increased with salinity which was in agreement with the experimental data. In the second case, a self-diffusion experiment was conducted in order to analyze the diffusion of an ionic tracer, and the model is predicted that the diffusion of anions increases with the effective porosity and ionic strength.

Lee *et al.*, (2009) performed experiments to investigate the effect of consolidation on the transport parameters which govern advection and dispersion. In view of this, the tests pertaining to the transport of ionic species were conducted using kaolinite clay, with the different dilutions of potassium bromide (KBr). The obtained results from batch tests indicated the high sorption of  $K^+$  ion and equilibrium was reached within 10-30 minutes. The sorption was observed to be more in the case of batch tests compared to that of dispersion or

solute transport tests. This might be because of lower solids-to-solution ratio and more efficient mixing process. From this study, it was inferred that the consolidation of kaolinite has no significant effect on sorption. This might be attributed to the minute alterations in porosity. The hydrodynamic dispersion coefficient ( $D_h$ ), effective diffusion coefficient ( $D^*$ ), and apparent tortuosity factor found to be declining with decreasing porosity. Furthermore, the obtained effective diffusion coefficient for  $Br^-$  was much higher than that for  $K^+$ , while it was vice versa for the values of hydrodynamic dispersion coefficient. The value of longitudinal dispersivity ( $\alpha$ ) was higher for  $K^+$  than  $Br^-$  and showed no clear trend with decreasing void ratio. In general, the experimental results suggested that the effect of consolidation on sorption is insignificant whereas the changes in transport parameters need to be considered more critically.

Huiming sun *et al.*, (2010) performed laboratory experiments and mathematical modelling to investigate the transport of kaolinite and lead ( $Pb$ ) under saturated conditions. Batch sorption experiments were conducted on kaolinite and quartz sand in order to obtain the adsorption isotherms of  $Pb$ . It was observed that  $Pb$  is being sorbed onto both the soils, but the sorption of  $Pb$  onto kaolinite was much higher i.e., 30 times than that of sand. In this study, the transport behaviour of  $Pb$  through kaolinite was studied in saturated sand columns. Further, an additional experiment was conducted by passing pure kaolinite through  $Pb$  contaminated sand. The obtained results inferred that the  $Pb$  sorbed onto the sand grains reduce the mobility of kaolinite and the mobile kaolinite were able to remove the  $Pb$  sorbed onto the sand grains thereby enhancing the mobility of  $Pb$ . In addition, the modelling studies were conducted and the obtained results from Langmuir model and an advective-dispersive transport model were found to be matching well with experimental data obtained from batch sorption and column studies.

Vincent and Craig (2013) conducted experiments to discern the effect of moisture on diffusion and porosity parameters of soil-cement mixtures. For this purpose, the titrated water was used as a conservative tracer in order to assess the diffusion properties of fourteen different soil-cement mixtures prepared in the laboratory. A single-reservoir diffusion test setup was used to determine the effective porosity ( $\eta_e$ ) and the effective diffusion coefficient ( $D_e$ ) through saturated, monolithic, soil-cement materials in order to evaluate the importance

of mixture design on  $\eta_e$  and  $D^*$  values. The corresponding values of  $D^*$  and  $\eta_e$  were found to be in the range of  $2.5 \times 10^{-10}$  to  $7 \times 10^{-10} \text{ m}^2/\text{s}$  and from 0.21 to 0.41, respectively. The results also indicated that the water content of the initial mixture has a substantial effect on the diffusive properties of the soil-cement material. The results further suggested that the designers should generally aim to minimize the water content of cement-based solidification-stabilization materials from a contaminant transport perspective.

Ghods *et al.*, (2012) conducted experiments to study the diffusion characteristics of chloride ion in concrete at different exposure conditions. The study was conducted on  $150 \times 150 \times 600$  mm prismatic concrete specimens cast with various water/ binder ratios, as well as different silica fume contents. The specimens were cured in a saturated calcium hydroxide ( $\text{Ca}[\text{OH}]_2$ ) solution up to 28 days and later subjected to different exposure conditions for three months in the region of Persian Gulf. The different exposure conditions in the present study were soil, atmosphere, submerged, tidal and splash zones. After the exposure period of three months, the specimens were ground to powder and analysed for chloride content at different depths from exposed surface. The diffusion coefficient ( $D$ ) and surface chloride content of concrete specimens were determined by fitting the nonlinear profiles of chloride content to Fick's second law of diffusion. Further, the effect of different exposure conditions was quantified. The obtained values were further employed in the design model of a service life concrete structure in the region of Persian Gulf.

## **2.6 SUMMARY AND CRITICAL APPRAISAL**

The reviewed literature demonstrates the utilization of lime for the effective modification and stabilization of problematic soils (Wilkinson *et al.*, 2010). The major finding observed from the literature was the potential of lime to modify the plasticity behaviour of soils. The variation of liquid limit of lime admixed soil was shown to have decrement with increasing lime percentage (Sakr *et al.*, 2009) and the vice versa in the case of plastic limit (Barker *et al.*, 2006), thereby causing a corresponding decrease in plasticity index making soil more friable and workable (Kavak and Baykal, 2012; Muhmed and Wanatowski, 2013). Lime was also used to enhance the behaviour of expansive soils which effectively controlled the swelling and shrinkage, henceforth reducing the damage and distortion of the superstructure

(Wilkinson *et al.*, 2010; Almkhtar *et al.*, 2010; Thyagaraj *et al.*, 2012). Other than the modification of plasticity and swelling characteristics, lime was also used to strengthen the soils (Lav and Lav, 2000; Nasrizar *et al.*, 2010; Al-Kiki *et al.*, 2011). This was mainly attributed to the cementation by means of pozzolanic reactions which led to the significant improvement in the long-term performance (Magdy and Mustafa, 2012; Tran *et al.*, 2012; Bekki *et al.*, 2015). However, in some cases, the addition of lime beyond certain limit was found to degrade the strength (Nasrizar *et al.*, 2010).

The pertinent literature shows the important research conducted on the utilization of lime for deep stabilization of soils such as building foundations, cutoff walls, and excavation supports (Rajasekaran and Rao, 2004). The deep stabilization techniques mainly include lime columns (*LC*), lime piles (*LP*) and lime slurry pressure injection (*LSPI*) (Rajasekaran and Rao, 2002; Wilkinson *et al.*, 2010). The soil modification/improvement during deep lime stabilization is primarily attributed to the migration of calcium and hydroxyl ions into the surrounding soil (Barker *et al.*, 2006), which resulted in the occurrence of immediate and long-term chemical and pozzolanic soil-lime reactions. The formations of cementitious products lead to the up gradation of the settlement, compressibility and reduction in the permeability (Rao and Mathew, 1995; Rajasekaran and Rao, 2002). From the works of Shen *et al.*, (2010), Muntohar and Juin-Liao (2006), Rao and Mathew (1995), it was inferred that lime migration was limited up to a radial distance of 2-4 times the diameter of the lime pile.

The morphological and micro structural changes occurring in the lime-treated soils were characterized by many advanced techniques. *SEM* studies (Chew *et al.*, 2004; Saeed *et al.*, 2013; Quang and Chai, 2015) showed the formation of pozzolanic compounds in lime-treated specimens. The *Ca/Si* ratio from *EDS* studies indicated the existence of *CSH* and *CASH* phases (Aravind and Sivapulliah, 2016). In the case of lime-treated soils, a reduction of peak intensities of clay minerals was observed from *XRD* studies (Nontananandh *et al.*, 2005; Lasledj and Almkhtar, 2008; Saeed *et al.*, 2015) which indicated the formation of cementitious compounds by pozzolanic reactions. The time-dependent changes induced in the thermal properties of lime-treated soils were investigated by *TGA-DTA* analysis (Horpibulsuk *et al.*, 2010; Ghosh and Subbarao 2001). Further, *FTIR* studies (Eisazadeh *et al.*, 2010; Saeed

*et al.*, 2013) were performed to study the molecular changes in the structure of lime-treated soils.

Tsai *et al.*, (2000), Lee *et al.*, (2009), Huiming sun *et al.*, (2010) studied the sorption capacity of various geomaterials for different contaminants by conducting batch sorption experiments. Kenneth *et al.*, (1991), Shackelford and Daniel (1991), Sato *et al.*, (1996), Zhang and Gjo (1996), Zhang *et al.*, (1998), Leroy *et al.*, (2005), Vincent and Craig (2013) made efforts to understand the fundamental mechanism involved in diffusion phenomena of soils. Zawawi *et al.*, (2004) employed accelerated diffusion to accelerate the migration of the ions by employing electric potential across the media.

However, the majority of the studies lack a fundamental understanding of the mechanism of lime stabilization that has occurred. Though parameters such as reactive nature of the soil and their compatibility in terms of sorption and diffusion characteristics determine the efficacy of stabilization technique, not many attempts were made to substantiate quantitatively. Based on the critical review of literature it is observed that many studies on deep stabilization using lime pile/column are found to be in disagreement regarding the dominant mechanisms governing soil stabilization. Majority have fallen short to consider some of the most influential properties such as the fabric and pore structure, and sorption affinity of in-situ soil, groundwater variation and presence of other ions in the neighborhood, as well as strength and microstructural variations within the lime pile/column.

Based on the above studies, it can be gathered that the improvement of engineering properties of the lime-treated soils is mainly controlled by the nature of soil-lime reactions. It was evident from the existing literature that the determination of the suitable method for chemical testing of lime-treated soils is lacking. In addition, ample attempts were not made to understand the mechanisms associated with the soil-lime interactions. The mineralogical and microstructural studies on the lime stabilization are mainly aimed at investigating its effect on the strength properties of soil. Nevertheless, a detailed comparative study on microstructure, mineralogy and thermal characteristics of lime-treated soils are inadequate. Hence, there is a need for the thorough investigation to completely characterize the microstructure, mineralogy and thermal properties of soil stabilized with lime.

# EXPERIMENTAL INVESTIGATIONS AND TESTING METHODOLOGY

---

### 3.1 GENERAL

In view of achieving the proposed objectives of the present study, three types of fine-grained geomaterials were selected, which includes two commercial clays: (a) white clay (denoted as *WC*); (b) Sodium bentonite (denoted as *BT*); and (c) sandy clay (denoted as *SC*) procured from East Coast, Nellore district of Andhra Pradesh, India. The basic characterization of these soils was carried out as per the guidelines reported in the standards and literature. In order to assess the efficacy of lime for stabilizing these materials, commercially available hydrated lime (denoted as *HL*) was procured and characterized for its chemical composition and purity.

### 3.2 PRELIMINARY CHARACTERIZATION

#### 3.2.1 Specific gravity, gradational characteristics and consistency limits of geomaterials

The specific gravity ( $G$ ) of the selected geomaterials was determined by employing ultracycrometer (Quantachrome, USA) as per the guidelines presented in ASTM D5550, where inert helium gas is used as the displacing fluid. The gradational characteristics of the selected geomaterials were determined as per ASTM D422 and the results are presented in the Figure 4.1. The consistency limits (viz., liquid limit,  $w_L$ ; plastic limit,  $w_P$  and plasticity index,  $PI$ ) were determined as per the guidelines provided by ASTM D4318. The hygroscopic moisture content of the selected geomaterials was obtained as per Shah and Singh (2006). Based on the particle size distribution and Atterberg limits, the selected geomaterials were classified as per ASTM D2487 and presented in Figure 4.2. The results from these investigations are presented in Table 4.1.



### 3.2.2 Specific surface area of geomaterials

The specific surface area (denoted as *SSA*) of the geomaterials was measured by employing ethylene glycol monoethyl ether (*EGME*) method (Cerato and Lutenecker, 2002; Arnepalli *et al.*, 2007). For this purpose, oven-dried soil samples were weighed to 2 gm, placed uniformly in a glass petridish and covered with watch glass. The selected geomaterials in triplicate were placed in a vacuum desiccator containing 250 g phosphorous pentoxide as a desiccant. Following, the samples were evacuated by applying vacuum till the weight of the sample reached a constant value. Further, the samples were mixed with 6 ml *EGME* solution of analytical grade to form homogeneous slurry and placed in the vacuum desiccator containing a mixture of 100 gm calcium chloride anhydrous and 20 ml *EGME* solution as a desiccant. This helps in maintaining a constant vapor pressure which is just sufficient to form a monolayer on the soil specimen as well as to minimize the loss of *EGME* from the monolayer that is formed on the external surface of the sample, and the interlayer spacing of the clay minerals of the soil. The initial weight of the *EGME* mixed soil slurry was measured using the high precision balance and the placed again in the desiccator for vacuum application so that *EGME* admixed specimen reaches equilibration. This process was repeated, until the weight of the *EGME* mixed soil attained a constant weight. Based on the experimental results, the *SSA* of the selected soils was obtained, as described in section 4.2.2.

## 3.3 CHEMICAL CHARACTERIZATION

### 3.3.1 Cation exchange capacity of the selected materials

The cation exchange capacity, abbreviated as *CEC*, is defined as the maximum quantity of total available cations (acid and base) that soil can hold at a given *pH*, for exchange with other cation species present in the soil solution. In the present study, the *CEC* of virgin geomaterials was determined using the guidelines presented in the codal provisions (IS 2720; ASTM D7503). Initially, the virgin soil sample was oxidized using hydrogen peroxide ( $H_2O_2$ ) by boiling the mixture of  $H_2O_2$  and the soil for an hour to remove any organic matter present in it. Then, 5 g of treated sample was oven-dried and saturated with sodium ( $Na^+$ ) ion by mixing with 50 ml 1N sodium acetate solution of *pH* 5. The mixture was digested in a hot

water bath for 30 minutes with intermittent stirring and later the sample was centrifuged at a speed of 5000 rpm for 15 minutes using a table top centrifuge (ELTEK, TC 4100D, India). The supernatant liquid was collected and stored for further analysis. The soil sample settled at the bottom of the centrifuge tube was again treated with 50 ml sodium acetate solution of same composition, digested and centrifuged. This process was repeated thrice to ensure saturation of potential sites completely with  $Na^+$  ion. Following, this sample was treated with 1N calcium chloride ( $CaCl_2$ ), and again digested and centrifuged. The whole process was repeated thrice, in order to ensure complete replacement of sodium ion that was sorbed during the previous step by the divalent calcium ion. This process ensures the saturation of all the exchangeable sites present in the soil by the calcium ion. Further, this sample was again treated with 50 ml 1N sodium acetate solution of  $pH$  7, digested and centrifuged thrice. The resulting supernatant from the last three steps was collected and analysed for concentration of calcium ion using atomic absorption spectrophotometer, *AAS* (Thermo Scientific iCE 3000, USA), as depicted in Figure 3.1. By following the above mentioned methodology, the cation exchange capacity of the selected geomaterials was obtained and the results are reported in section 4.2.3.



Figure 3.1 Photographic view of atomic absorption spectrometer used in this study

### 3.3.2 X-ray fluorescence spectroscopy

The elemental composition of virgin geomaterials and hydrated lime was determined from the X-ray fluorescence (*XRF*) studies. *XRF* analysis was carried out at the central electrochemical research institute (CECRI), Karaikudi, Tamil Nadu, India using a table top X-ray analytical microscope (*XGT-2700*, Horiba, Japan) as shown in Figure 3.2, operating at 30 kV and 1.0 mA. Since the X-ray analytical microscope uses X-rays for elemental analysis, there is no need to process samples beforehand. To obtain the representative chemical composition, analyses of 100 seconds each on different points of the sample were repeated several times. The obtained elemental composition of the selected materials in their oxide form is presented in the Table 4.2



Figure 3.2 Photographic view of X-ray analytical microscope used in this study

### 3.3.3 Simultaneous thermo gravimetric - differential thermal analysis

In the present study, the thermo gravimetric-differential thermal analysis analysis (*TGA-DTA*) was performed on lime-treated soils using Netsch STA 409 PC/PG instrument as shown in Figure 3.3. Prior to the analysis, the representative specimens were oven-dried for 24 hours at 40 °C and pulverized into fine powder using a mortar and pestle. Following, approximately

20 mg of the sample was weighed up to four decimals precision in a micro analytical weighing balance. The weighed sample was placed in alumina crucibles and thermal analysis was performed under argon gas atmosphere with a flow rate of 10 mL/min over a temperature range of 35 °C to 1000 °C at a rate of 10 °C/min. (Wild *et al.*, 1993; Horpibulsuk *et al.*, 2010; Sharma *et al.*, 2012). During the initial trial experiments, most of the samples exhibited continuous weight loss upon heating, owing to presence of free moisture at the time of analysis. This created difficulties in obtaining the initial weight of the sample. In order to overcome this difficulty, sample was equilibrated in a furnace atmosphere of 30 °C until it reached a constant weight (initial dry weight). Later, the heating was continued at a constant rate of 10 °C per min and both the weight gain/loss and corresponding temperatures were recorded. The weight at 1000 °C was considered to be the final weight of the sample. The obtained results are presented in the section 4.5.1.



Figure 3.3 Photographic view of thermo gravimetric analyzer used in this study

### 3.3.4 Fourier transform infra-red spectroscopy

Fourier transform infra-red (*FTIR*) spectroscopy is an advanced analytical tool employed for investigating the clay mineral properties in terms of the molecular changes within their

structural units (Eisazadeh *et al.*, 2011 and 2012). This technique follows the principle of measuring the absorption at characteristic wavelength of chemical bonds that vibrate independently of one another, and thereby the associated functional groups can be identified (Madejova and Komadel, 2001). In the present study, the infra-red (*IR*) spectra of lime-treated soils were obtained using a bench-top *FTIR* spectrometer (Perkin Elmer, Spectrum 100, USA) as illustrated in Figure 3.4, equipped with an *IR* source, middle *IR* (*MIR*) detector, and advanced universal attenuated total reflectance (*UATR*) accessory, for reliable analysis of small powder samples.



Figure 3.4 Photographic view of Fourier transform-infrared spectrometer used in this study

Prior to the analysis, the specimens were oven-dried at 40 °C for 24 hours. The *FTIR* instrument was initially calibrated for background signal by scanning without a specimen. During sample analysis, a pinch of the powdered soil sample was loosely poured onto the crystal surface of sample plate. Following, sample was pressed on to surface of plate with a micrometer-controlled pressure pin under controlled rate, in order to ensure proper contact. The scan range used was *MIR* spectral range of 650-4000  $\text{cm}^{-1}$  and spectra of all samples were recorded with a resolution of 4  $\text{cm}^{-1}$  and 64 accumulations. For each sample, 64 scans in the *MIR* range was conducted in the reverse scan direction with starting frequency of 4000  $\text{cm}^{-1}$  and ending frequency of 650  $\text{cm}^{-1}$ . The obtained spectra with wave number ( $\text{cm}^{-1}$ ) as the

abscissa and transmittance (%) as the ordinate characterized by several peak minima are presented and discussed in the next chapter under the section 4.5.2, in detail.

### 3.4 MINERALOGICAL CHARACTERIZATION

The mineralogical characteristics of the selected virgin geomaterials as well as lime-treated soils were determined using analytical X-ray powder diffraction technique, *XRD* (PANalytical X'Pert Pro, The Netherlands), as depicted in Figure 3.5. The operating conditions were 45 kV and 30 mA, with Cu-K $\alpha$  radiation ( $\lambda=1.5418$  Å), and scanning was carried out over a range of  $2\theta$  values from 10 ° to 90 °, with 0.16° step size, and scan rate of 1.08 °/s. Prior to the *XRD*, the specimens were oven-dried at 40 °C for 24 hours and pulverized into fine powder using mortar and pestle. The dry powdered samples were placed on clean sample holders and mounted on the machine to obtain the X-ray patterns of various soils considered in this study. The mineralogical compositions of the selected soils were determined by following the above mentioned procedure and same is reported in section 4.2.5 and 4.6.1.



Figure 3.5 Photographic view of X-ray powder diffractometer used in this study



### 3.5 MICROSTRUCTURAL CHARACTERIZATION

In the present study, microstructural analysis was carried out using the Philips *FEI* Quanta 200 scanning electron microscope (*SEM*) as shown in Figure 3.6. The micrographs were obtained in a range of magnification from 25X to 5000X. Further, the energy dispersive spectrometry (*EDS*) facility coupled with *SEM* was availed for procuring the elemental composition of specified locations in the samples. Multiple locations were analysed and average of them was considered. Prior to the *SEM* analysis, the representative specimens of virgin as well as lime-treated soils were lyophilized using freeze-drying technique with the help of a lyophilizer (Lark Innovative, India), as illustrated in Figure 3.7. This process was done to assure the moisture free specimens without significantly altering its pore structure.



Figure 3.6 Photographic view of scanning electron microscope used in this study

Further, the lyophilized samples were mounted on aluminum stubs using an electrically conductive tape and cleaned using a hot air-blower in order to avoid possibility of column contamination by loose particles upon building of desired vacuum. Following, the specimen

surface was made electrically conductive by sputter coating with a thin layer of gold in vacuum at a current of 50 mA for 10 minutes (Sharma *et al.*, 2012). This minimizes the accumulation of electrons and consequent charge build-up on the specimen during analysis. The gold-coated specimen was placed on the sample stage inside the chamber, and the chamber was pumped to vacuum for collecting the micrographs and *EDS* spectra. All the microscopic data were obtained at a working condition of 30 kV accelerating voltage and 10 mm working distance under high vacuum condition. The obtained *SEM* micrographs, *EDS* results (energy in keV versus intensity in counts) were analysed using *EDAX* Genesis software and details are presented in the section 4.2.6 and 4.7.



Figure 3.7 Photographic view of lyophilizer used in this study



## **3.6 GEOTECHNICAL CHARACTERIZATION**

### **3.6.1 Compaction characteristics of geomaterials**

The compaction characteristics (viz., optimum moisture content, *OMC* and maximum dry unit weight, *MDD*) of virgin geomaterials were determined by conducting standard Proctor test as per ASTM D698. The required quantity of air-dried soil passing through 425  $\mu\text{m}$  sieve was homogeneously mixed with different moisture contents and compacted in the mould in three approximately equal layers. In order to ensure uniform moisture distribution, the wet soil samples were stored in air-tight containers for 24 hours maturation prior to compaction. The compaction characteristic curves were established by plotting the variation of dry unit weight with the moisture content from the results of compaction tests as shown in Figure A- 1 (refer Appendix). In order to minimize the amount of effort as well as the sample required, a miniature compaction test was conducted as developed by Sridharan and Sivapullaiah (2005) in further characterizations of soil-lime mixes and the obtained results are presented in the Table 4.4. The test is performed by compacting the soil into a cylindrical mould of 115  $\text{cm}^3$  volume, and the number of blows, hammer weight and drop height are 36, 1 kg and 160 mm, respectively. The obtained results are discussed in the section 4.4.1.

### **3.6.2 Unconfined compressive strength of geomaterials**

The unconfined compressive strength (*UCS*) of the virgin geomaterials and lime-treated soils were determined by conducting standard unconsolidated unconfined (*UU*) test (as depicted in Figure 3.8) by following the ASTM D2166 guidelines. The sample preparation involved same procedure as for miniature compaction test mentioned above. In this case, the cylindrical *UCS* specimens of 38 mm diameter by 76 mm height (length-to-diameter ratio of 2) were prepared in cylindrical split moulds by static compaction method. Afterwards, specimens were carefully extruded from the mould and immediately sealed air-tight in order to minimize the moisture loss owing to surface evaporation. For conducting the test, sample is placed in the triaxial cell with perspex discs on either ends of it. Further, the triaxial cell with sample was placed over the testing platform and attached to the load cell at the top, and the specimen was subjected to compressive stresses at a strain rate of 0.5 mm per minute. The

load and deformation values were recorded at different time intervals to obtain the stress-strain curves. The loading was continued until either the sample failed (load value decreased with increased strain) or total strain reached 20 %. It is important to mention that specimens of each sample were triplicated for strength evaluation, so as to ensure repeatability of the test data. By following the above mentioned methodology, the unconfined compressive strength characteristics of virgin as well as lime-treated geomaterials were assessed, and the details are reported in section 4.2.7 and 4.4.2.



Figure 3.8 Photographic view of unconfined compressive strength test conducted in this study

### 3.7 DETERMINATION OF OPTIMUM LIME CONTENT

Optimum lime content (*OLC*) can be defined as the total amount of lime required to provide sufficient quantity of free calcium to satisfy the initial charge deficiency of soil clay minerals (also denoted as initial consumption of lime, *ICL* or lime fixation point,  $L_m$ ), and still in excess for long-term pozzolanic reactions. In the present study, the *OLC* for the selected geomaterials was determined using the conventional and standard Eades and Grim *pH* test (Eades and Grim, 1966; ASTM D6276). According to this test, the *OLC* corresponds to the

lowest percentage of *HL* required to maintain the *pH* of a soil-lime-water solution equal to that of a saturated lime solution ( $\approx pH$  12.4). The experimental methodology adapted for determining the *OLC* is discussed in the following.

Initially, approximately 25 g of air-dried soil was mixed with different proportions of *HL* varying from 0 to 20 percent by dry weight of soil in polypropylene bottles, and was mixed with 100 ml deionised water at liquid to solid (*L/S*) of 4. The soil with zero percentage *HL* content was considered as the control for comparison purposes. Another bottle having 2 g of *HL* alone was also prepared in order to represent the saturated lime solution. Later, all bottles were continuously agitated in a mechanical shaker at 100 rpm to ensure thorough mixing. The temperature was consistently maintained to  $25 \pm 1$  °C throughout the experiment. The *pH* and *EC* values of the various soil-lime suspensions as well as the saturated lime solution were measured and recorded at the end of 1 hour using a water quality analyzer (Elico, PE138, India). From the obtained results, the graph was plotted between *HL* content along the abscissa versus *pH* along the ordinate. Further, the *OLC* values were determined as the amount of *HL* corresponding to *pH* 12.4, and are discussed in the section 4.3.1.

### **3.8 DETERMINATION OF BUFFERING CAPACITY**

The buffer capacity of soil plays a predominant role in determining its *OLC* for lime stabilization. It is defined as the amount of  $H^+$  or  $OH^-$  ions in the soil that must be neutralized in order to respectively raise or drop the soil solution *pH* by one unit (Kissel *et al.*, 2005; Weaver *et al.*, 2004). The buffer capacity of the virgin soils was determined as per the standard procedure of acid/base titration, by following the guidelines presented in literature (Young *et al.*, 1990 and 2009). Initially, different molal concentrations ranging from 0 to 0.2 of acid ( $HNO_3$ ) and base (NaOH) solutions were prepared and stored in volumetric flasks. Later, different concentrations of soil-acid mixtures were made by mixing 4 g soil with 40 ml acid solution, corresponding to liquid to solids ratio, *L/S*, of 10 in polypropylene bottles. These solutions were placed in a mechanical shaker and continuously agitated for an equilibration time of 24 hours. The *pH* of the soil suspension was recorded at the end of equilibration time to evaluate buffer capacity of soils by measuring the change in *pH* of the soil due to addition of range of acid molal concentrations to it. Similar efforts were also made

to evaluate the soil buffering capacity by treating with different molal concentration of base solutions. Based on the observed change in the  $pH$  of the soil, the titration curves (i.e.,  $pH$  versus acid/base concentration in centimol  $H^+/OH \cdot kg^{-1}$ ) for various soils were developed and same is presented in section 4.3.2. Further, the  $pH$  and electrical conductivity ( $EC$ ) of the virgin geomaterials were measured by employing water quality analyzer (Elico, model PE138, India).

### 3.9 PROPERTY EVALUATION OF LIME-TREATED SOILS

In order to accomplish the secondary goal of assessing the significant influence of lime content on the macro-level geotechnical properties (compaction characteristics and  $UCS$ ) of the selected geomaterials, conventional laboratory tests were also conducted on soil specimens prepared with different lime proportions varying from 0-20 % by dry weight of soil. Further, advanced chemical, mineralogical and microstructural characterization of these samples were carried out using the analytical tools such as  $TGA-DTA$  and  $FTIR$ ,  $XRD$  and  $EDS$ ,  $SEM$ , respectively. Using the obtained results, attempts were made to comprehend the underlying micro-level mechanisms which have caused the macro-level changes in terms of the qualitative and semi-quantitative estimation of new reaction products as well as alterations of virgin clay minerals present in the soil.

Since the study interested in evaluating the impact of placement moisture content on the mechanical behaviour of lime-treated soils,  $UCS$  tests were conducted on soils treated with lime corresponding to  $OLC$  and compacted over a range of moisture contents. The three moisture contents considered were: (a)  $OMC$ ; (b) 2 % above  $OMC$  (i.e., wet side of the optimum, termed as  $WMC$ ); and (c) 2 % below  $OMC$  (i.e., dry side of the optimum, termed as  $DMC$ ) for each soil- $OLC$  mixture. In order to assess the influence of curing period and temperature on properties of lime-treated soils, the fabricated specimens were cured up to 28-days in temperature and relative humidity ( $RH$ ) controlled humidity chamber (Rays Scientific Instruments, HC 02, India), as shown in Figure 3.9. The two different combinations of curing conditions were chosen being  $25 \pm 1$  °C &  $60 \pm 5$  %  $RH$  and  $40 \pm 1$  °C &  $75 \pm 5$  %  $RH$ , respectively



Figure 3.9 Photographic view of humidity chambers used in this study

### 3.9.1 Sample preparation for lime-treated soils

During the process of sample preparation for evaluating the compaction characteristics of lime-treated specimens, required quantity of air-dried soil passing through 425  $\mu\text{m}$  sieve was homogeneously mixed with different lime contents varying from 0-20 % by dry weight of soil and mixed with different moisture contents. Following, the miniature proctor compaction test was performed and obtained results are presented in section 4.4.1. The test was repeated for each soil-lime mix under similar testing conditions. Precautionary measures were taken to produce a homogenous soil-lime mixture with a desired initial density for all specimens. The method of gradual moistening was followed for the preparation of all the soil-lime mixtures to achieve the best performance (Mooney and Toohey, 2010). A mechanical blender was employed for mixing of the soil-lime mixtures; otherwise, some amount of lime may be trapped in the neighbourhood of large clods of soil; and therefore, cannot disseminate properly within the matrix (Bozbey and Garaisayev, 2010).

Later, sample preparation for the study pertaining to influence of lime content on the *UCS* of the soil was carried out by uniformly mixing air-dried soil with different lime contents at their respective *OMC* value, as obtained from the compaction results. In order to avoid any

soil-lime reactions prior to the compaction, the dry soil was initially mixed with moisture content up to its plastic limit, and these samples were matured in air-tight containers for 24 hours. Further, the matured soil was mixed with pre-determined lime content and additional water to attain the desired moisture content. The lime mixed samples were prepared by adopting the procedure mentioned in section 3.6.2. After the sample preparation, the proper sealing of specimens was ensured as it disables carbon dioxide ingress; and thus, diminishes carbonation process during curing which is detrimental to strength gain as it causes structural disintegration of stabilized soil-lime matrix (Yunus *et al.*, 2012). Later on, specimens were cured for up to 28-days in the temperature and humidity controlled chamber to ensure more uniform soil-lime interactions and thus producing more consistent results. Following, UCS tests were conducted on cured specimens and the obtained results are presented in section 4.4.2. Based on the observations made from the *UCS* results obtained for different soil-lime mixtures, the respective *OLC* of selected soils was determined according to guidelines provided in the literature, which is discussed in further sections. In addition to these tests, further evaluation of the effect of placement moisture content on *UCS* of lime-treated soil was carried out on soils blended with lime content corresponding to its *OLC* value at various moisture contents of *DMC*, *OMC* and *WMC*, respectively obtained from the compaction and *UCS* results. These samples were fabricated and cured for a period ranging from 0 to 240 days at curing conditions as mentioned above, for evaluating the influence of curing conditions as well. At reaching the supposed curing period, the specimens were retrieved and tested for *UCS*. The obtained results are presented in section 4.4.3.

Subsequently, the selected fragments of *UCS* specimens were also tested for evaluating the microstructural, chemical and mineralogical characteristics by employing advanced analytical tools such as *SEM*, *TGA-DTA* and *FTIR*, *XRD* and *EDS* by following the procedure as mentioned earlier. The respective results are discussed in detail in the further sections.

## 4.1 GENERAL

This chapter presents the results obtained using experimental methodologies described in the previous chapter. Selected materials were characterized for physical, chemical, mineralogical, microstructural and geotechnical properties.

## 4.2 PRELIMINARY CHARACTERIZATION OF GEOMATERIALS

### 4.2.1 Specific gravity, gradational characteristics and consistency limits of geomaterials

As discussed in the section 3.2.1, the specific gravity, grain size distribution and Atterberg limits were determined as per the standard procedures and presented in the Table 4.1.

Table 4.1 Physical characteristics of geomaterials

Properties	Value		
	<i>WC</i>	<i>BT</i>	<i>SC</i>
Specific gravity, <i>G</i>	2.65	2.78	2.69
Hygroscopic moisture content (%)	4.5	11.7	4.9
Specific surface area (m <sup>2</sup> /g)	45	360	135
Cation exchange capacity (meq./100g)	21	105	90
<b>Consistency limits (percent by weight, %)</b>			
Liquid limit, <i>w<sub>L</sub></i>	52	350	42
Plastic limit, <i>w<sub>P</sub></i>	27	27	15
Plasticity index, <i>PI</i>	25	323	26
<b>Particle Size Distribution (percent by weight, %)</b>			
Gravel size (> 4.75 mm)	0	0	0
Sand size (> 75 μm and ≤ 4.75 mm)	0	0.9	43.3
Silt size (> 2 μm and ≤ 75 μm)	15	31	12.7
Clay size (≤ 2 μm)	85	69	44
Unified soil classification system ( <i>USCS</i> )	<i>CI-CH</i>	<i>CH</i>	<i>CI</i>

The specific gravity of the selected geomaterials is in the range of 2.6-2.8, which reflects that these geomaterials are clays or silty clays. The liquid limit of *BT* is much higher than the *WC* and *SC*; this might be due to the presence of clay mineral montmorillonite. The clay fraction is found to be more in *WC* compared to that of *BT* and *SC*. Based on the obtained

results the *WC*, *BT*, *SC* are classified as medium to high compressible, highly compressible and medium compressible clays as per *USCS*.

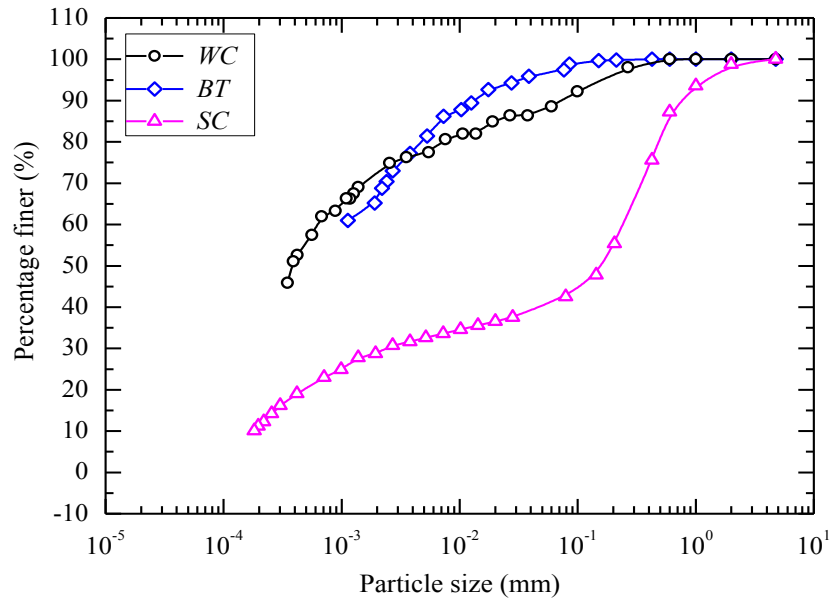


Figure 4.1 Particle size distribution characteristics of the selected geomaterials

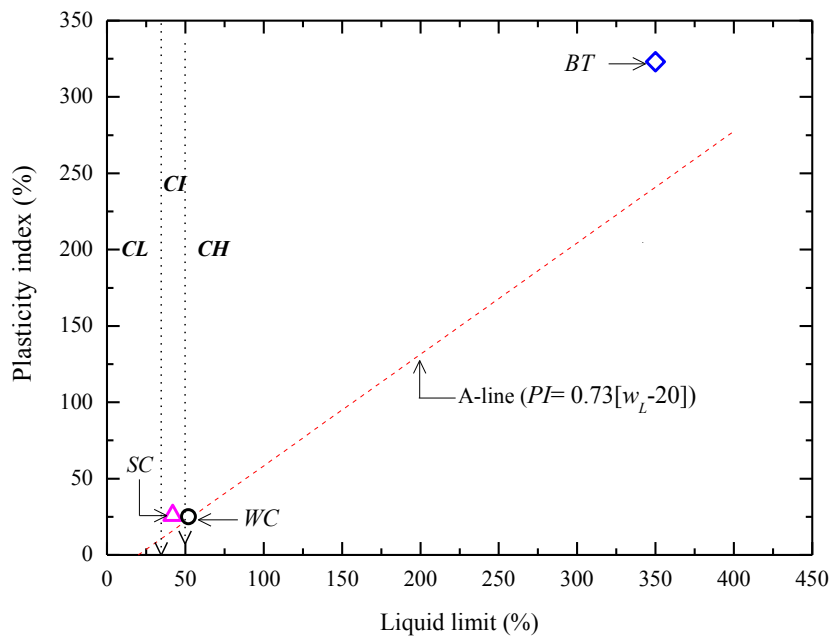


Figure 4.2 Plasticity chart



#### 4.2.2 Specific surface area

As discussed in the section 3.2.2, the specific surface area (*SSA*) of the selected geomaterials was determined using ethylene glycol monoethyl ether (*EGME*) method. The *SSA* of the soil specimens were determined using the following relationship (equation 4.1) proposed by Cerato and Lutenegger (2002). The weight of *EGME* required to form a monomolecular layer on a square meter of surface is 0.000286 g/m<sup>2</sup>. The variation of *EGME* that sorbed on the different soils with time was obtained and the same is presented in the form of Figure 4.3. From the experimental results, the *SSA* values obtained for various soil samples are provided in the Table 4.1.

$$SSA \text{ (m}^2\text{/g)} = \frac{W_c}{0.000286 \times W_s} \quad (4.1)$$

where

$W_c$  = weight of *EGME* sorbed by the material corresponding to monolayer formation (g)

$W_s$  = air-dried weight of the soil considered (g)

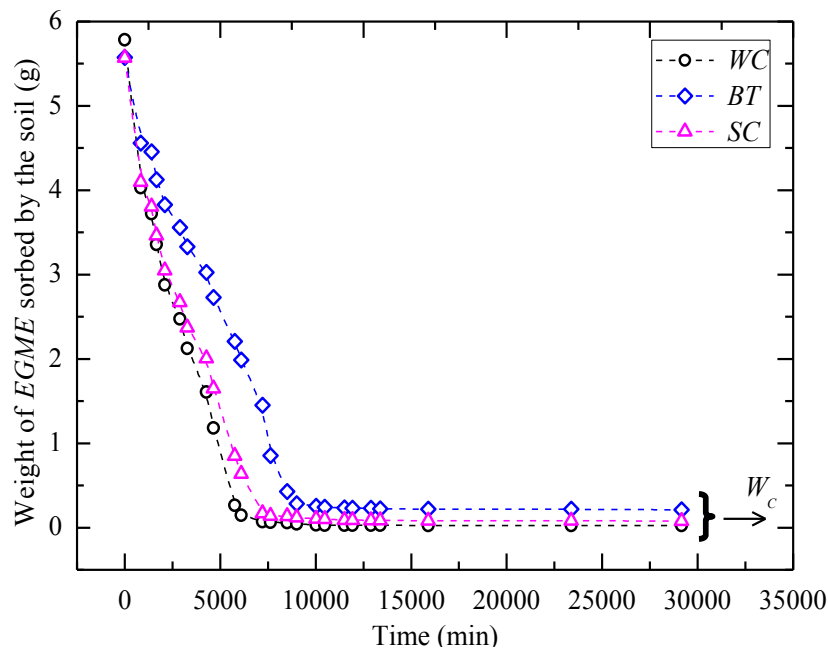


Figure 4.3 Variation of ethylene glycol monoethyl ether weight with time

### 4.2.3 Cation exchange capacity

The cation exchange capacity of geomaterials was determined as per the methodology described in the section 3.3.1, by following the guidelines presented in the codal provisions (IS 2720; ASTM D7503). The *CEC* was calculated as per the following relationship and the obtained results are presented in Table 4.1.

$$CEC \text{ (meq. / 100g)} = \frac{\text{Concentration of } Ca^{2+} (\mu\text{g/ml}) \times 100 \times \text{volume of extract (ml)}}{\text{Equivalent molecular weight of the } Ca^{2+} \times 1000 \times \text{weight of the sample (g)}} \quad (4.2)$$

The maximum *CEC* values were obtained for *BT* followed by *SC*, whereas *WC* is found to have minimum *CEC* Values. This can be attributed to the combined influence of characteristic *SSA* and mineralogical nature of these materials.

### 4.2.4 Elemental composition of geomaterials

As discussed in section 3.3.2, the elemental composition of virgin geomaterials and hydrated lime was determined from the X-ray fluorescence (*XRF*) studies. The obtained elemental composition of the selected geomaterials in their oxide form is presented in the Table 4.2. The predominant elements present in the selected geomaterials are in aluminum (*Al*), silicon (*Si*), magnesium (*Mg*), potassium (*K*), sodium (*Na*), titanium (*Ti*), iron (*Fe*), and calcium (*Ca*). The *HL* is found to have major concentration of calcium (*Ca*), with traces of other elements such as *Si*, *Mn*, *Mg* & *Sr*.

### 4.2.5 Mineralogical properties of geomaterials

As discussed in section 3.4, the mineralogical characteristics of the selected untreated geomaterials were determined using analytical X-ray powder diffraction technique. From the obtained diffractograms as depicted in Figure 4.4, the major minerals were identified using ICDD data base and the same is presented in Table 4.3. The mineralogical composition of clay fraction (<2 $\mu\text{m}$ ) of selected geomaterials was also determined, and the same is presented in the Figure 4.5. As reported in Figure 4.4, the X-ray diffractogram of *WC* indicated the presence of significant amount of non-swelling mineral, kaolin (kaolinite) as well as the non-

clay mineral such as quartz. Similarly, in the case of *BT*, kaolinite, quartz and high-swelling minerals such as montmorillonite were identified. The X-ray diffractogram of *SC* consisted mostly of quartz, with traces of colusite, a tin-bearing mineral belonging to the sphalerite group.

Table 4.2 Elemental compositions of selected geomaterials

Oxide constituents (%)	Sample type			
	<i>WC</i>	<i>BT</i>	<i>SC</i>	<i>HL</i>
<b>SiO<sub>2</sub></b>	60.39	59.49	62.26	1.65
<b>Al<sub>2</sub>O<sub>3</sub></b>	32.99	17.34	14.76	0.06
<b>K<sub>2</sub>O</b>	0.79	0.93	2.05	---
<b>CaO</b>	1.52	2.49	1.28	96.1
<b>TiO<sub>2</sub></b>	1.89	3.69	0.97	0.01
<b>Fe<sub>2</sub>O<sub>3</sub></b>	2.03	14.20	12.28	0.07
<b>Na<sub>2</sub>O</b>	---	---	5.46	---
<b>MgO</b>	---	---	0.21	0.46
<b>P<sub>2</sub>O<sub>5</sub></b>	---	0.32	0.11	0.20
<b>MnO<sub>2</sub></b>	0.01	0.19	0.11	1.06
<b>SrO</b>	0.01	0.02	0.02	0.22
<b>CuO</b>	0.01	0.03	0.02	---

--- Below detection limits

Table 4.3 Major minerals present in the selected geomaterials

Geomaterial	Minerals
<i>WC</i>	Kaolinite, Quartz
<i>BT</i>	Quartz, Montmorillonite, Kaolinite
<i>SC</i>	Quartz, Colusite

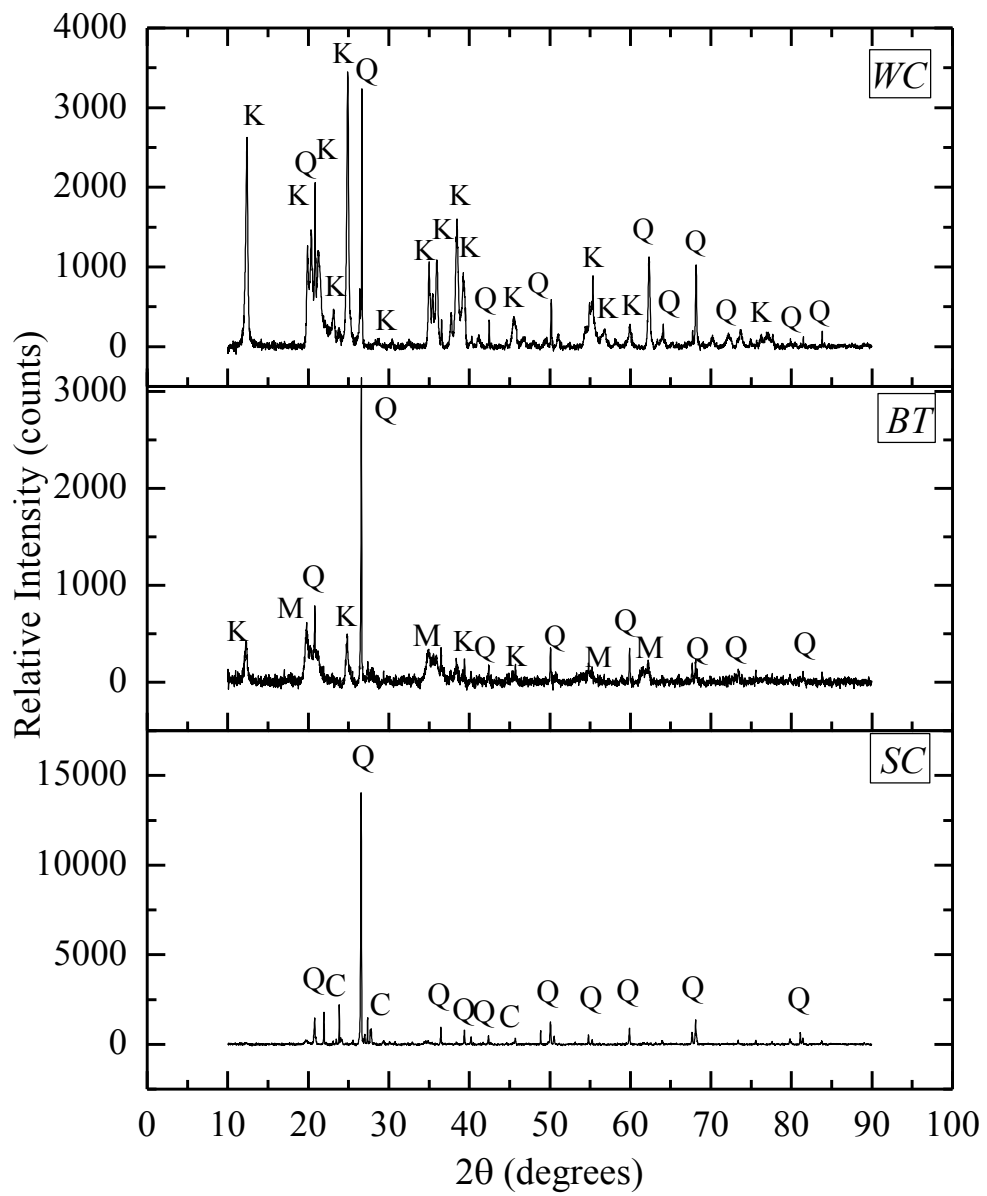


Figure 4.4 X-ray diffractograms of selected geosamples

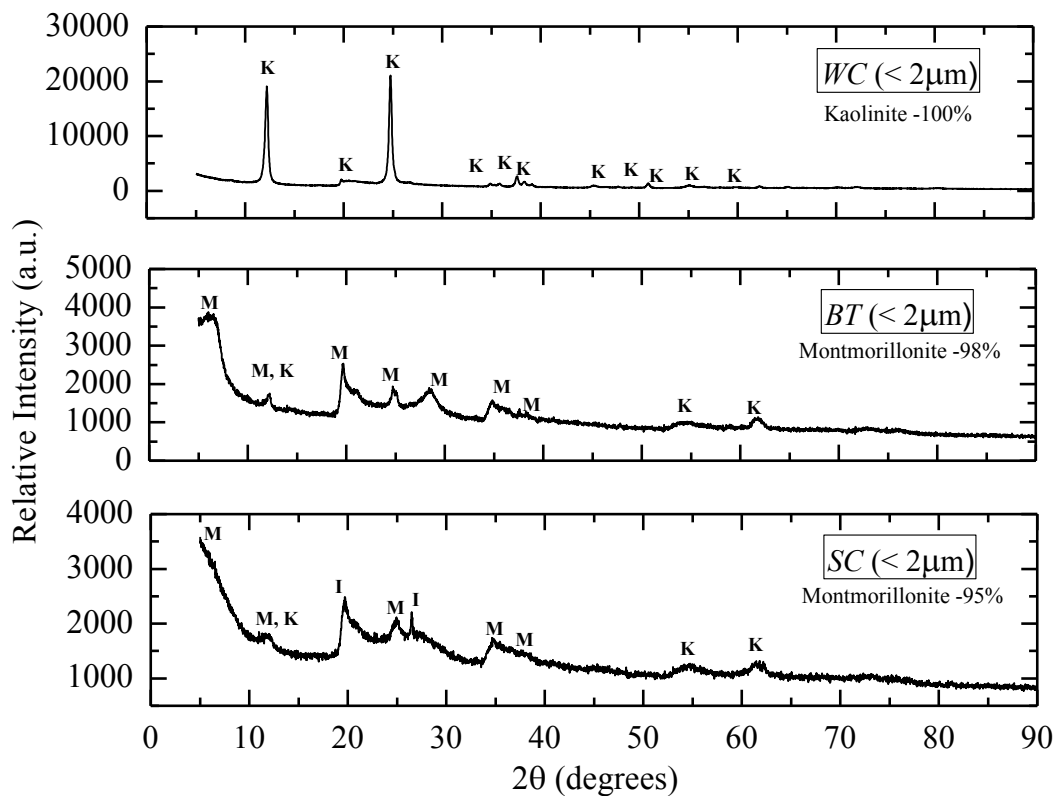


Figure 4.5 X-ray diffractograms of clay-size fraction of selected geomaterials

#### 4.2.6 Microstructural properties

The microstructural analysis of the selected geomaterials was conducted as per the methodology presented in section 3.5. The obtained *SEM* micrographs along with *EDS* spectra of the geomaterials corresponding to *WC*, *BT* and *SC* respectively are presented in Figure 4.6. The *SC* has more percentage of silt- and sand-size particles than the clay-size particles, which is specifically observed in the micrograph. The *EDS* results also showed a significant amount of silica (*Si* and *O*) representing the sand-size and silt-size particles present in the *SC* soil and the background indicates the amorphous nature of the soil. Moreover, the *EDS* results of *WC* and *BT* are in agreement with the *XRD* results reported in the previous section. These soil types are composed of mostly silica (*Si*) and alumina (*Al*), with traces of *Na*, *K*, and *Ca*. The admixture, *HL* is observed to be an amorphous powder consisting of primarily calcium (*Ca*).

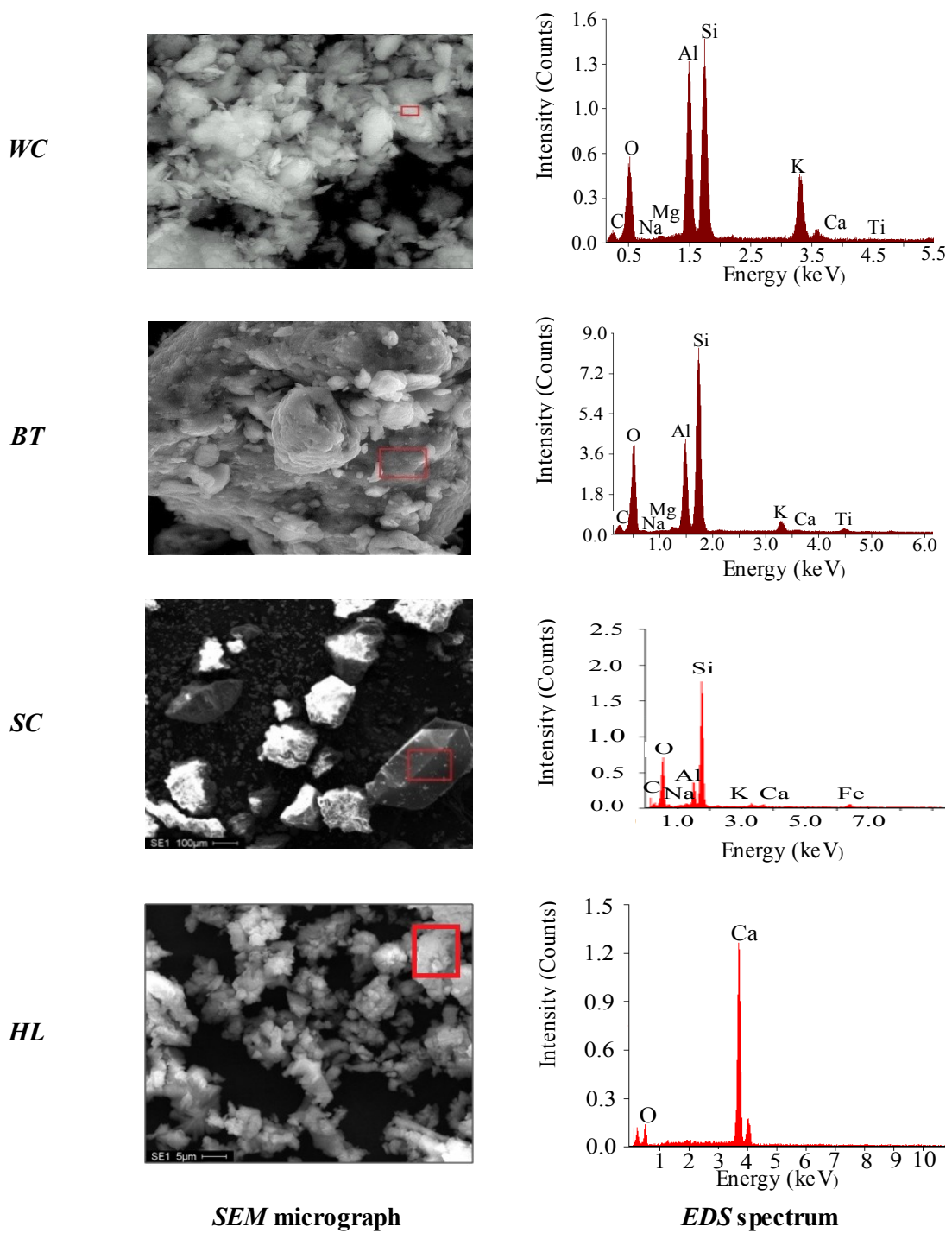


Figure 4.6 Scanning electron microscope & energy dispersive spectroscopy of selected geomaterials

#### 4.2.7 Geotechnical properties

##### *Compaction characteristics of geomaterials*

As discussed in section 3.6.1, the compaction characteristics (viz., optimum moisture content, *OMC* and maximum dry unit weight, *MDD*) of virgin geomaterials were determined by conducting standard Proctor test as per ASTM D698. The obtained results are presented in Figure A- 1 and Table 4.4. The sodium bentonite is found to have maximum *OMC* followed by white clay and sandy clay whereas it is vice versa in case of *MDD*. This can be attributed to the presence of swelling mineral montmorillonite in *BT* as well as the surface charge properties of geomaterials.

Table 4.4 Compaction characteristics of geomaterials

Compaction Characteristics	Geomaterial		
	<i>WC</i>	<i>BT</i>	<i>SC</i>
Maximum dry unit weight, <i>MDD</i> (kN/m <sup>3</sup> )	15.9 (16.1)	12.8 (12.7)	16.9 (18.3)
Optimum moisture content, <i>OMC</i> (%)	20.5 (18.2)	29.3 (26.5)	16.8 (14.2)

Note: Values reported in italics within the paranthesis represent the miniature compaction characteristics.

##### *Unconfined compressive strength of geomaterials*

As discussed in section 3.6.2, the unconfined compressive strength (*UCS*) of the virgin geomaterials was determined by conducting standard unconsolidated unconfined test. The obtained results are presented in the Table 4.5. The white clay exhibited higher strength followed by sodium bentonite and sandy clay. This can attributed to the clay fractions present in the geomaterials.

Table 4.5 Unconfined compressive strength of geomaterials

	Geomaterial		
	<i>WC</i>	<i>BT</i>	<i>SC</i>
Zero day <i>UCS</i> (MPa)	0.425	0.288	0.115

### 4.3 INFLUENCE OF SOIL PH ON THE PERFORMANCE OF LIME-TREATED SOILS

As highlighted in section 1.3, the primary aim was to evaluate the influence of virgin soil *pH* and buffer capacity upon the determination of *OLC* required for mobilizing the pozzolanic soil-lime reactions to the great extent and realizing the desired degree of soil stabilization. The study also attempted to understand the inherent limitations of conventional Eades and Grim *pH* test used for determination of *OLC*. Studies were also conducted to determine the chief role played by the pore fluid chemistry in terms of the type of ions present in the pore solution in governing the geological properties of virgin soil (viz., *pH* and mineralogy), which in turn influences the rate of pozzolanic reactions during lime stabilization and its efficacy.

For the sake of brevity, this study was conducted on soils with diverse physical and mineralogical properties (viz., *WC*, *BT* and *SC*). The *OLC* tests were carried out following the methodology described in section 3.7. In view of assessing the limitations of conventional Eades and Grim *pH* test, the *pH* and *EC* measurements were continued beyond the proposed duration of 1 hour, up to 24 hours and at an elevated temperature of  $40\pm 1$  °C, in order to evaluate the variations with temperature. Supplementary blank solutions with different lime concentrations varying from 0-20 % *HL* were also analyzed in this study so as to estimate the lime saturation point as well as to compare the relative effects in different soils. Furthermore, conventional Eades and Grim *pH* tests were carried out on soils with modified initial *pH* value of 2, 7 and 12, in order to simulate the acidic, neutral and alkaline geological conditions in the field, respectively. The *pH* modified soil samples were prepared by equilibrating the virgin soil to *pH* 2, *pH* 7 and *pH* 12 by titration. For this purpose, air-dried soil fraction finer than 425  $\mu\text{m}$  was mixed with deionised water to form a slurry and was allowed for 24 hours equilibration. During the preparation of soil slurry as well as throughout the experimentation the liquid to solid ratio of 4 and room temperature of  $25\pm 1$  °C was maintained in order to avoid the effect of *L/S* ratio and temperature on the soil *pH*. Prior to the equilibration of the soil with different *pH* values acidic solution, i.e., 1 molar solution of nitric acid ( $\text{HNO}_3$ ) and alkaline solution, i.e., 1 molar solution of sodium hydroxide ( $\text{NaOH}$ ) were prepared and titrated with the soil slurry to prepare soil samples having different *pH* values. Every 24 hours



of equilibration of soil slurry, the soil  $pH$  and electrical conductivity,  $EC$  (mS/cm) was measured. The titration of the soil slurry, either with 1M acidic or alkaline solution was continued until the desired  $pH$  value of the modified soil was achieved.

In the case of  $WC$ , the  $pH$  of virgin soil was recorded as 5.5; hence, the acidic solution was used for titration to obtain  $pH$  2 whereas alkaline solution was used to increase soil  $pH$  to 7 and 12. Similarly, for  $BT$  as well as  $SC$  the virgin soil  $pH$  was noted as 10.2 and 8.6 respectively; therefore, the acidic solution was used to lower  $pH$  to 7 and 2; and basic solution was used for raising  $pH$  to 12. Once the  $pH$  of soil slurry reached the desired value, the surplus solution was decanted, and the slurry was oven-dried and pulverized to prepare finely powdered soil specimens representing the  $pH$  2,  $pH$  7 and  $pH$  12. Following, the primed soil samples were used for evaluating the  $OLC$ , as discussed in the following.

#### 4.3.1 Optimum lime content of geomaterials

The  $pH$  of a virgin, as well as modified soil gets enhanced with the addition of lime, owing to the rise in the concentration of  $OH$  ions in the soil-lime suspension (Chorom and Rengasamy, 1995). The  $OLC$  of the virgin soil as per the Eades and Grim method was obtained as presented in the Table 4.6, and is found be in the following order  $OLC_{BT} < OLC_{WC} < OLC_{SC}$  (as depicted in Figure 4.7). However, this order has changed to  $OLC_{WC} < OLC_{BT} < OLC_{SC}$  when the optimal lime content was assessed using 24- hours of equilibration (Figure 4.7). The variation between  $OLC$  values corresponding to 1 hour and 24 hours equilibration time indicate that  $pH$  of the soil suspension is changing dynamically even after the specified equilibrium time of 1 hour suggested by ASTM D6276. The results indicate that  $OLC$  of  $WC$  corresponds to 1 hour and 24 hours equilibration time remains practically constant around 1 percent, whereas for  $BT$ ,  $OLC$  has increased by almost 0.6 percent from 1 hour to 24 hours equilibration time. Similarly, for  $SC$  there is an increase of  $OLC$  from 1.33 percent to 2.5 percent. The variations in  $pH$  of the soil suspension with time beyond 1 hour equilibration time might be attributed to the progressive interaction of clay minerals with the ions present in suspension and subsequent cation exchange. The cation exchange and ensuing change in soil  $pH$  value will continue unless and until all the available electro negativity on clay surface have been neutralized (Chorom and Rengasamy, 1995).

Table 4.6 Optimum lime content values of selected geomaterials

Geomaterial	OLC after 1 hour (%)	OLC after 24 hours (%)
<i>WC</i>	0.96	1.00
<i>BT</i>	0.89	1.50
<i>SC</i>	1.33	2.50

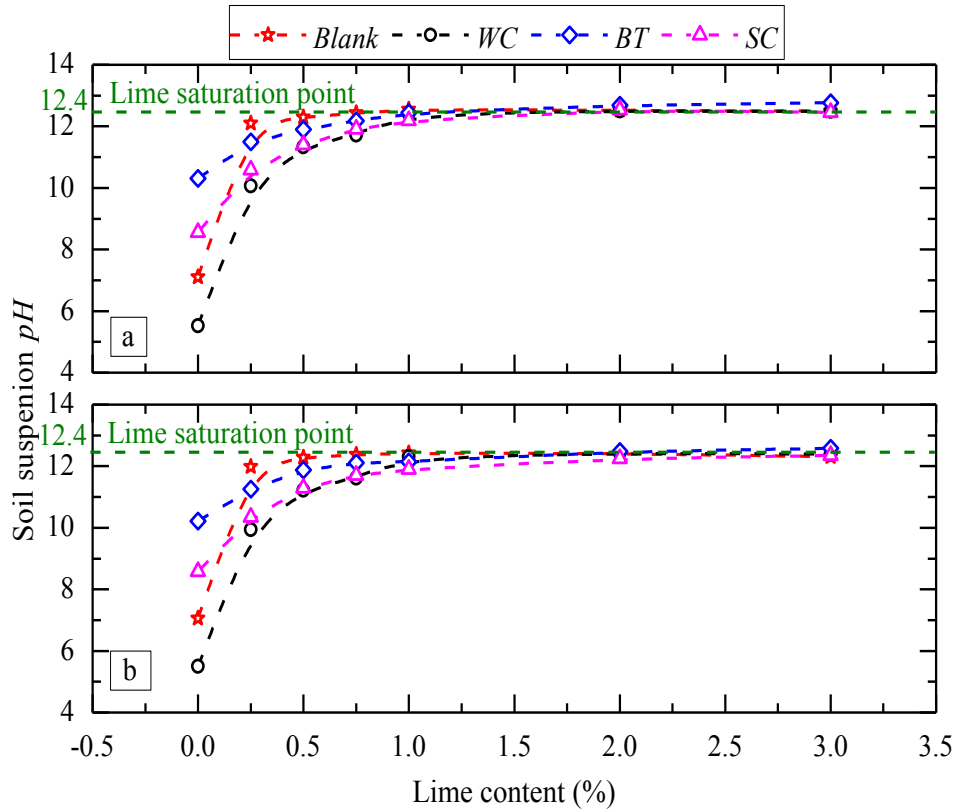


Figure 4.7 Variation of  $pH$  of the soil suspension with lime content for various geomaterials corresponding to (a) 1-hour; (b) 24 hours equilibration

From the results obtained, it can be opined that *WC* contain low reactivity minerals with low cation exchange capacity attains equilibrium  $pH$  of 12.4 within a short interaction time of 1 hour whereas highly reactive type clay minerals present in *BT* and *SC* continue to react for longer period and hence, the *OLC* value corresponding to 24 hours interaction time is higher than that of 1 hour interaction time. The specifically increasing trend of *OLC* value with equilibration time is possibly due to decrease in  $pH$  over long-term soil-lime reactions. Based on the above discussions it can be realized that the equilibration time of 1 hour in the conventional  $pH$  tests for *OLC* determination (Eades and Grim 1996, ASTM D6276) does not stand valid for wide variety of soils, especially, soils containing highly reactive clay minerals

such as montmorillonite and illite, highly reactive clay minerals demands more than 24 hours of equilibration time for attaining equilibrium  $pH$  of 12.4 as well as enough calcium ion concentration. While shorter periods of interaction such as 1-2 hours may be sufficient for low reactive soil types such as white clay. Based on the observations reported, it can be noted that both Eades and Grim  $pH$  test and ASTM D6276 procedure failed to account for the reactive nature of clay minerals present in the soil while determining  $OLC$  values based on 1 hour equilibration time. Further, it can be concluded that the above-mentioned methodologies under predict optimum lime content values in the case of highly reactive clays.

#### 4.3.2 Buffering capacity of geomaterials

The buffering capacity of the soil plays a predominant role in determining its  $OLC$  value. With this in view, the buffer capacity of a virgin as well as  $pH$  modified geomaterials was determined by following the methodology discussed in section 3.8 and the obtained results are shown in Figure 4.8, Figure 4.9 and presented in the form of Table 4.7.

$WC$  suspension has a lower initial  $pH$  of 5.5 than  $BT$  ( $pH$  10.2) and  $SC$  suspensions ( $pH$  8.6). As shown in Figure 4.8, the titration curve of  $WC$  with  $HNO_3$  indicates that there is an immediate drop in  $pH$  value to 1.5 when the acid input level reaches 0.025 moles/litre. Beyond this point, there is negligible change in the  $pH$  of soil suspension. Further, the similarity in shapes of titration curves for  $WC$  and that of blank indicates that the contribution of soil in  $WC$  suspension in resisting the  $pH$  change upon titration with the acidic solution is insignificant (Yong *et al*, 1990). In the titration curve of  $BT$ , the suspension  $pH$  drops sharply from about  $pH$  10.2 to  $pH$  2 when the acid concentration reaches 0.1 moles/litre. Beyond this point, little change in soil suspension  $pH$  is observed with a further input of acidic solution. The  $SC$  soil shows a moderate resistance to change in  $pH$  value until the concentration of acidic solution reaches 0.075 moles/litre; beyond, the soil solution  $pH$  starts to drop gradually from 1.7 to 0.6.

The buffer capacity for each of the geomaterials was deciphered from the negative slope of the respective titration curve in the  $pH$  range 2 to 8. Over the range of  $pH$  values,  $BT$  has slightly higher buffer capacity (13.4 centimol  $H^+ \cdot kg^{-1}$  soil) than  $SC$  (10.6 centimol  $H^+ \cdot kg^{-1}$

soil). However, kaolinitic soil *WC* exhibited insignificant buffer capacity in the *pH* range of 2 to 8 as the *pH* variation with the mild acid addition is similar to that of the blank, to all intents and purposes.

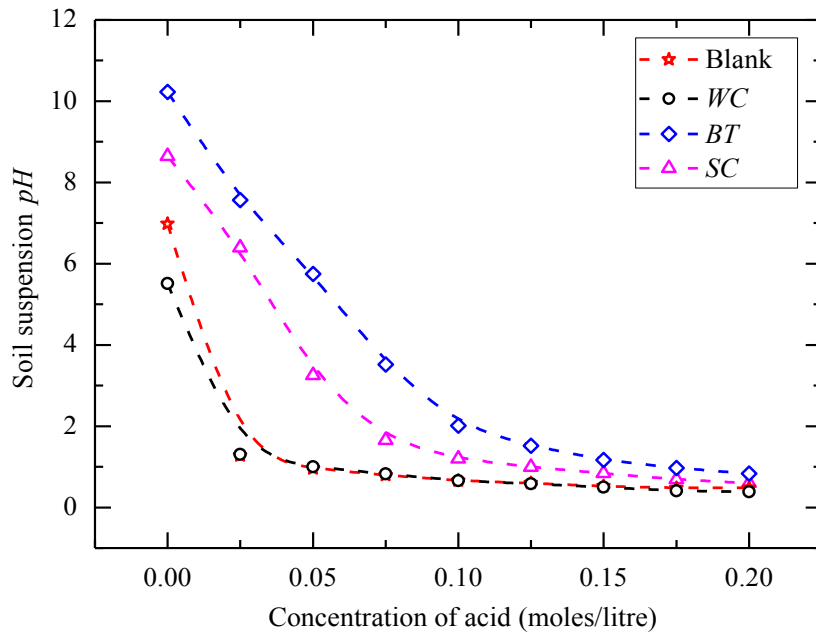


Figure 4.8 Variation of *pH* of the soil suspension with acid titration for determining buffer capacity of virgin geomaterials

The titration curves of *WC*, *BT* and *SC* (as shown in Figure 4.9) upon addition of alkaline solution displayed similar trends as the blank solution. The *pH* of all suspensions became more or less identical beyond a certain concentration of 0.1 moles/litre. However, the rate of change of *pH* of various geomaterials with respect to alkali concentration was observed to be different for different geomaterials for initial concentrations up to 0.01 moles/litre. From the respective alkaline titration curves, the buffer capacity for *WC*, *BT* and *SC* was determined and presented in the Table 4.7. Nevertheless, these values cannot be considered as true buffer capacity of geomaterials since none of them exhibits resistance to change in alkaline suspension *pH*.

Taken as a whole, it can be deduced that *WC*, *BT* and *SC* have exhibited very little resistance to *pH* value changes on acidic/alkaline solution input at the initial stages. This is due to the fact that  $H^+$  ions supplied during the initial stages of titration might not have

participated in cation exchange reactions, and hence resulted in a drastic change in  $pH$  of the soil suspension upon the addition of trace level concentrations of acidic solution (Federer and Hornbeck, 1985). On the contrary, during the latter part of the titration, soils  $BT$  and  $SC$  have exhibited a noticeable resistance towards the  $pH$  change upon titration with the moderate concentration of acid solutions. Incidentally, this observation can be substantiated in terms of the magnitude of soil cation exchange capacity. Since the cation exchange capacity of kaolinitic soil  $WC$  is very low, and hence, the resistance against  $pH$  change offered by this material is practically same across the wide range of concentrations of the acidic solution. In the case of alkaline solution titration, by the addition of low concentrations of alkali i.e.,  $NaOH$ , immediate adsorption of monovalent  $Na^+$  cations onto the negatively charged clay platelets occur via weaker vander Waals forces (Van Olphen, 1963; Mitchell and Soga, 2005). Therefore, the increasing  $OH^-$  concentration in the solution causes a sudden rise in its  $pH$  value.

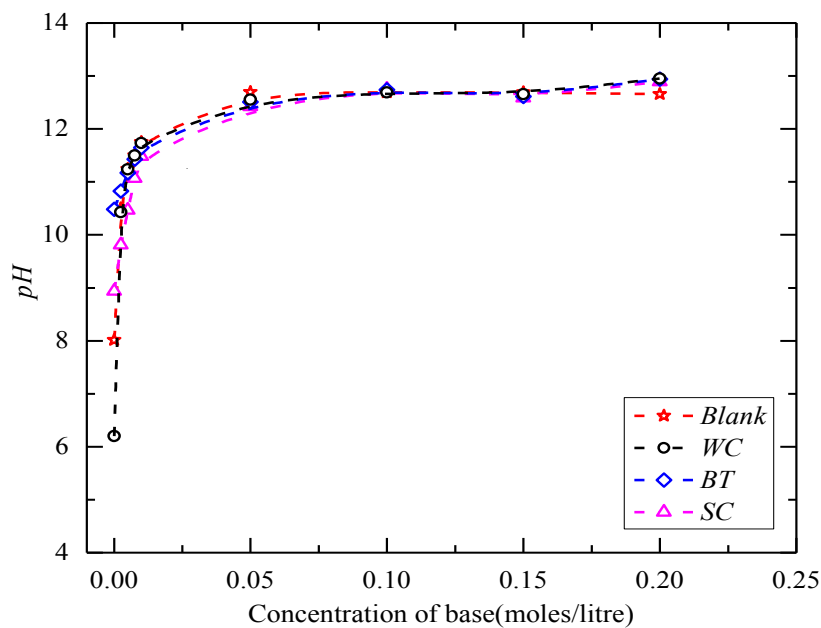


Figure 4.9 Variation of  $pH$  of the soil suspension with alkali titration concentration for determining buffer capacity of virgin geomaterials

Table 4.7 Buffer capacity values of selected geomaterials

Geomaterial	Buffer capacity based on acid titration (centimol $H^+$ . $kg^{-1}$ soil)	Buffer capacity based on base titration (centimol $OH^-$ . $kg^{-1}$ soil)
<i>WC</i>	5.9	1.8
<i>BT</i>	13.4	8.6
<i>SC</i>	10.6	3.9

Further, as the alkaline solution concentration increases the resistance to  $pH$  change increases and the  $pH$  remains more or less constant. This is attributed to preferential cation exchange reactions caused by replacement of higher valence cations having low concentration on clay surface by the very high concentration monovalent  $Na^+$  ions present in the suspension (Chorom and Rengasamy, 1995). In contrast to *BT* and *SC*, *WC* apparently does not seem to have any substantial involvement in suspension  $pH$  variation. This phenomenon indicates that *WC* has negligible cation exchange capacity and reactivity towards electrolytes. Moreover, the buffer capacity results emphasize the trend of *OLC* values obtained for different geomaterials. For same initial  $pH$ , the soil with higher buffer capacity will require more amount of lime in order to attain a solution  $pH$  12.4, and hence, will be characterized by higher *OLC*.

#### 4.3.3 Effect of clay mineralogy on optimum lime content

The philosophy of Eades and Grim  $pH$  test is that the lime content corresponding to *OLC* should rise the soil suspension  $pH$  to 12.4. From the studies conducted by the previous researchers, it has been noticed that the virgin soil  $pH$  also plays a significant role in determining *OLC*. For example, when lime is added to different buffer capacity soils, the one having a higher initial  $pH$  will exhibit a lower *OLC* and vice versa. In other words, if two soils have similar initial  $pH$ , *OLC* of these materials should be identical, unless and otherwise the soil mineralogy and buffering capacity of these materials are different. In order to evaluate these phenomena the conventional *OLC* determination tests were also conducted on  $pH$  modified geomaterials, i.e., virgin soil  $pH$  value has been modified to 2, 7, and 12. From the critical synthesis of the results obtained for virgin as well as  $pH$  modified soils, it is evident that the modified soils which were adjusted towards the acidic side exhibited higher *OLC* value when compared to those soils altered towards the basic  $pH$  conditions (as depicted in Figure 4.10).

As  $pH$  of the soil decreases from its original value, the  $OLC$  increases and vice versa; probably due to the fact that for a lower  $pH$  value of soil the amount of lime required for a rise in  $pH$  to 12.4 is higher, for the given soil mineralogy. Moreover, the variation in  $OLC$  followed the same order of  $OLC_{BT} < OLC_{SC} < OLC_{WC}$  for a given  $pH$  value, thereby pronouncing the effect of higher cation exchange capacity of  $BT$  followed by  $SC$  and  $WC$ . This is different from the case of virgin soils where  $SC$  showed higher  $OLC$  than  $BT$ , which emphatically proves the inevitable consequence of its original  $pH$  of 8.6 which is much lower than that of  $BT$  ( $pH$  of 10.2)

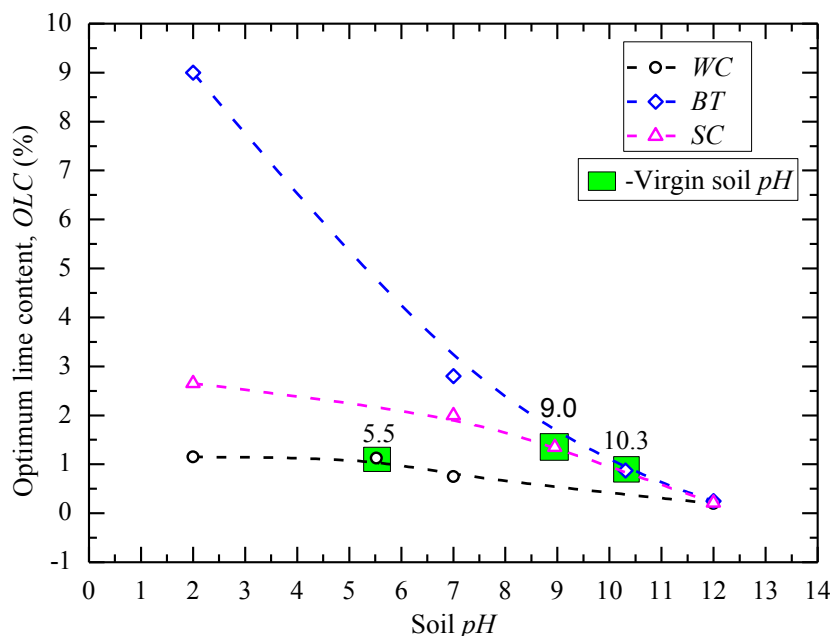


Figure 4.10 Variation of optimum lime content with soil  $pH$  for different soils

#### 4.3.4 Effect of cations on the electro kinetic properties of geomaterials

In order to validate the effect of various acid [ $HNO_3$ ] and alkaline [ $NaOH$ ,  $Ca(OH)_2$ ] cation types and their concentrations on  $OLC$  and buffer capacity, electrokinetic properties of the soils have been evaluated. For this purpose, the variations in  $EC$  of the virgin as well as  $pH$  modified geomaterial samples were assessed. As shown in Figure 4.11, the  $EC$  of white clay, sodium bentonite and sandy clay increased with the addition of  $NaOH$  concentration up to 0.1 moles/litre owing to enormous supply of  $Na^+$  and  $OH^-$  ions. Though, at low concentrations of  $NaOH$  up to 0.1 moles/litre some  $Na^+$  ions are adsorbed on to clay mineral surface (Van

Olphen, 1963), yet, sufficient supply of ions from excess NaOH maintains the persistent increase in *EC*. In addition, *pH* and *EC* for all geomaterials were almost same and merging with that of blank at different concentrations. This demonstrates that monovalent cations are more or less indifferent to various soil minerals and their reactive nature (Alkan *et al*, 2005).

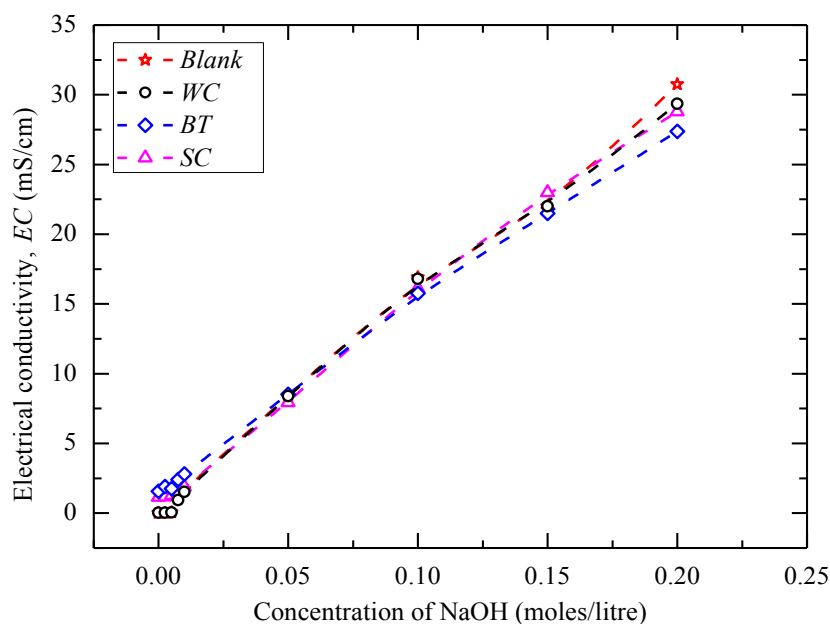


Figure 4.11 Variation of electrical conductivity of soil suspension with NaOH titration

Similarly, *EC* of geomaterials increased with  $\text{Ca}(\text{OH})_2$  concentration up to two percent by dry weight of soil, and remained constant thereafter, except for *BT* as shown in Figure 4.12. As shown in Figure 4.12, the *EC* of all geomaterials became constant after addition of 1 percent  $\text{Ca}(\text{OH})_2$  to the soil suspension, as the soil-lime suspension attained the electrochemical properties of the saturated lime solution. Based on the above observation it can be presumed that the precipitation of excess  $\text{Ca}(\text{OH})_2$  occurs only after lime saturation (i.e., 1 percent of lime by dry weight of soil), and hence, no further remarkable changes occur in *pH* for *WC* and *SC*. Yet another reason for constant *pH* might be the balanced adsorption of  $\text{OH}^-$  onto positive sites or desorption of  $\text{H}^+$  ions by de-protonation of surface hydroxyl groups at high *pH* (Alkan *et al*, 2005). Also, at very high *pH*,  $\text{Ca}^{2+}$  cations are hydrolyzed as  $\text{CaOH}^+$  and get adsorbed on the de-protonated surfaces of clay minerals and cause charge neutralization and lowering of suspension *pH* and *EC* values (Alkan *et al*, 2005). But, *EC*



value of *BT* and *SC* continues to rise beyond 1 percent due to extended cation exchange reactions as well as desorption of cations from clay mineral surface by breaking of unstable bonds. This might be also attributed to relatively stronger dissolution of reactive  $Si^{4+}$  and  $Al^{3+}$  ions from the smectitic clay mineral structure of *BT* and *SC* into pore solution at high *pH*. This shows that even though the change in *pH* is solely due to change in  $H^+$  and  $OH^-$  concentration there is momentous influence from the dissolved cations (viz.,  $Si^{4+}$ ,  $Al^{3+}$ ,  $Mg^{2+}$ ,  $Na^+$ , etc.) as well when it comes to variations in *EC* value (Al-mukhtar *et al.*, 2010).

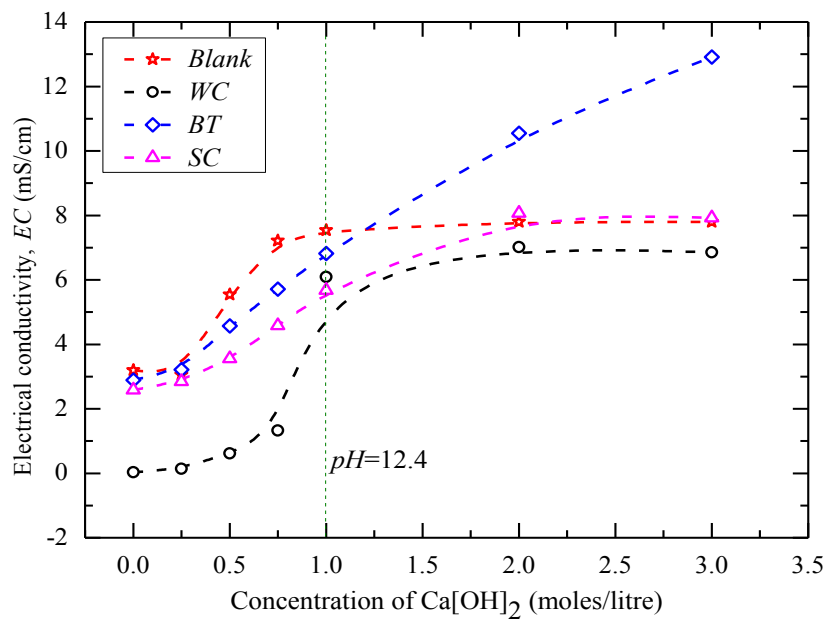


Figure 4.12 Variation of electrical conductivity of soil suspension with  $Ca(OH)_2$  titration

The *EC* variation with  $HNO_3$ , as shown in Figure 4.13, presents more or less linearly increasing trend with respect to electrolyte concentration, in the order of  $WC > SC > BT$ . The *EC* of *WC* coincides with that of the blank solution, and this behavior reflects the effect of buffer capacity as well. Due to the relatively higher buffer capacity of *BT*, it can accommodate more ions from solution by strong ion exchange reaction. Therefore, the rate of change of *pH* as well as *EC* is comparatively lesser for *BT*.

In addition, by comparing *pH* and *EC* variations of geomaterials in the presence of different electrolyte concentrations of  $Na^+$  and  $H^+$ ; it can be noted that for all three soils, the measured *EC* value for the given molar concentration of  $NaOH$  is lower when compared to

the addition of  $\text{HNO}_3$  of identical molar concentration. This is ascribed to the fact that stronger  $\text{H}^+$  ions with higher charge density are not easily adsorbed on to clay mineral surface as weaker  $\text{Na}^+$  ions, and hence,  $EC$  will be higher in  $\text{HNO}_3$  solution due to a lower rate of ion exchange and isomorphous substitution. Similarly,  $\text{Ca}(\text{OH})_2$  is supposed to exhibit higher  $EC$  than  $\text{NaOH}$  solution due to the higher valency of  $\text{Ca}^{2+}$  ions. However, in the present study,  $EC$  values are lowest in  $\text{Ca}(\text{OH})_2$  solutions because the concentrations used here are very low compared to that of  $\text{NaOH}$  and  $\text{HNO}_3$ .

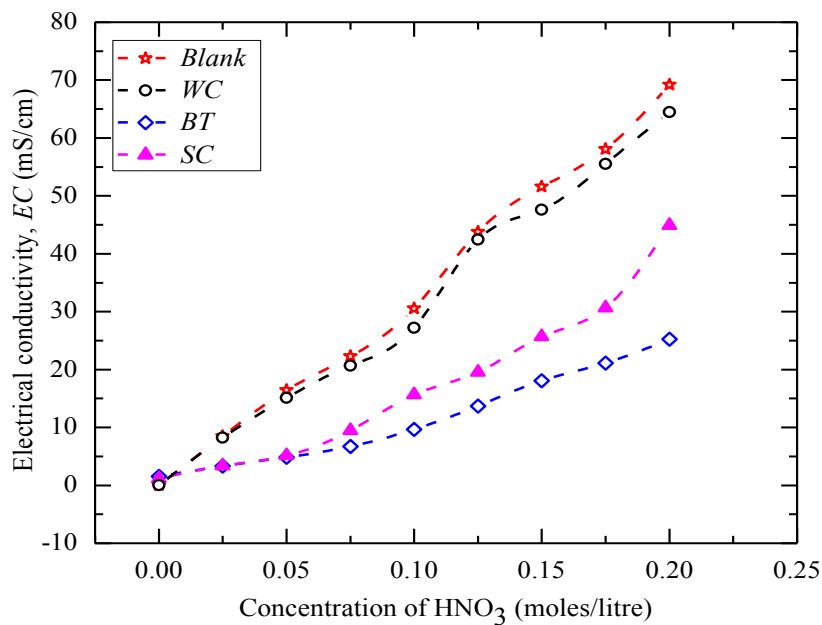


Figure 4.13 Variation of electrical conductivity of soil suspension with  $\text{HNO}_3$  titration

#### 4.4 STRENGTH EVALUATION OF LIME-TREATED SOILS

To determine the significant variations of the macro-level compressive strength properties of the selected geomaterials treated with varying lime content and curing temperature, laboratory  $UCS$  tests were conducted following the methodology presented in the sections 3.6.2 and 3.9.1. In addition,  $UCS$  tests were also conducted on lime-treated soil with varying placement moisture content, in order to assess the key role of moisture and curing temperature on the rate of pozzolanic reactions and subsequent strength improvement. Since, the majority of geotechnical properties of  $BT$  and  $SC$  are identical including the mineralogical

compositions to an extent (refer Figure 4.5), the geomaterials *WC* and *BT* are only considered for evaluating the strength gain upon lime treatment.

#### 4.4.1 Compaction characteristics of lime-treated soils

Compaction tests were performed on the *BT* and *WC* soils mixed with different percentages of lime (0-20 %). Figure 4.14 shows compaction curves for *BT* and *WC* soils with addition of different percentages of lime content (0-20 %). From the plots presented in Figure 4.14, the maximum dry density (*MDD*) and optimum moisture content (*OMC*) of *BT* and *WC* soils were determined, and are presented in Table 4.8. It is observed that the compaction curves shifted downward and towards the right with increasing lime content which implies that the *MDD* of the mix reduced and *OMC* of the soil increased than that of untreated soil. It is attributed to the flocculation-agglomeration process which is initiated due to the addition of lime, resulting in the formation of big clusters, thereby increasing the void ratio which is reflected in the decrease of *MDD* (Jawad *et al.*, 2014). From the shape of compaction curves, another important observation made is that addition of lime has flattened the compaction curves. This indicates that the desired density can be achieved over a relatively wider range of moisture content. This in other way manifests the improved workability of the soil achieved due to the addition of lime (Hussain 2009).

It was found that, in comparison with the untreated sample, the *MDD* values of *BT* and *WC* soils decreased by 1.5 % to 5.5 % and 5.3 % to 14 % for an increase in lime content from 2 % to 20 %. The *OMC* values have been found to increase by 2 % to 37 % and 20 % to 51 % for *BT* and *WC* soils due to stabilization with 2 % to 20 % lime. The increase of moisture content was also attributed to the pozzolanic reactions of the soil (Sarkar *et al.*, 2012).

Table 4.8 Variation of compaction characteristics of geomaterials with lime content

Lime content (%)	<i>BT</i>		<i>WC</i>	
	Compaction characteristics			
	<i>OMC</i> (%)	<i>MDD</i> (kN/m <sup>3</sup> )	<i>OMC</i> (%)	<i>MDD</i> (kN/m <sup>3</sup> )
0	26.5	12.753	20.4	15.794
2	27.0	12.557	24.5	14.911
4	28.1	12.459	25.2	14.617
6	28.4	12.459	26.4	14.519
8	29.0	12.459	26.9	14.225
10	29.8	12.361	27.4	13.930
12	30.2	12.361	28.0	13.832
14	31.3	12.361	29.1	13.832
16	32.4	12.164	29.8	13.734
18	35.4	12.066	30.6	13.636
20	36.3	12.066	30.8	13.636

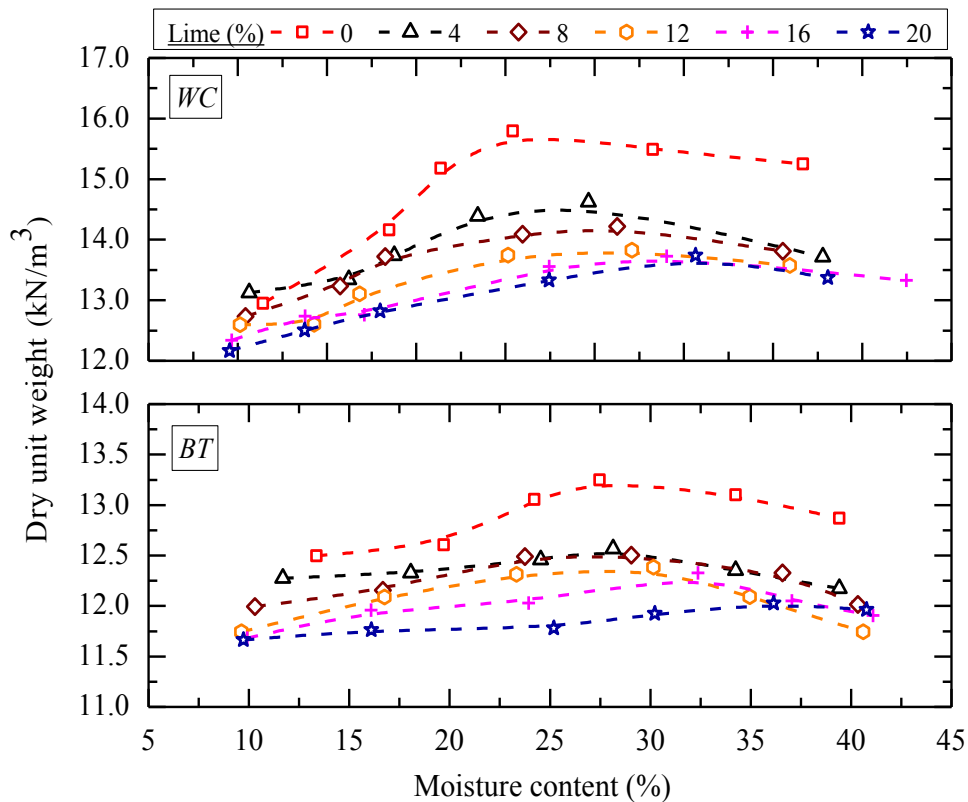


Figure 4.14 Compaction curves for different soil-lime mixtures of white clay and sodium bentonite

#### 4.4.2 Compressive strength characteristics of lime-treated soils

The effect of lime addition on the strength development was evaluated using the unconfined compressive strength (*UCS*) tests as per the methodology presented in the sections 3.6.2 and 3.9.1. Since the majority of geotechnical properties of *BT* and *SC* are identical including the mineralogical compositions, the geomaterials *WC* and *BT* are only considered for evaluating the strength gain upon lime treatment. Figure 4.15 presents the  $UCS_{28\text{-day}}$  of *WC* and *BT* treated with various lime contents ranging from 0-20 % and cured at 25 °C.

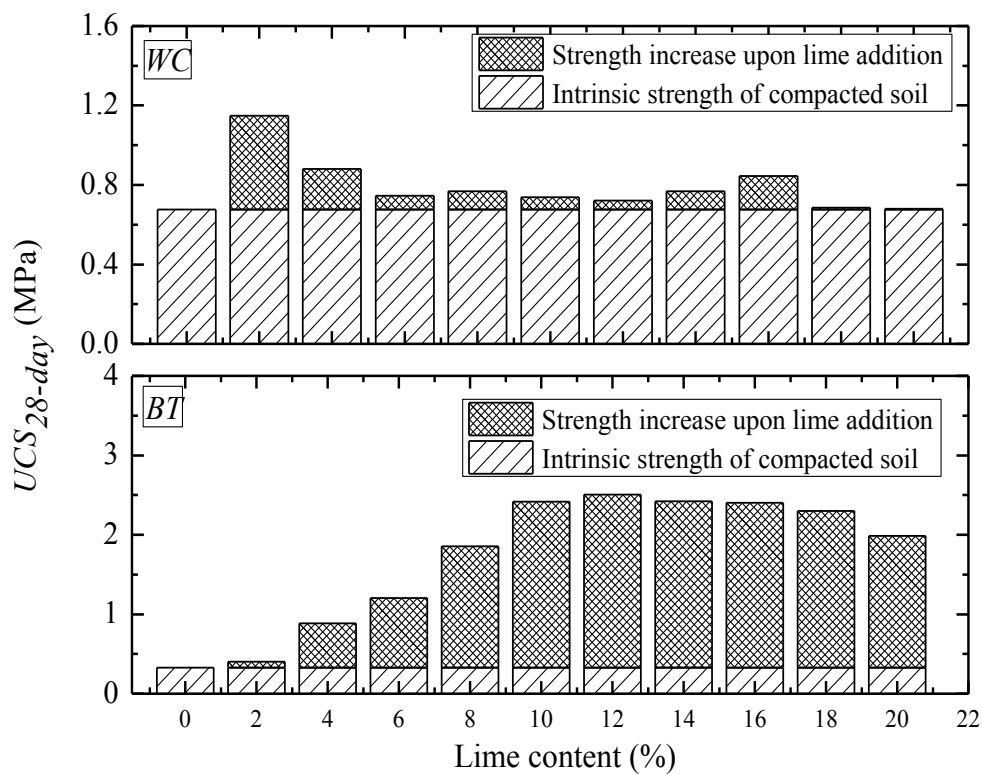


Figure 4.15 Unconfined compressive strength of 28-day cured lime-treated white clay and sodium bentonite at 25 °C

In lime-treated soils,  $UCS_{28\text{-day}}$  values of *WC* and *BT* increased from 0.68 Mpa and 0.35 Mpa to 1.15 Mpa and 2.5 MPa with increasing lime contents up to a lime content of 2 % and 12 % for *WC* and *BT*, respectively. This indicates an increase of approximately 1.7 and 7.1 times in comparison to the strength of virgin *WC* and *BT* soils, respectively. The increase in strength gain might be attributed to the pozzolanic activity. Further, the  $UCS$  value decreased

to 0.69 Mpa and 2 MPa with 20 % lime for *WC* and *BT*, respectively. This decrement in the strength might be due to the carbonation of excess lime present in the soil-lime systems as well as due to sliming effect (Ismail, 2004). Nevertheless, the rate of strength gain is not following any particular order which is due to the variation in the rate of pozzolanic reactions and corresponding deposition of cementitious products with the fraction of lime added. Further, the failure pattern altered from ductile behaviour for the virgin soil to brittle behaviour for lime-treated soils, as evaluated with respect to the ratio of maximum stress to maximum strain. The virgin soil specimens failed at considerably higher strain values when compared to the lime-treated specimens. The axial strain at peak *UCS* ranged from 1.5 % - 2.75 % and 2 % - 3 % for lime-treated *BT* and *WC*.

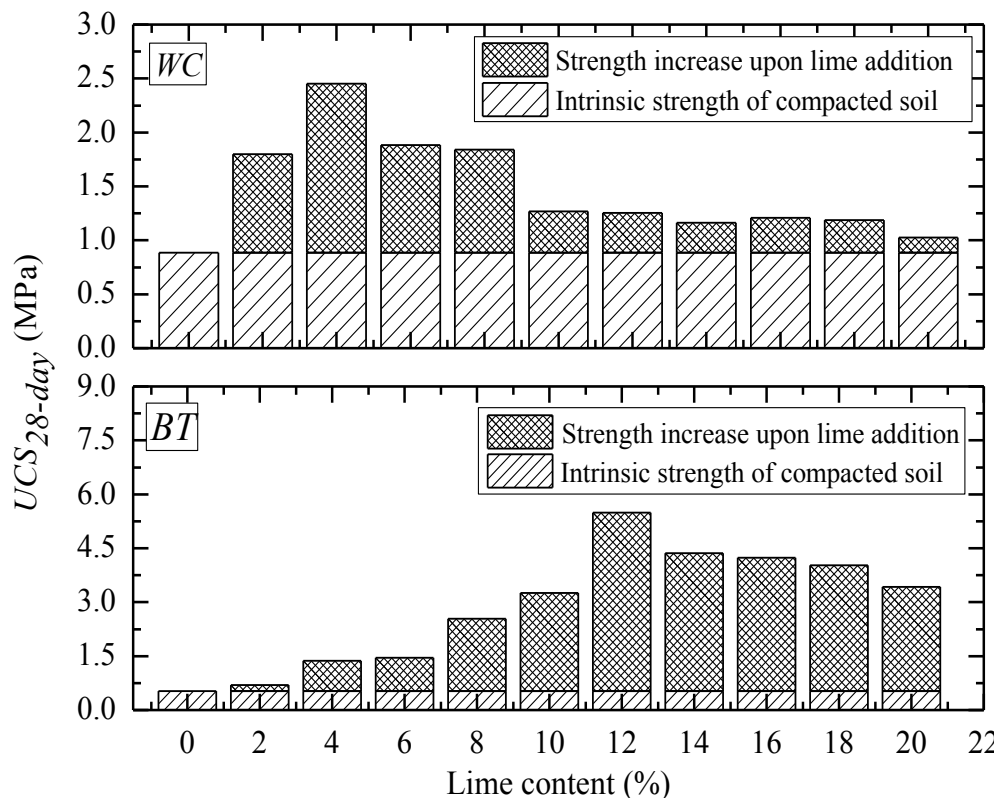


Figure 4.16 Unconfined compressive strength of 28-day cured lime-treated white clay and sodium bentonite at 40 °C

Figure 4.16 presents the *UCS* strength of *WC* and *BT* treated with various lime contents ranging from 0-20 % at 40 °C after a curing period of 28-day. In lime-treated soils, 28-day

*UCS* values of *WC* and *BT* increased from 0.9 MPa and 0.5 MPa to 2.5 MPa and 5.5 MPa with increasing lime contents up to a lime content of 4 % and 14 % for *WC* and *BT*, respectively. This indicates an increase of approximately 2.7 and 11 times in comparison to the strength of virgin *WC* and *BT* soils.

Further, the *UCS* value decreased to 1 MPa and 3 MPa with 20 % lime for *WC* and *BT*, respectively. In the case of *BT*, the virgin strength at 40 °C has increased 1.38 times to that at 25 °C. Similarly the virgin strength of *WC* increased 1.31 times compared to that of samples at 25 °C. This might be due to enhanced bonding of soil particles at elevated temperatures. However, in the case of lime-treated soils, substantial improvement of strength was observed at elevated temperature. This might be attributed to the increase in the solubility of the reactive silica and alumina found in clay and also the reactivity of lime. This leads to a greater extent of formation of pozzolanic compounds, and thereby, more stable fabric can be accomplished.

Further, the electrokinetic properties (viz., *pH* and *EC*) of soils treated with varying quantities of were determined by using ELICO make PE138 water quality analyzer. Due to the characteristic soil-lime interactions, the *OH* ion concentration in the system increases and produces an alkaline environment. This level of alkalinity is high enough for the dissolution of clay mineral structure and initiates the pozzolanic reactions (Arabani and Karami, 2007). Figure 4.17 depicts this phenomenon as it can be seen that the *pH* of the pore solution increases proportionally with lime content, owing to supply of more *OH* ions by lime and water molecules associated with the clay minerals. Moreover, due to increase in the ion concentration, the mobility of these ions increases, this in return proliferates the *EC* of the soil. Thus, the representative graphs presenting *pH* and *EC* variations of lime-treated soils explicitly display a phenomenal increase with lime treatment.

Figure 4.18 depicts the plots of *pH* versus lime content obtained for *WC* and *BT* as per Eades and Grim *pH* test following the procedure described in section 3.6. The lime content in percent which raised soil suspension *pH* at 25 °C to 12.4 was referred as *OLC<sub>pH</sub>* (Cherian and Arnepalli, 2015). It is important to note that the soil-lime suspensions at 40 °C did not attain *pH* 12.4 (corresponding to lime saturation) even for 20 % lime content in them. This is

supposed to have occurred due to practically lower lime dissolution capacity at a higher temperature, which in turn reduced lime saturated suspension  $pH$  to 12 (National Lime Association).

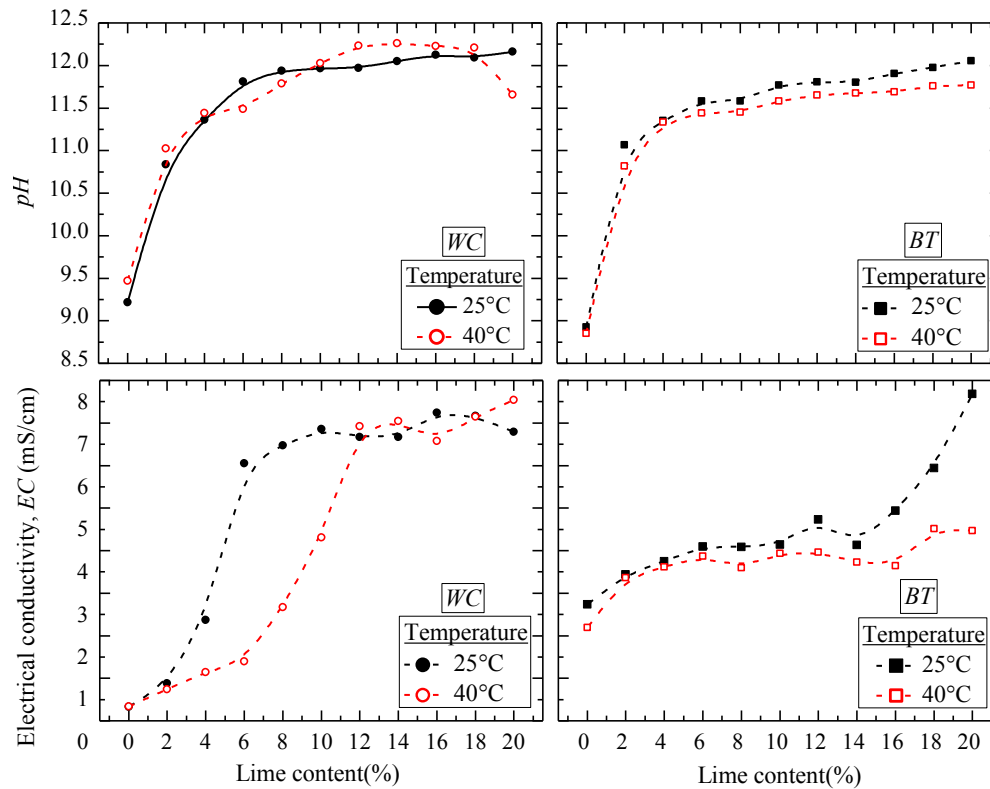


Figure 4.17  $pH$  and electrical conductivity of lime-treated white clay and sodium bentonite at 25 °C and 40 °C

Accordingly, the  $OLC$  values for  $WC$  at 25 °C and 40 °C were measured to be 2 % and 1.7 %, whereas 2.7 % and 2.2 % for  $BT$ , respectively. This indicated that both soils required more or less similar proportions of lime for immediate alteration of physicochemical characteristics. However, it is worth to note that the protocol of Eades and Grim  $pH$  test is true only in terms of attaining solution  $pH$  12.4 which is essentially required for reactive silica and alumina dissolution and eventually initiating the pozzolanic reactions. Yet, this test does not provide reliable and substantial information relative to either potential reactivity of particular soil, or magnitude of increased strength realized upon its treatment with  $OLC$  (Cherian and Arnepalli, 2015).



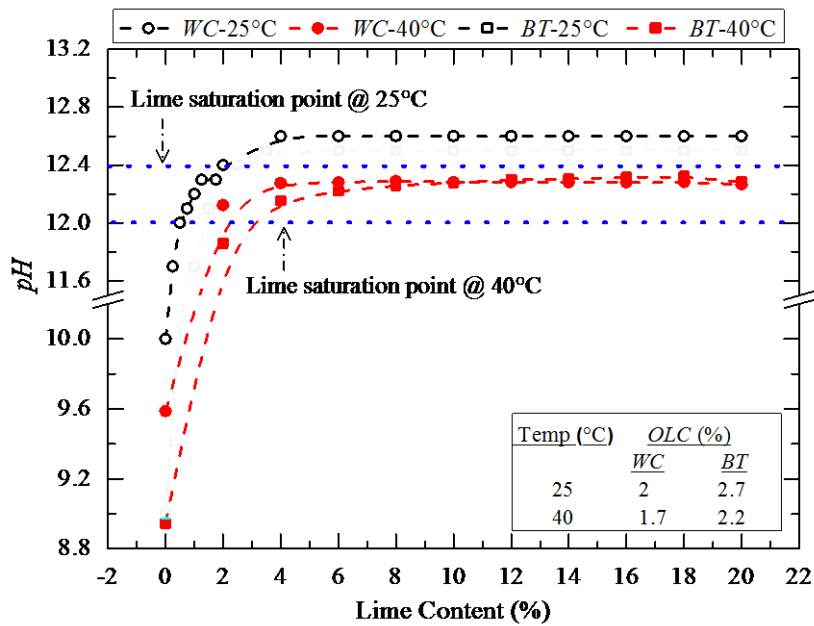


Figure 4.18 Determination of optimum lime content using Eades and Grim  $pH$  test

Similarly, from the 28-day  $UCS$  values obtained for  $WC$  and  $BT$  when treated with different lime contents, the lime content corresponding to maximum  $UCS$  value was selected as  $OLC_{UCS}$ . Based on the observed  $UCS$  results, the  $OLC_{UCS}$  value for  $WC$  and  $BT$  was determined as 2 % and 10 % lime when cured at 25 °C, and 4 % and 12 % corresponding to curing at 40 °C, respectively. Table 4.9 depicts the  $OLC$  values obtained from both tests; hence, it was observed that  $OLC_{pH}$  and  $OLC_{UCS}$  @ 25 °C for  $WC$  are same. It means that 2 % of lime was sufficient to fully satisfy the whole requirement for cation exchange as well short-term pozzolanic reactions. However,  $OLC_{pH}$  @ 25 °C for  $BT$  is almost 4 times lower than the respective  $OLC_{UCS}$  @ 25 °C which indicated the considerably higher rate of lime consumption for pozzolanic reactions when compared to  $WC$ . As a whole, these observations primarily infer back to the relatively poorer reactive nature of  $WC$  owing to the lower activity of clay as well as  $SSA$  values compared to  $BT$ . Based on these accounts, the lime content corresponding to the maximum 28-day  $UCS$  was selected as  $OLC$  for further experimental studies in order to eliminate any chances of risk and to ensure the complete mobilization of the long-term chemical and pozzolanic soil-lime reactions.

Table 4.9 Comparison of optimum lime content of geomaterials

Soil Type	Temperature (°C)	OLC (%)	
		Based on Eades and Grim (1966)	Based on UCS value
<i>WC</i>	25	2	2
	40	1.7	4
<i>BT</i>	25	2.7	10
	40	2.2	12

#### 4.4.3 Effect of placement moisture content and curing period on the lime-treated soils.

As discussed in section 3.9, the impact of placement moisture content on the compressive strength of lime-treated soil was studied by following the methodology presented in the section 3.9. The characteristic curves showing the variations in the strength of soil-lime mixture against placement moisture content and curing temperature are presented in Figure 4.19 and Figure 4.20, for *WC* and *BT* respectively, in terms of maximum *UCS* strength. In the case of virgin soils, the 28-day *UCS* value of *WC* was observed to be almost 1.5 and 1.2 times higher than that of *BT*, for 25 °C and 40 °C temperatures, respectively. More or less similar trend was observed for other curing periods as well; however, the drift in *UCS* values with respect to placement moisture content was dissimilar for *WC* and *BT*. Figure 4.19 indicated that the virgin *WC* specimens possessed inferior strength at *DMC* and *WMC* when compared to soil holding *OMC*. At *OMC*, the *UCS* value of *MC* obtained after 7-day curing was 0.518 MPa; further, it was reduced by 15 % at *DMC* and 40 % at *WMC*, for samples cured at 25 °C. Similarly, for samples cured at 40 °C 7-day *UCS* value was 0.6 MPa at *OMC* and was decreased by 4 % and 35 % at *DMC* and *WMC*, respectively. The slight increase in strength for virgin soils compacted at *DMC* when compared to *WMC* might be due to an increase in the total suction resulting from a lower moisture content in the void spaces. Whereas, for *BT* the virgin *UCS* value was observed to be the minimum at *DMC* and maximum at *WMC*, consistently for all curing conditions. Though the change was marginal, it was presumed that this might have resulted because of relatively higher reactive nature of *BT*. For instance, the moisture content supplied at *OMC* might not be sufficient to fully mobilize the pozzolanic reactions; as a consequence, the rate of strength gain advanced up to *WMC*. Further, it can be deduced from these results that the consistent increase in virgin soil strength upon prolonged curing up to 8-months could be related to the re-arrangement of soil fabric and its subsequent hardening under controlled humidity as well as temperature (Mitchell and Soga, 2005).

At *OMC*, the 28-day *UCS* value of lime-treated *WC* corresponding to 25 °C and 40 °C increased by 1.5 and 2 folds, respectively. Similarly, for lime-treated *BT* around 4.5 folds increase in 28-day *UCS* value at *OMC* was noticed for both curing temperatures. Further, the drift in *UCS* values with respect to placement moisture content was observed to follow the same trend for lime-treated soils as well. In lime-treated *WC* specimens prepared to *DMC* and *WMC*, there was noticeable strength loss when compared to *OMC*; whereas the lime-treated *BT* exhibited maximum strength at *WMC*. The major reason for the decrease in strength at *DMC* is related to the combined effect of increased suction, and also to the insufficient supply of moisture which is essential to drive the long-term pozzolanic reactions and by extension, realize strength improvement to the maximum level.

Further, it is assumed that decrease in strength of lime-treated soils at lower placement moisture content might be attributed to increase in the volume of air voids present in the compacted specimens and flocculated fabric arrangement, which in turn reduced particle-to-particle contact between soil grains. The impedance in the formation and development of cementitious reaction products in the wet of optimum may be due to various reasons. Primarily, the increase in strength occurs only until all internal porous cavities of compacted soil are filled with moisture and fines and mobilizes maximum strength in the specimen. Any moisture content more than sufficient might act as a lubricant, and thereby, results in the decrease of internal friction angle of the soil, and hence, its shear strength (Winterkorn and Fang, 1972). Yet again, compaction at *WMC* results in a more parallel orientation of soil fabrics, thereby diluting soil structure and reducing strength (Muntohar 2005). Nevertheless, it should be noted that despite exhibiting a loss of strength with increasing or decreasing moisture content, the *UCS* values of lime-treated *WC* and *BT* soils were still higher than those of untreated counterparts.

From the results presented here, it is evident that curing at 40 °C contributed to the significant enhancement of *UCS* strength at all placement moisture content and curing periods. The increase is in the order of 35 % for *WC* and 24 % for *BT* as of 28-day test results, for lime-treated soils compacted at *OMC*. By comparing the relative strength of virgin and lime-treated specimens at *OMC* after 8-months curing, the temperature rise to 40 °C yielded acceleration from 2.4 to 3.2 times for *WC* and 4.9 to 5.6 times for *BT*, respectively.

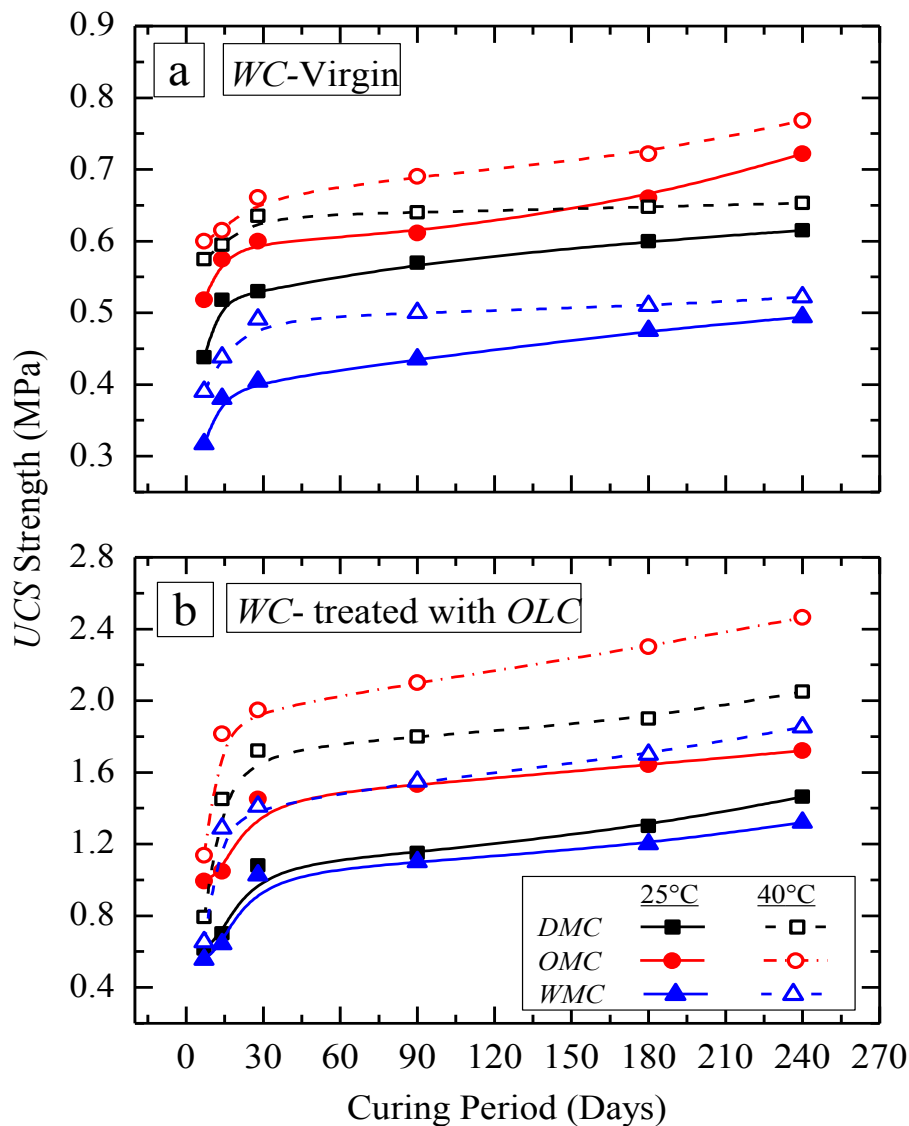


Figure 4.19 Effect of compaction and curing conditions on *UCS* of (a) virgin; (b) lime-treated white clay

Likewise, for both soils compacted at *DMC* and *WMC* dramatic strength improvement was observed in more or less similar rates. It is suspected that this might have resulted from the dramatic acceleration of pozzolanic reactions upon exposure to elevated temperature, as indicated by the previous researchers (George *et al.*, 1992, Narmluk and Nawa, 2014). All other factors being the same, a higher curing temperature is deemed to cause the greater extent of formation of pozzolanic compounds and thereby more stable fabric can be accomplished (Morsey and Haikal, 2004). In addition to these facts, the general comparison of *UCS* data related to *WC* and *BT* confirmed that the degree of strength improvement of virgin specimens was more apparent in *WC* which has higher clay content. However, upon

lime treatment, *BT* gained higher strength compared to *WC*. This result depends on the reactive nature of the clay minerals present in the soil (viz., reactive silica and alumina, *SSA*, *CEC*, etc.) and consequent formation and growth of crystalline reaction compounds (Marto *et al.*, 2013; Cherian and Arnepalli, 2015), which can be further established by advanced microstructural evaluation.

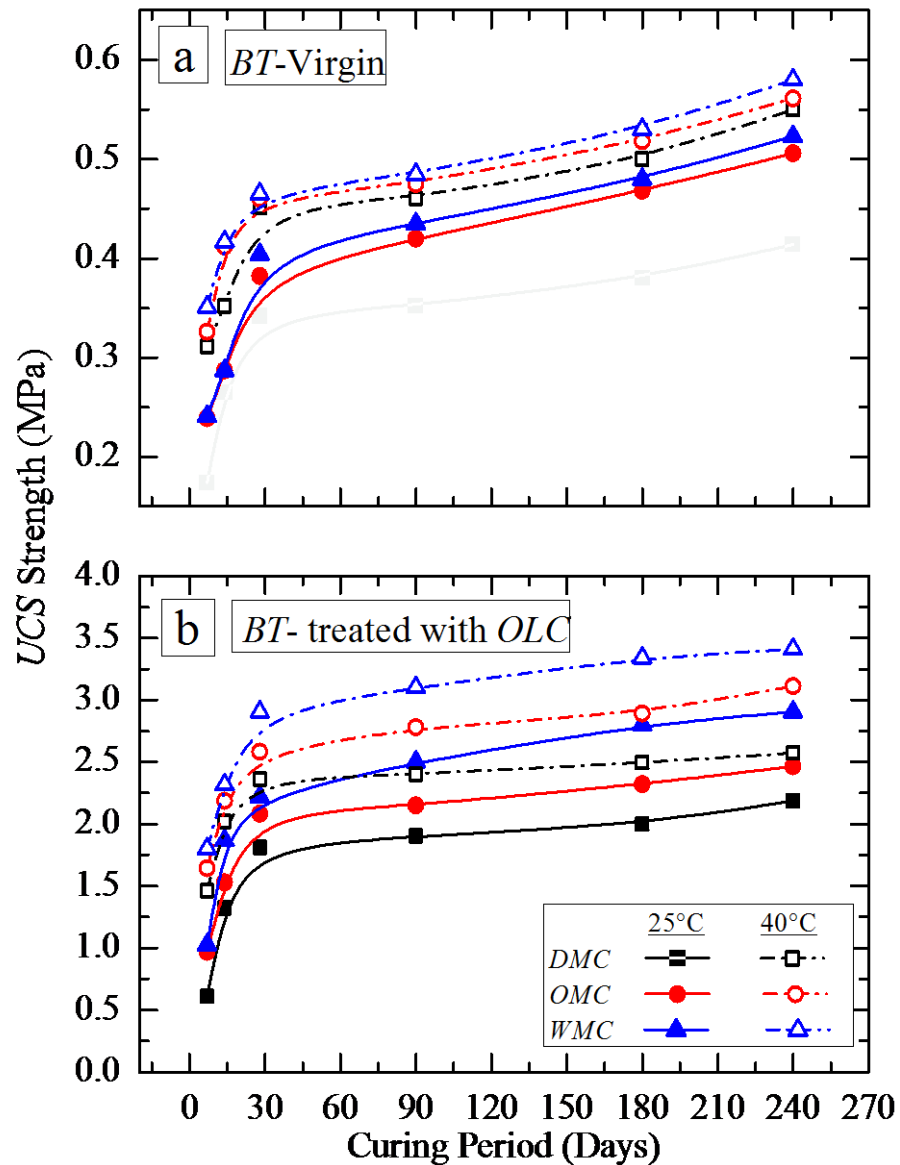


Figure 4.20 Effect of compaction and curing conditions on *UCS* of (a) virgin; and (b) lime-treated sodium bentonite

From the *UCS* studies, it is clear that the intrinsic strength of white clay is more than the strength gained upon lime addition as shown in Figure 4.15. Whereas, the strength gained by

sodium bentonite upon lime addition is much higher to that of its intrinsic strength as shown in Figure 4.15. In view this; further studies were carried out only on sodium bentonite to understand the mechanisms responsible for drastic strength improvement upon lime treatment. Further, in order to predict the underlying micro-level mechanisms which have caused the macro-level changes, the qualitative and semi-quantitative estimation of new reaction products as well as alterations of virgin clay minerals were also carried out by employing the sophisticated techniques such as *XRD*, *TGA-DTA*, *SEM-EDS*, *FTIR*. The obtained results are compared vis-à-vis virgin soil properties in order to identify the predominant mechanisms involved in stabilization process, and to precisely quantify the degree of improvement achieved.

## **4.5 VARIATIONS IN CHEMICAL CHARACTERISTICS OF LIME-TREATED SOILS**

### **4.5.1 Simultaneous thermo gravimetry - differential thermal analysis**

The physicochemical processes involved in the short-term and long-term lime stabilization mechanism plays a predominant role in determining the hydro-mechanical behaviour of the treated soil matrix. Hence, the precise quantification of these processes becomes a key aspect of lime stabilization study in order to account for the influence of reactive nature of the virgin soil as well as the compatibility between soil and lime. In this study, the chemical composition of lime-treated *BT* fragments after a curing a period of 28-day at 25 °C was assessed by employing the thermo-gravimetry and differential thermal analysis (*TGA-DTA*) technique as per the methodology presented in the section 3.3.3. By the appropriate interpretation of the data obtained from these tests, it is anticipated to develop a better understanding of the chemical modifications imparted by pozzolanic soil-lime reactions and resulting variations in the mechanical and hydraulic behaviour of lime-treated soil.

The results obtained from the *TGA* analysis of 28-day cured *BT* treated with lime percentages varying from 0 to 20 % (by dry weight of soil) are depicted in Figure 4.21. The total loss on ignition (*LOI*) up to 1000 °C for various samples during the analysis is determined to be less than 20 %.

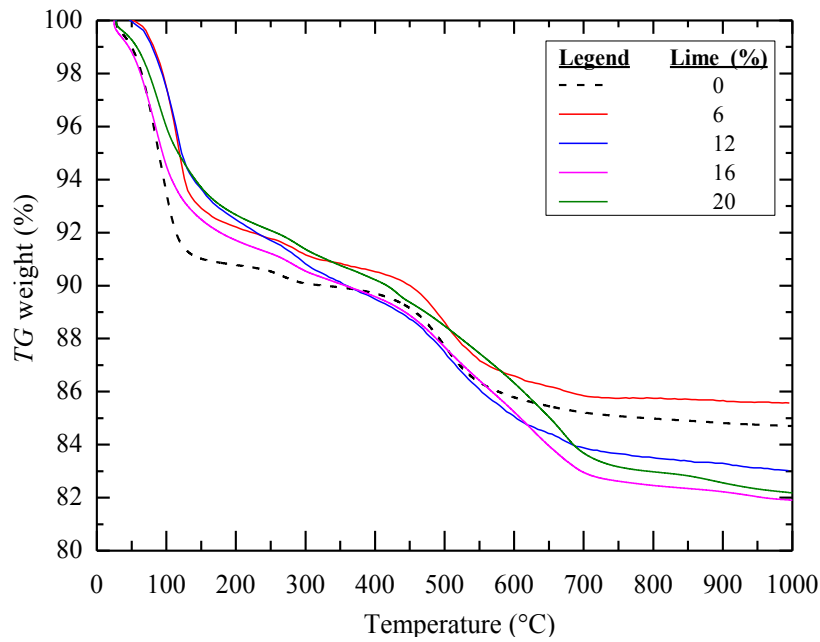


Figure 4.21 Comparison of thermo gravimetric curves obtained for virgin and lime-treated sodium bentonite

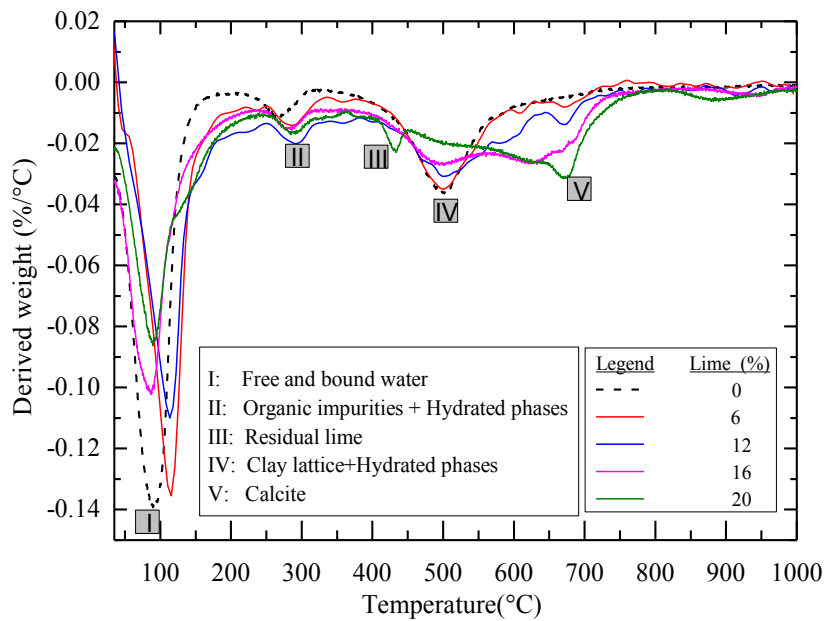


Figure 4.22 Comparison of derivative thermo gravimetric curves obtained for virgin and lime-treated sodium bentonite

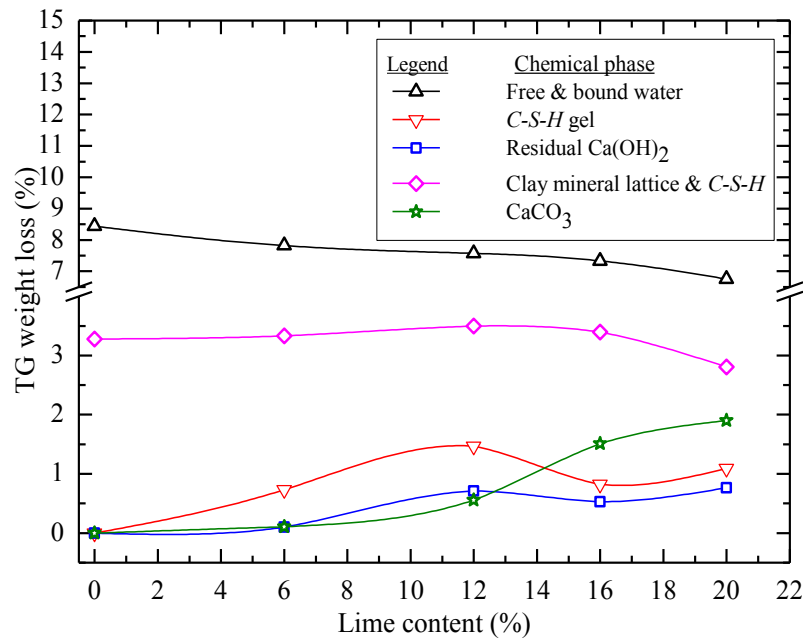


Figure 4.23 Thermo gravimetric weight loss of various phases present in 28-day cured lime-treated sodium bentonite at 25 °C

Similarly, Figure 4.22 shows the *DTG* decomposition profiles and characteristic peaks of different phases such as free and bound water, organic impurities and gel water, hydroxides such as  $\text{Ca}(\text{OH})_2$ , clay lattice water, and carbonates such as  $\text{CaCO}_3$ . It is worthy to note that *TG* weight loss curves of all samples look more or less alike; however, substantial differences can be observed from the corresponding *DTG* decomposition profiles (Figure 4.22). Hence, the *DTG* profiles provide better visualization of the evolution of pozzolanic reaction and carbonation in the cured lime-treated soils. Further, Figure 4.23 provides the relative weight losses corresponding to different chemical phases present in the analyzed soil samples

### ***Dehydration losses***

The virgin *BT* with 0 % lime corresponds to reference sample, which shows an initial rapid and substantial weight loss of about 8.4 %, located between 50 °C and 200 °C as a result of free and bound water dehydration (Dellisanti *et al.*, 2006; Bray and Redfern, 1999). The free water describes the inter-lamellar water not linked to the exchangeable cation as well as water between clay particles, whereas bound water describes water linked to exchangeable cation and water between clay particles (Al-Mukhtar *et al.*, 2012). The weight loss of free and bound water decreases proportionally with increasing lime content (Figure 4.23); it can be



implicitly taken as the estimate of the degree of pozzolanic reactions and progressive hydration of reaction products and gel formation.

On closer observation (refer Figure 4.24(a)) it is further noticed that the dehydration profile of free and bound water for 6 % and 12 % lime is becoming narrower with a decrease of Full Width at Half-Maximum, *FWHM* and exhibits a shift in the peak position with the relatively higher onset and offset temperatures. The previous studies mentioned that the probable temperature ranges of various reactions can vary considerably depending upon the various factors such as grain size of the clay aggregates, individual crystal size, packing, heating rate, type and flow of purging gas and particle distribution (James, 2013). However, no specific reasons could be deduced for this behaviour in the dehydration peaks corresponding to free and bound water present in soil samples from the current knowledge available in the literature.

Additional loss of water observed in the temperature interval of 200-340 °C is assumed to have occurred from the various hydration products formed during pozzolanic soil-lime reactions such as *CSH* and *CASH* (Kontori *et al.*, 2009; Eisazadeh *et al.*, 2010). Nonetheless, *CSH* dehydration and dehydroxylation occurs gradually and differently over a wide temperature range up to 800 °C (Zhang and Ye, 2012). Moreover, the decomposition of minute fractions of organic matter present in the virgin soil takes place in 280-320 °C temperature range, which is reflected by a tiny peak in the *DTG* profile of virgin soil. On a further close observation of Figure 4.24 (a & b), a corresponding increase in the observed weight loss up to the optimum of 12 % lime content can be noticed. Beyond, weight loss is found to decrease thereby indicating the retardation of pozzolanic reactions. This might be attributed to the inadequacy of necessary ingredients such as moisture and reactive clay minerals as well as accelerated carbonation process. This reasoning also substantiates the *UCS* results (refer to Figure 4.15) which exhibit strength increment in lime-treated soils up to 12 % ( $\sim OLC_{UCS}$ ) and gradual decrement thereafter. Another important point to be noted is that the observed shift in the *CSH* dehydroxylation peak towards higher temperature evidences progressive crystallization of *CSH* gel. In general, the peak shift can also be related to the presence of different phases of hydrated gels characterized by varying *Ca/Si* ratio in the lime-treated soil mixture (Ukrainczyk *et al.*, 2006).

### ***Dehydroxylation losses***

The broad shoulder between 350 °C to 450 °C on the *DTG* curve ( Figure 4.24(c)) indicates weight loss due to dehydroxylation of residual or excess free lime that has not participated in any chemical or pozzolanic reactions during 28-day curing of lime-treated soil (Kolias *et al.*, 200, Robin *et al.*, 2014; Vitale *et al.*, 2016). It is assumed that added lime is being consumed during the pozzolanic reaction as well as carbonation process during the curing period (Sharma *et al.*, 2012). Nevertheless, the observed increment in *TG* weight loss of lime primarily reflects that the pozzolanic reactions are not fully mobilized in the early stages of curing. Besides, 20 % lime shows a distinct dehydroxylation peak of lime in sharp contrast to all other samples which indicates the appreciable amount of unreacted lime present in it. This observation substantiates the significant strength loss for 20 % lime as surplus free lime might impart lubrication effect, which in turn results in the deterioration of shear strength of treated soil (Ismail, 2004).

Similarly, the untreated *BT* shows a well-defined decomposition peak from 450 °C to 590 °C attributed to dehydroxylation of clay lattice water as well as hydration products, as shown in Figure 4.24(d) (Drits *et al.*, 2012). The consistent broadening of the peak indicates the loss of crystalline nature owing to delamination of clay lattice by the lime attack; however, no significant peak shift is noticed. The corresponding *TG* weight loss in this temperature range is observed to increase up to the optimum of 12 % lime and further decline (Figure 4.23). This is primarily attributed to interference of *CSH* dehydroxylation which also contributes to additional weight loss in this temperature interval.

### ***Decarbonation losses***

The decarbonation losses between 590-630 °C and 630-720 °C account for the amount of amorphous calcium carbonates and well-crystallized calcite, respectively (Jimenez *et al.*, 2008; Vedalakshmi *et al.*, 2003).

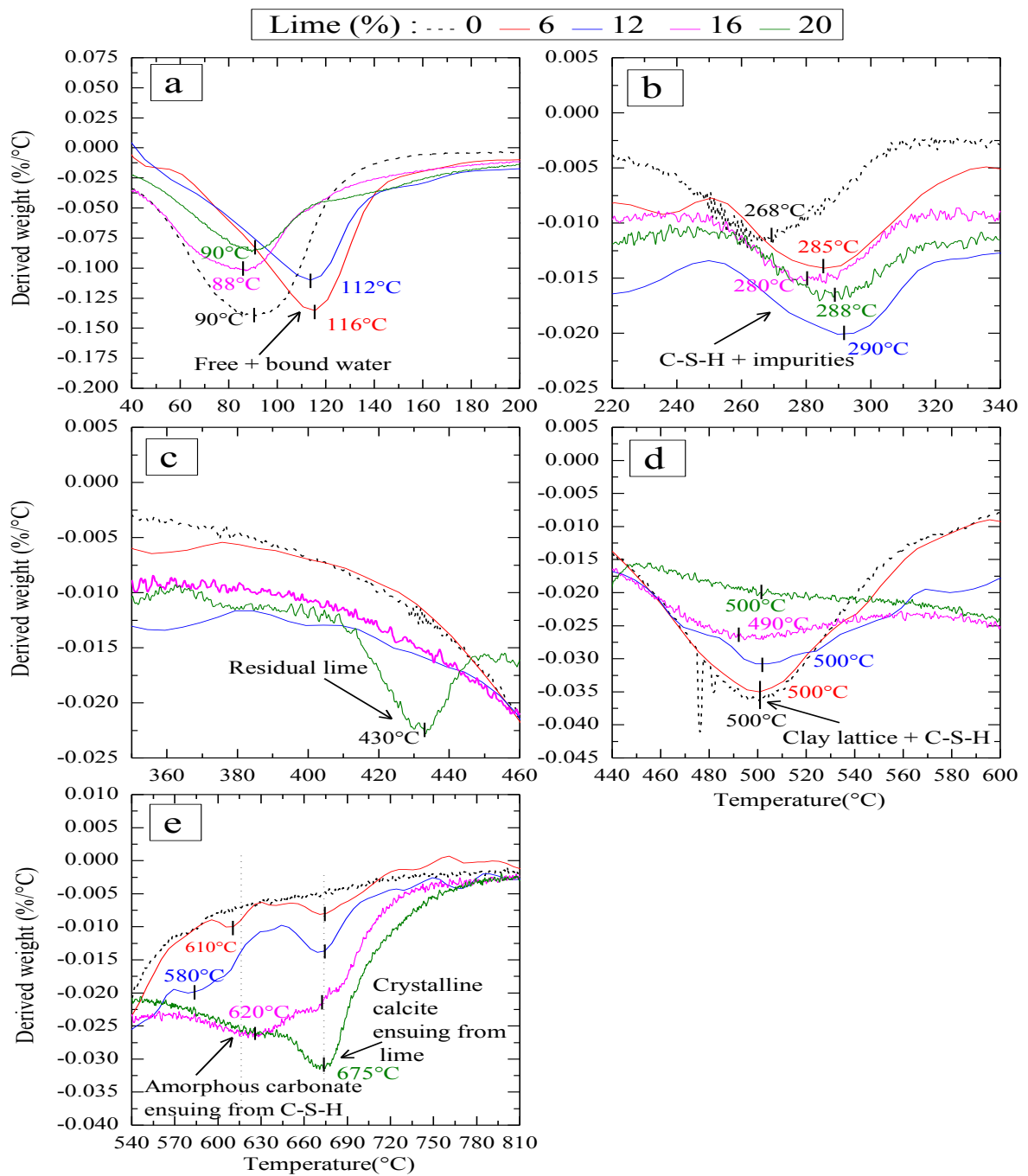


Figure 4.24 Derivative thermo gravimetric curves of lime-treated sodium bentonite over different temperature ranges

Most of the crystalline calcite is presumed to have formed during the curing period by detrimental lime carbonation reactions, and it mainly dissociates at high temperature in TGA

(Villain *et al.*, 2007). Conversely, the calcium carbonate ensuing from the *CSH* carbonation may correspond to more amorphous phases which dissociate at a relatively lower temperature (Mackenzie *et al.*, 1988). As it can be noticed in Figure 4.24(e), the peak due to the carbonated amorphous phases has narrowed and shifted to a higher temperature while the peak area of well-crystallized calcite has doubled. However, it can be observed that corresponding peaks of two phenomena overlap thereby making it difficult to assert the temperature ranges specifically. As a consequence, the total *TG* weight loss ensuing from decarbonation reaction is determined by considering the lower and upper bound temperatures of 590 °C and 720 °C. Moreover, it is noteworthy that reliable quantification of carbonated phases and calcite from *DTG* profiles shown in Figure 4.24(e) are cumbersome due to a series of overlapped decompositions of structural OH groups from different phases of *CSH* gel as well as calcite and other carbonated phases present in soil (Gabrovsek *et al.*, 2006).

#### 4.5.2 Fourier transform-infra red spectroscopy

As mentioned in the section 3.3.4, *FTIR* analysis was conducted on the lime-treated *BT* fragments after a curing a period of 28-day at 25°C as per the methodology presented in the section 3.3.4. The Figure 4.25 represents the *IR* spectra obtained for *BT* soil treated with varying lime contents from 0 to 20 %, compacted and cured for 28-day in a humidity chamber. From the interpretation of the *IR* spectrum of untreated as well as lime-treated *BT* soil, the chemical compositions could be confirmed in terms of the vibration properties of their characteristic chemical bonds. For better identification of the important features present in the *IR* spectrum, significant regions are selected and presented in separate Figure 4.26 and Figure 4.27 for virgin & lime-treated *BT*, respectively. As shown in Figure 4.26 and Figure 4.25, the *IR* spectra of untreated as well as lime-treated *BT* were consistent and showed a major group of bands at 3694, 3620 and 3420  $\text{cm}^{-1}$  attributed to *O-H* bonds of inner surface hydroxyl groups present in the clay minerals as well as water molecules adsorbed on their negatively charged surface. A prominent absorption band was also observed at 1636  $\text{cm}^{-1}$  mainly attributed to *O-H* as well as *H-O-H* bond of water. Another characteristic set of bands was present between 1100 and 900  $\text{cm}^{-1}$ , attributed to stretching vibrations of *Si-O* and *Al-O* bonds which are characteristics of silicate chains present in clay minerals. The other two

bands at 795 and 688  $\text{cm}^{-1}$  of relatively very low intensities might be attributed to bending vibrations of *Si-O-Si* bonds present in clay minerals.

As can be observed from the Figure 4.27 (a) to (c), the first group of *MIR* bands between 3700 and 3400  $\text{cm}^{-1}$  is quite consistent with the characteristic *O-H* linkages in the structure of adsorbed and molecular water, for all soil-lime mixes from 0 to 20 % lime content. With the change in lime concentration, not significant peak shift was noticed in this region of the *IR* spectra; however, there was a considerable broadening of peaks. Moreover, the percentage transmittance increased with increasing lime content for up to 12 % lime content in the approximate rates of 8 %, 13 % and 9 %, for 3694, 3620 and 3420  $\text{cm}^{-1}$ , respectively. Beyond 12 % and further up to 20 % lime content, there was a negligible reduction in percentage transmittance value by about 2 %. In other words, it can be stated that the characteristic absorbance in this band group decreased with increasing lime content up to optimum lime content and decreased with further increase in lime content. This trend is also matching very well with the *UCS* results, where maximum strength gain was observed for 12 % lime content, and beyond, strength was found to decline with the addition of more amount of lime. Hence, it can be assumed that the relative changes in the *IR* spectrum induced by lime addition occurred by the consumption of molecular and adsorbed water for hydration of cementitious products formed by pozzolanic reactions. The rate of reactions is accelerated with increasing lime content up to *OLC* value, where a maximum reduction in absorbance value was noted. Beyond, pozzolanic reactions either declined or ceased owing to the scarcity of reactive silica and alumina content; therefore, the additional lime remained as excess free lime. Hence, no further notable changes were observed in *IR* spectrum.

While considering the band at 1636  $\text{cm}^{-1}$ , the untreated *BT* showed a very sharp band corresponding to transmittance value of 85 %, and it continued to increase with increasing lime content up to 93 % for 20 % lime content. In other words, the absorbance at 1636  $\text{cm}^{-1}$  decreased with increasing lime content up to *OLC* and beyond also. As this band is attributed to molecular water and the trend is almost matching with the broad band in the range of 3700 to 3400  $\text{cm}^{-1}$ , the chief cause for the decrease in absorbance might be increasing rates of pozzolanic reactions and subsequent hydration of reaction products. In addition to this narrow and sharp band, another sharp band is noticed near 1418  $\text{cm}^{-1}$  which is not present in the *IR*

spectrum of untreated *BT* soil. This band is the characteristic of *Ca-O* linkages in the lime, and it is observed that the transmittance value decreased with increasing lime content from no peak (or ~ 100 % transmittance) for 0 % lime content up to 84 % transmittance for 20 % lime content. Conversely, another characteristic narrow and less prominent band at 1103  $\text{cm}^{-1}$  in the untreated soil corresponding to *Si-O* bond in the clay mineral structure was observed to gradually disappear with the addition of lime. This might be probably owing to the disintegration of clay mineral structure during lime treatment as a result of accelerated rates of dissolution of structural silica and alumina contents in highly alkaline medium.

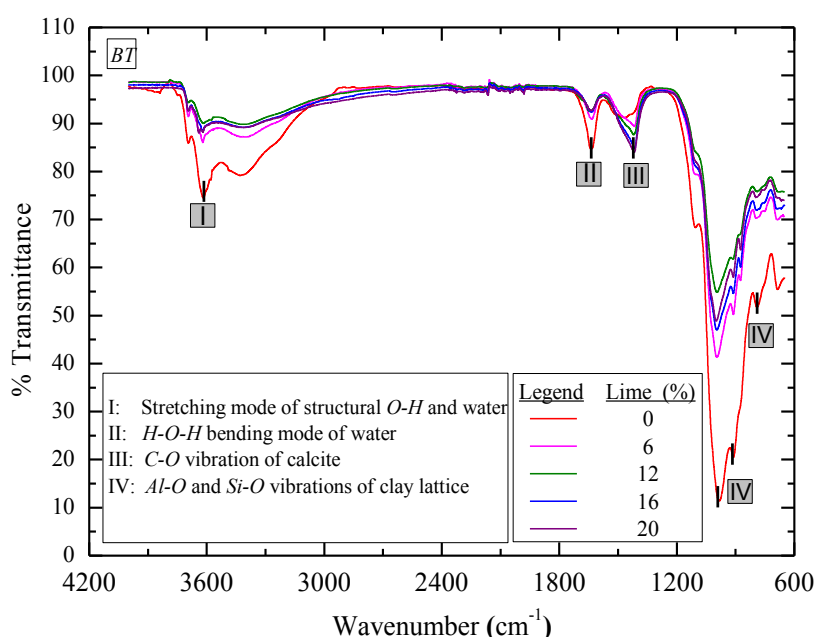


Figure 4.25 Infra-red spectra for lime-treated sodium bentonite after 28-day curing at 25 °C

In a similar manner, the set of bands present between 1100 and 900  $\text{cm}^{-1}$  are attributed to stretching vibrations of *Si-O* and *Al-O* bonds of silicate chains present in clay minerals also showed continuous increment in percentage transmittance (%T) value. It is worth to note that the increasing trend of %T was followed up to *OLC* value of 12 % lime content, and further, there was a negligible but slight decrement in %T value. It is believed that this variation might be due to the possible error in sample handling and operational limitations of attenuated total reflection (*ATR*) technique, where the applied mechanical pressure on the sample as well as contact area plays a significant role in governing the accuracy of results.

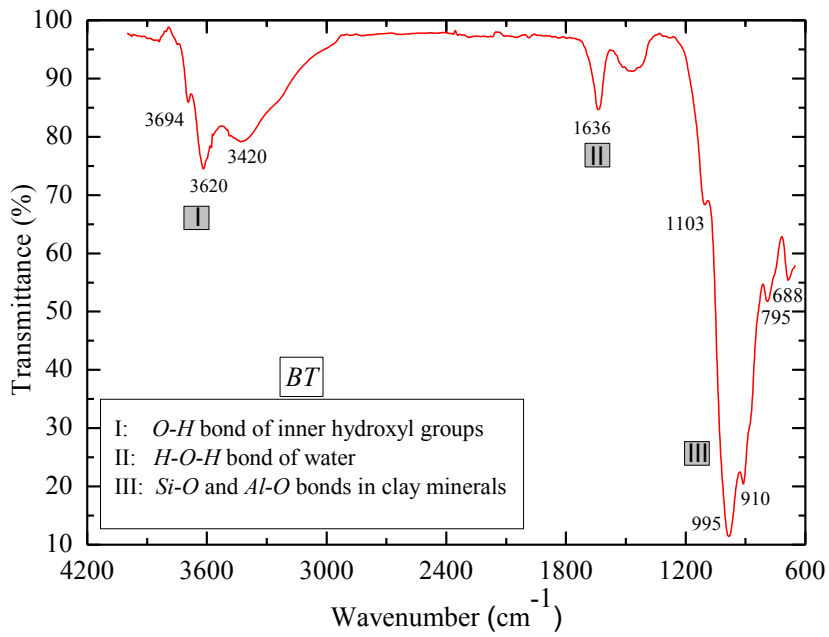


Figure 4.26 Major bands identified in the infra-red spectra for virgin sodium bentonite after 28-day curing at 25 °C

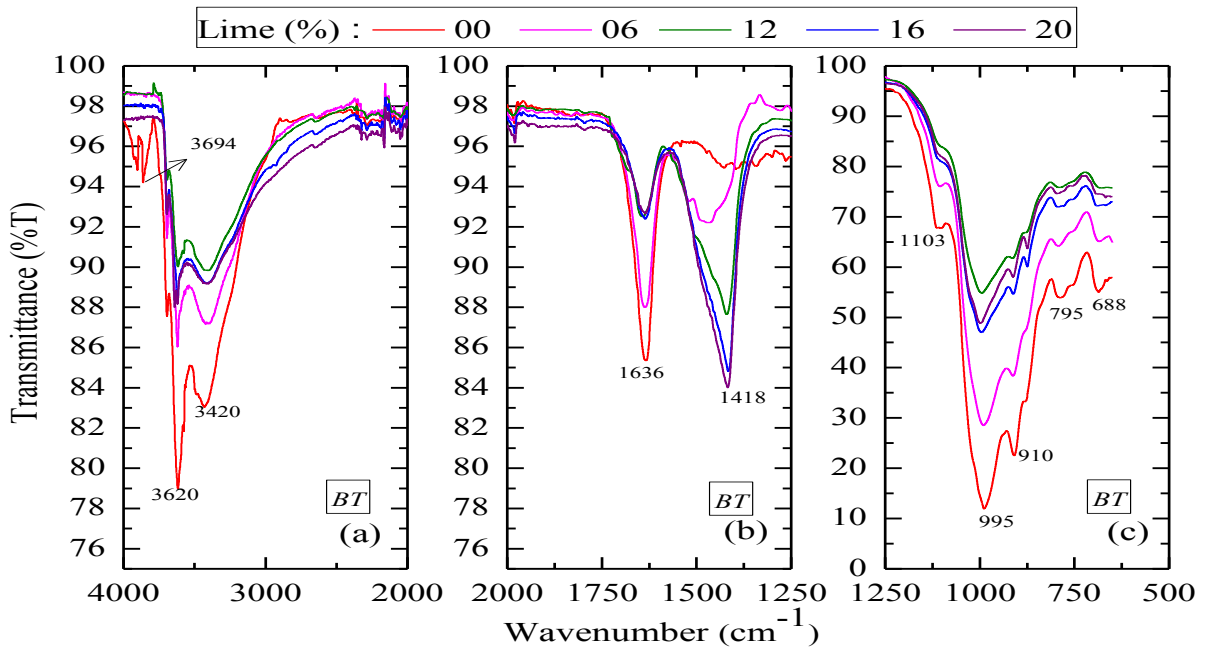


Figure 4.27 Major bands identified in the infra-red spectra for lime-treated sodium bentonite soil after 28-day curing (a) *O-H* bond of inner hydroxyl groups; (b) *H-O-H* bond of water and *Ca-O* bond of lime; (c) *Si-O* and *Al-O* bonds in clay minerals

## 4.6 VARIATIONS IN MINERALOGICAL CHARACTERISTICS OF LIME-TREATED SOILS

### 4.6.1 X-Ray diffraction

As mentioned in the section 3.9, the *XRD* studies were conducted on lime-treated *BT* after a curing a period of 28-day at 25°C by following the same methodology described in section 3.3. The Figure 4.28 represents the x-ray diffractogram obtained for hydrated lime (*HL*) used for stabilization of soils in this study. The peak identification, as well as the semi-quantitative analysis, was conducted using commercial X-Pert Highscore Plus software package. The composition of *HL* was quantified to be 93 % portlandite ( $\text{Ca}[\text{OH}]_2$ ) and 7 % calcite ( $\text{CaCO}_3$ ). The peak with the highest intensity of more than 20, 000 counts was observed at 34.07° 2 $\theta$  angle, corresponding to the characteristic primary peak of portlandite ( $\text{Ca}[\text{OH}]_2$ ). In addition, many other peaks with significant intensities were identified to be attributed to portlandite at 18.02°, 28.64°, 47.09°, 50.88°, 54.31°, 56.11°, 59.34°, 62.56°, and 64.24° 2 $\theta$ . The peaks identified for calcite were of the order of less than 1000 counts for the primary peak at 29.34°, and other two peaks were observed at 39.39° and 48.41° 2 $\theta$  angles with negligible intensities overlapping with background signal.

The x-ray diffractogram of untreated *BT* soil was also analyzed and most of the intense peaks corresponded to montmorillonite mineral with a monoclinic crystal system (Figure 4.29), and the chemical composition of montmorillonite was given as  $\text{H}_2\text{Al}_{1.93}\text{Ca}_{0.06}\text{Fe}_{0.06}\text{K}_{0.27}\text{Mg}_{0.31}\text{Na}_{0.21}\text{O}_{12}\text{Si}_{3.71}$ . The remaining less intense peaks corresponded to quartz with a hexagonal crystal and chemical composition of  $\text{SiO}_2$ . The highest peak intensity for montmorillonite was 3990 counts at 5.97° 2 $\theta$ , and rest of the peaks were positioned at 21.69°, 25.19°, 27.35°, 29.41°, 34.89°, 44.69°, 45.70°, 55.23°, 61.69°, 62.01°, 64.10°, 68.2° 2 $\theta$ , respectively. The highest intensity peak for quartz was located at 26.56° 2 $\theta$  with 7000 counts, and other major peaks were at 20.8°, 36.45°, 39.39°, 40.2°, 42.40° and 50.1° 2 $\theta$ . Similarly, the *XRD* analysis was conducted for different *BT*-lime mixes and the Figure represents the comparison of the obtained results.



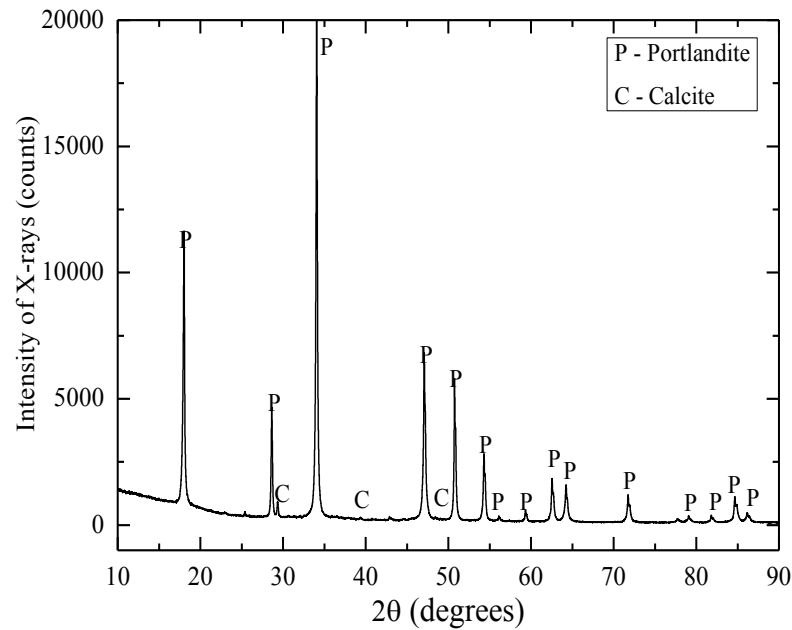


Figure 4.28 X-ray diffractogram of hydrated lime

As shown in Figure 4.30, the treating with lime and 28-day curing in controlled conditions induced significant alterations in the mineralogical properties of *BT* soil due to the short-term soil-lime interactions and consequent formation of new products. This is clearly indicated by the characteristic peak shifts and broadening effects as well as presence and absence of peaks at specific  $2\theta$  positions. On closer observation and comparison with X-ray diffractogram of untreated soil, it can be identified that the highest intensity peak for quartz located at  $26.56^\circ$   $2\theta$  with 7000 counts in untreated *BT* was suppressed to 3548 counts for *BT* treated with 12 % lime (i.e., *OLC* value). This trend was consistently followed with a further increase in lime content up to 20 % and is also observed for other peaks of quartz as well. Similarly, the highest peak intensity for montmorillonite at  $5.97^\circ$   $2\theta$  with 3990 counts was reduced to 2181 counts for *BT* treated with 12 % lime and further to 1858 counts for *BT* treated with 20 % lime. A similar trend was noticed for other major peaks of montmorillonite as well. Hence, it is assumed that the continuous reduction in peak intensities occurred due to the attack of lime on clay mineral lattices and concurrent dissolution of reactive silica and alumina.

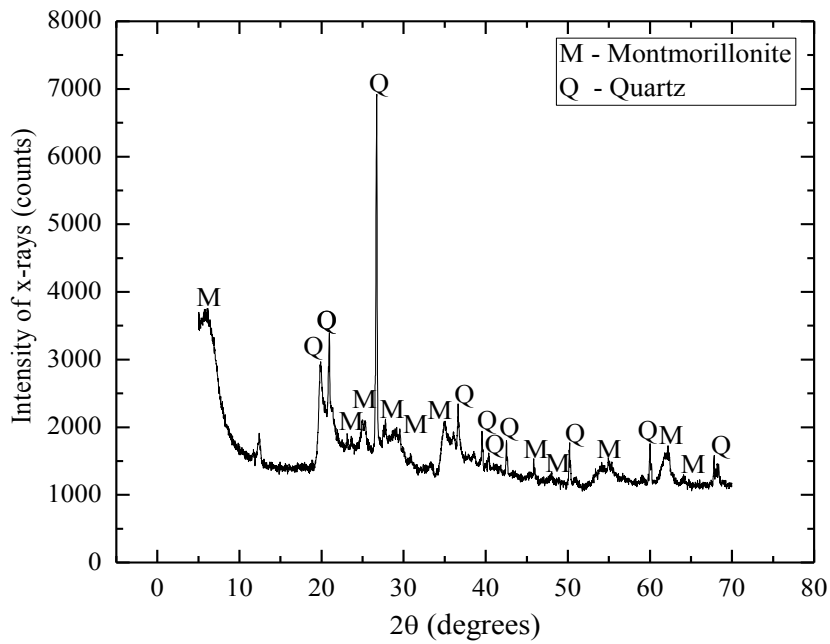


Figure 4.29 X-ray diffractogram of virgin sodium bentonite

Further, at  $2\theta$  of  $29.44^\circ$  and  $50.05^\circ$ , the intensity in counts was observed to increase with increase in lime content from 0 to 20 %, which is probably corresponding to portlandite ( $\text{Ca}[\text{OH}]_2$ ). However, the peak at  $18.03^\circ$   $2\theta$  position which also corresponded to portlandite showed reduction in intensity up to 16 % lime content; but 20 % lime content showed a shoot up in intensity which might be attributed to excess free lime present in the sample after the pozzolanic reactions ceased. Also, at peak positions of  $12.22^\circ$ ,  $20.69^\circ$  and  $44.69^\circ$  corresponding to montmorillonite in untreated *BT*, the intensity was observed to increase with lime content up to *OLC*, beyond the intensity either decreased or remained without further change when higher lime contents were added to *BT*. This trend is very well matching with the *UCS* and *FTIR* observations, and hence, it is supposed that these peak growths corresponded to formation and deposition of new cementitious products as a result of pozzolanic soil-lime reactions. Moreover, a new peak at  $11.18^\circ$  was also observed in lime-treated *BT* soil which was absent in both pure lime & in untreated *BT*.

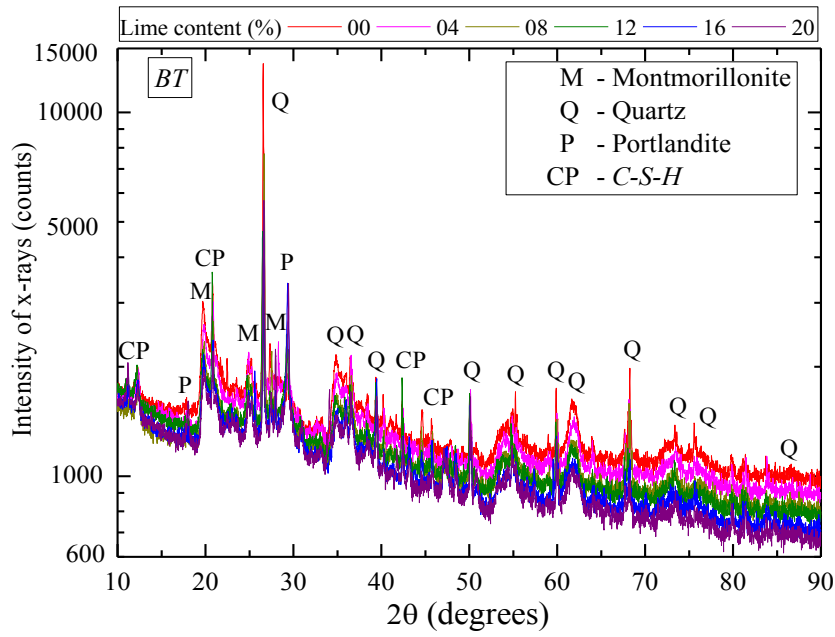


Figure 4.30 X-ray diffractograms of lime-treated sodium bentonite with varying lime content

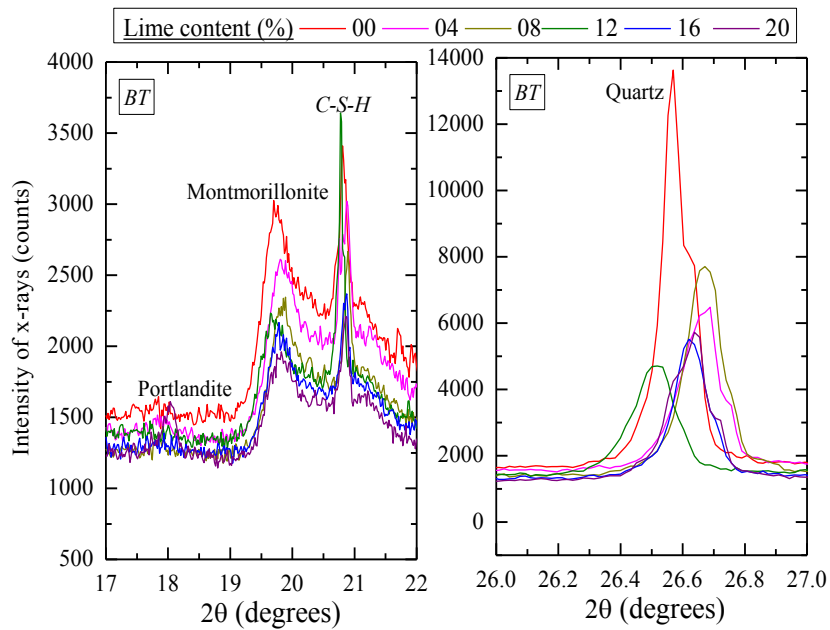


Figure 4.31 Major sections of X-ray diffractograms of lime-treated sodium bentonite with varying lime content

By observing Figure 4.31 which shows the zoomed sections of X-ray diffractograms of lime-treated *BT* soil, it can be seen that at  $2\theta$  positions of  $20.69^\circ$  and  $26.56^\circ$ , except for 12 %

lime (i.e., *OLC*) which showed maximum intensity all others followed continuously decreasing trend with the addition of lime. This also pointed towards the significant impact of *OLC* in governing the structural and chemico-mineralogical modifications of *BT* up on lime treatment, and indirectly the degree of stabilization achieved.

#### 4.6.2 Energy dispersive spectroscopy

In this thesis, energy dispersive spectroscopy was carried out on the lime-treated *BT* after a curing a period of 28-day at 25 °C in order to quantify the elemental information of the sample volume in terms of both normalized weight % and normalized atomic % concentrations as per the methodology presented in section 3.4. The elemental changes induced by the lime stabilization were studied by monitoring the intensity of peaks with different percentages of lime. *EDS* spectrums of the virgin and lime-treated soils with 6, 12 and 20 % are shown in Figure A- 6, Figure A- 7, Figure A- 8 and Figure A- 9 (Refer to Appendix). In addition, the *Si:Al*, *Ca:Si* and *Ca:Al* ratios for different soil-lime mixes are presented in Table 4.10. The predominant peaks in the *EDS* spectra are aluminum (*Al*), silicon (*Si*), magnesium (*Mg*), sodium (*Na*), iron (*Fe*), and calcium (*Ca*) for both the virgin and lime-treated samples, whereas calcium (*Ca*) showing much greater intensity for the lime-treated specimens. As a whole, *EDS* analysis offered mineralogical evidence of the changes which occurred in *BT* soil when treated with lime. This was further supported by changes in physical properties such as compaction characteristics, compressive strength, etc measured on the same samples.

Table 4.10 Elemental composition of lime-treated sodium bentonite cured for 28-day at 25 °C

Percentage of lime added to the soil (%)	Peak intensity counts			Peak intensity ratio		
	<i>Al</i>	<i>Si</i>	<i>Ca</i>	<i>Si/Al</i>	<i>Ca/Si</i>	<i>Ca/Al</i>
0	8.80	21.02	0.44	2.39	0.02	0.05
6	8.66	18.81	2.40	2.17	0.13	0.28
12	6.63	14.23	4.99	2.15	0.35	0.75
20	8.63	18.54	6.69	2.14	0.36	0.77

In case of virgin and lime-treated *BT*, significant changes can be observed from the *EDS* results in terms of *Si:Al* ratio. There was a higher reduction in the *Si:Al* ratio of samples

treated with lime content ranging from 0-20 %. This was consistent with the higher extraction of silica from the clay mineral structure. As can be seen from the Table 4.10, *Ca:Si* ratios for the lime-treated soils are found to be increasing significantly with that of virgin soil. This behaviour might be attributed to the formation of a new compound whose structure contains calcium as well as silica which contributed to a much higher *Ca:Si* ratio with increasing lime content.

#### **4.7 VARIATIONS IN MICROSTRUCTURAL CHARACTERISTICS OF LIME-TREATED SOILS**

##### **4.7.1 Scanning electron microscopy**

To understand the macro-behaviour of lime-treated soils in a more realistic manner, micro structural developments were studied using scanning electron microscopy (*SEM*). In order to study the comparative strength behaviour and microstructure of lime-treated soils, *BT* specimens stabilized with different lime percentages (0-20 %) and cured for 28-day 25°C were studied using *SEM* micrographs by employing the same methodology described in section 3.5. In the analysis of each sample, many areas were scanned so that the representative structure could be determined. Therefore the images reported in the following section are those representing the typical microstructure and composition of that soil mixture. Figure 4.32 shows the microstructure of virgin *BT* soil and *BT* soil stabilized with 6, 12 and 20 % of lime at a magnification of 2,000X. The virgin sample exhibited a dispersed film-like structure similar to that of montmorillonite which is predominant mineral in the soil (Mitchell and Soga, 2005).

From the *SEM* micrographs, it is apparent that particle sizes increased appreciably with an increase in lime content, probably owing to cation exchange reactions and concurrent flocculation phenomena which form larger agglomerates. As noted earlier, lime-treated soil specimens exhibited higher strength values with respect to different lime percentages. It is an indication that the development of cementing products with various percentages is responsible for such a difference. Due to lime treatment, soil fabric transformed to flocculated structure from dispersed structure as can be seen in Figure 4.32 (a) and (b). One

common characteristic of all the soil samples stabilized with lime was the abundance of hydration products which can be clearly seen by cementing phases. From the Figure 4.32 (c), growth of new material at edges and surface of the original soil particles can be seen clearly. The development of cementitious products increased with lime content up to 12 % which is also in good agreement with the variation of *UCS* results. This was further confirmed from the *EDS* and *TGA* results. Afterwards, with an increase in lime content, there was a decrease in *UCS*; this might be due to the carbonation effect. From the Figure 4.32 (d), the traces of unreacted lime can be seen in the form of white deposits which is further confirmed by *TGA* results. However, it was observed that determination of the pozzolanic reaction products in lime-treated *BT* samples was very challenging due to their relatively very low concentrations.

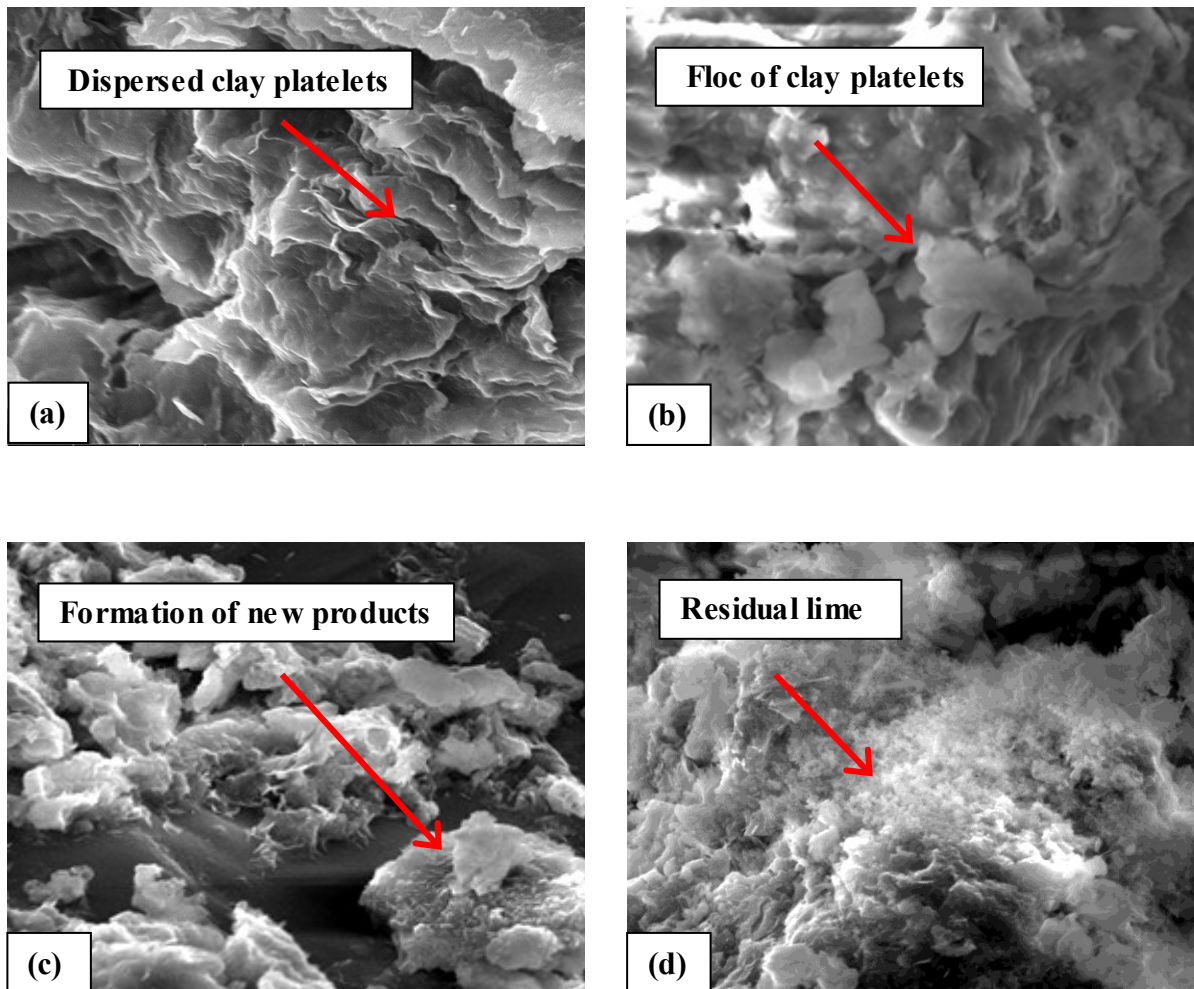


Figure 4.32 Scanning electron micrograph of lime-treated sodium bentonite cured for 28-day at 25 °C with (a) 0 % lime; (b) 6 % lime; (c) 12 % lime; (d) 20 % lime

## 5.1 GENERAL

This chapter presents the summary and conclusions of all the results discussed in the previous chapter. For the sake of brevity, the conclusions are categorised into three sections, and are presented as below.

## 5.2 INFLUENCE OF INHERENT SOIL PROPERTIES ON *OLC*

Due to the interplay of so many parameters such as soil mineralogy and virgin soil *pH*, cation exchange capacity, buffer capacity, etc, it becomes quite difficult to identify the optimum lime content, which would have the most significant influence on the efficacy and extent of stabilization in contaminated soils. In the present study, attempts have been made to evaluate the influence of *pH* and reactive nature of the virgin soil on the determination of optimum lime content, using the traditional Eades and Grim test (ASTM D6276; Eades and Grim, 1966). Further, the influence of various cation types such as  $Ca^{2+}$ ,  $Na^+$  and  $H^+$  and their varying concentrations over the electro kinetic properties of soils was also studied by conducting tests as per guidelines provided by ASTM standards.

The conclusions of this study are as follows:

- Conventional *pH* tests failed to account for reactive nature of clay minerals while determining *OLC* based on 1 hour equilibration time.
- Under virgin soil *pH* condition, *OLC* of geomaterials varies as  $WC < BT < SC$ .
- Under virgin soil *pH* condition, the buffer capacity of geomaterials varies as  $WC < SC < BT$ , for acidic and basic titrations.
- The buffer capacity values obtained by NaOH titration cannot be considered as the true property of geomaterials since none of them exhibited resistance to change in suspension *pH* with the addition of NaOH solution.

- For all other conditions being constant, *OLC* is inversely proportional to virgin *pH* and directly proportional to the buffer capacity of soil.
- The *EC* of geomaterials increases in the order of cation type as  $H^+ > Ca^{2+} > Na^+$ .

### 5.3 COMPRESSIVE STRENGTH BEHAVIOUR OF LIME-TREATED SOILS

The objective of this study was to assess the significant influence of lime content on the macro-level geotechnical properties (compaction characteristics and *UCS*) of the selected geomaterials. Also, the effect of compaction state in terms of placement moisture content and curing temperature on *UCS* characteristics of lime-treated soils was evaluated. The results obtained from this study illustrated the role of an *OLC* and placement moisture content that maximises the unconfined compressive strength of an engineered lime-treated cohesive soil. Following are the major conclusions that can be drawn from this study:

- With the addition of lime, the compaction response of *BT* and *WC* soils tends to be flatter.
- Virgin white clay having more clay content compared to sodium bentonite exhibited relatively greater magnitude and rate of *UCS* improvement, as fine clay particles filled internal porous cavities of compacted specimen and mobilised complete strength.
- For virgin and lime-treated white clay *DMC* and *WMC* compaction states showed a decrease in *UCS* compared to *OMC*, which is in line with the variation of its dry unit weight with respect to moisture content.
- For virgin as well as lime-treated sodium bentonite, the *UCS* increased proportionally with placement moisture content up to *WMC*, probably owing to extended long-term pozzolanic reactions driven by higher moisture content.
- *UCS* value of both soils after lime treatment significantly increased with curing period, owing to formation and deposition of pozzolanic reaction products which strongly binds the soil particles into a hard matrix.

Irrespective of the lime content, compaction state and curing period, both virgin and lime-treated white clay as well as sodium bentonite exhibited relatively higher strength at 40 °C



curing when compared to 25°C; this is attributed to the accelerated kinetics of pozzolanic reactions at elevated temperatures.

A concluding inference from this work is that the controlled and uniform placement of soil-lime mixtures with optimum lime and moisture contents shows superior results, beyond any doubt. Further, this research has taken note that the degree of strength gain of in-situ lime-treated soils is subjected greatly to prevailing temperature. The study also emphasizes that insufficiency of free lime and reactive clay minerals, as well as inadequate curing period, can subsequently lead to the relatively inferior performance of lime-treated soils.

#### 5.4 CHARACTERIZATION OF LIME-TREATED SOILS

The main objective of this study was to assess the chemico-mineralogical and microstructural variations occurring during short-term curing of lime-treated soils. The qualitative and quantitative estimation of relative quantities of hydration products, calcite and residual lime was enabled by detailed analysis of the *XRD*, *TGA-DTA*, *FTIR*, and *SEM-EDS*. Further, these results were correlated with 28-days *UCS* of *BT* treated with varying lime contents, which in turn provides a direct inference on the degree of pozzolanic soil-lime reactions as well as the unfavorable lime carbonation phenomena. The major conclusions from the study are as follows:

- The major mineral detected in the clay fraction of *BT* soil is montmorillonite.
- The addition of the lime resulted in the formation of new reaction products. These reaction products were detected as calcium silicate hydrates (*CSH*) in *SEM-EDS* and *XRD*.
- The peak intensities corresponding to the formation of *CSH* were found to be increasing up to 12 % lime addition and decreased beyond which is agreement with the *UCS* results.
- The *TGA-DTA* analysis showed that the weight loss of free and bound water decreased proportionally with increasing lime content which correlates to the degree of pozzolanic reactions and progressive gel hydration of reaction products.

- In *TGA-DTA*, the increasing weight loss of *CSH* up to the optimum lime content of 12 % indicates a higher degree of clay-lime reactions; further decrease in *CSH* weight loss might be owing to retardation of pozzolanic reactions attributed to lime carbonation.
- Most of the amorphous and crystalline calcium carbonate observed in *TGA-DTA* analysis ensues from the carbonation of excess lime and hydration products during curing of lime-treated soils.
- *Ca:Si* ratios from *EDS* were tentatively assigned to the development of a gel compound micro-structure of pozzolanic products which found to be increasing with lime content.
- *FTIR* and *EDS* results also provided reliable justification for the variations in the *UCS* behaviour of lime-treated soils.

The results of the characterization of lime-treated soils evidence the formation of hydration products and calcite in the lime-treated soil during curing. Thus, the present study demonstrates that the thorough analysis of micro-level studies enables reliable interpretation of the kinetics of pozzolanic soil-lime reactions occurring in lime-treated soils and the behaviour of ensuing physico-mechanical modifications.

## **FUTURE SCOPE OF RESEARCH WORK**

---

The major focus of the present study is limited to the evaluation of the short-term strength behaviour of lime-treated soils under different curing conditions, in view of understanding the predominant physico-chemical mechanisms of soil-lime reactions involved in the process of stabilization. However, the short-term effects of lime treatment can also lead to drastic changes in the volume change as well as the permeability properties. Hence, this study can be further extended to the evaluation of the influence of key parameters such as clay mineralogy and curing conditions up on the variations of volume change and permeability characteristics of lime-treated soils. Furthermore, there is scope for assessing the long-term performance of lime-treated soils in terms of stiffness and durability properties, keeping view of field applications. The advanced characterization tools employed in this study can aid to identify the compatibility between diverse soil types and stabilizers and determining their optimum design mixes, for achieving desirable improvement.

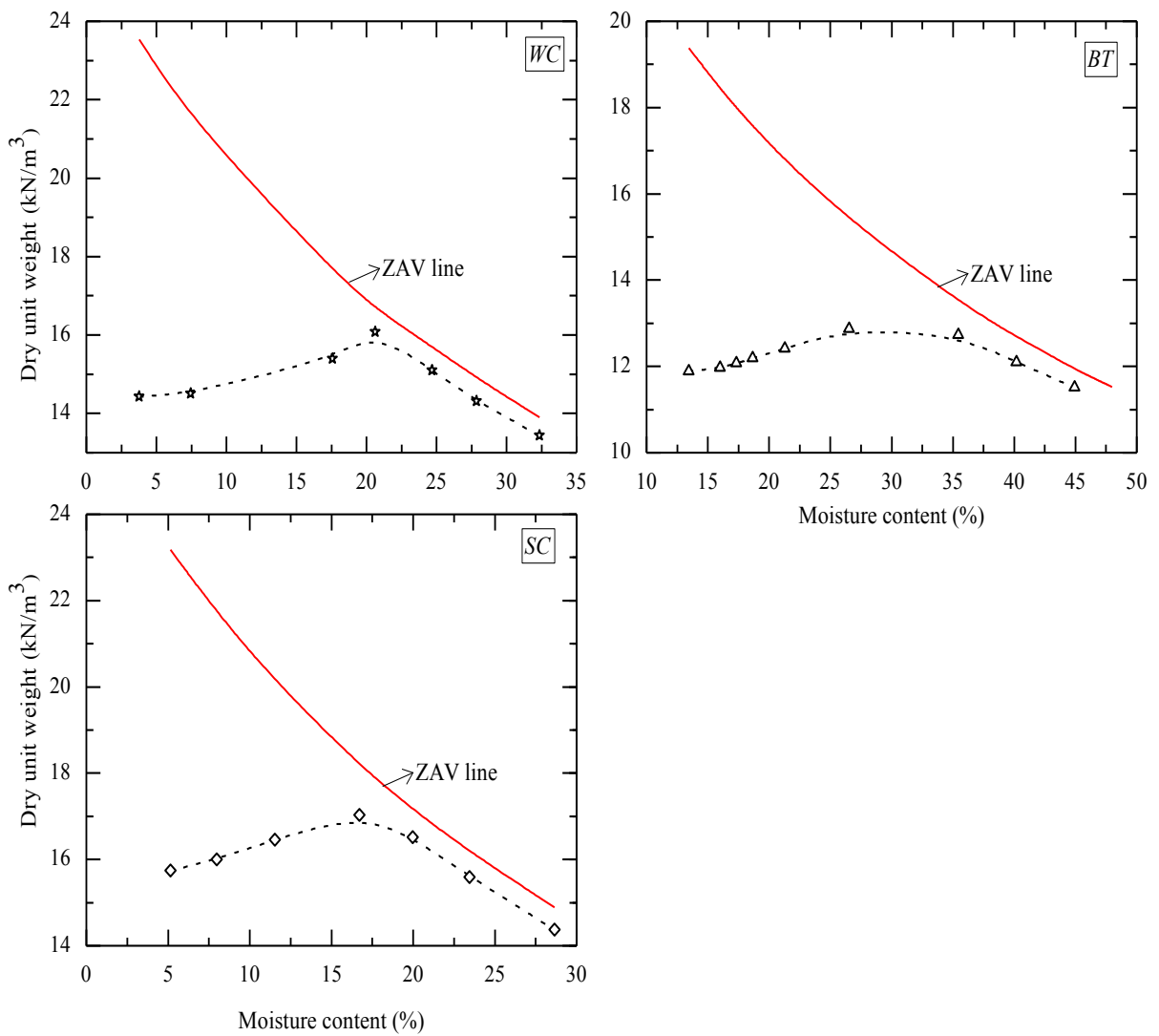


Figure A- 1 Standard proctor compaction curves for selected geomaterials

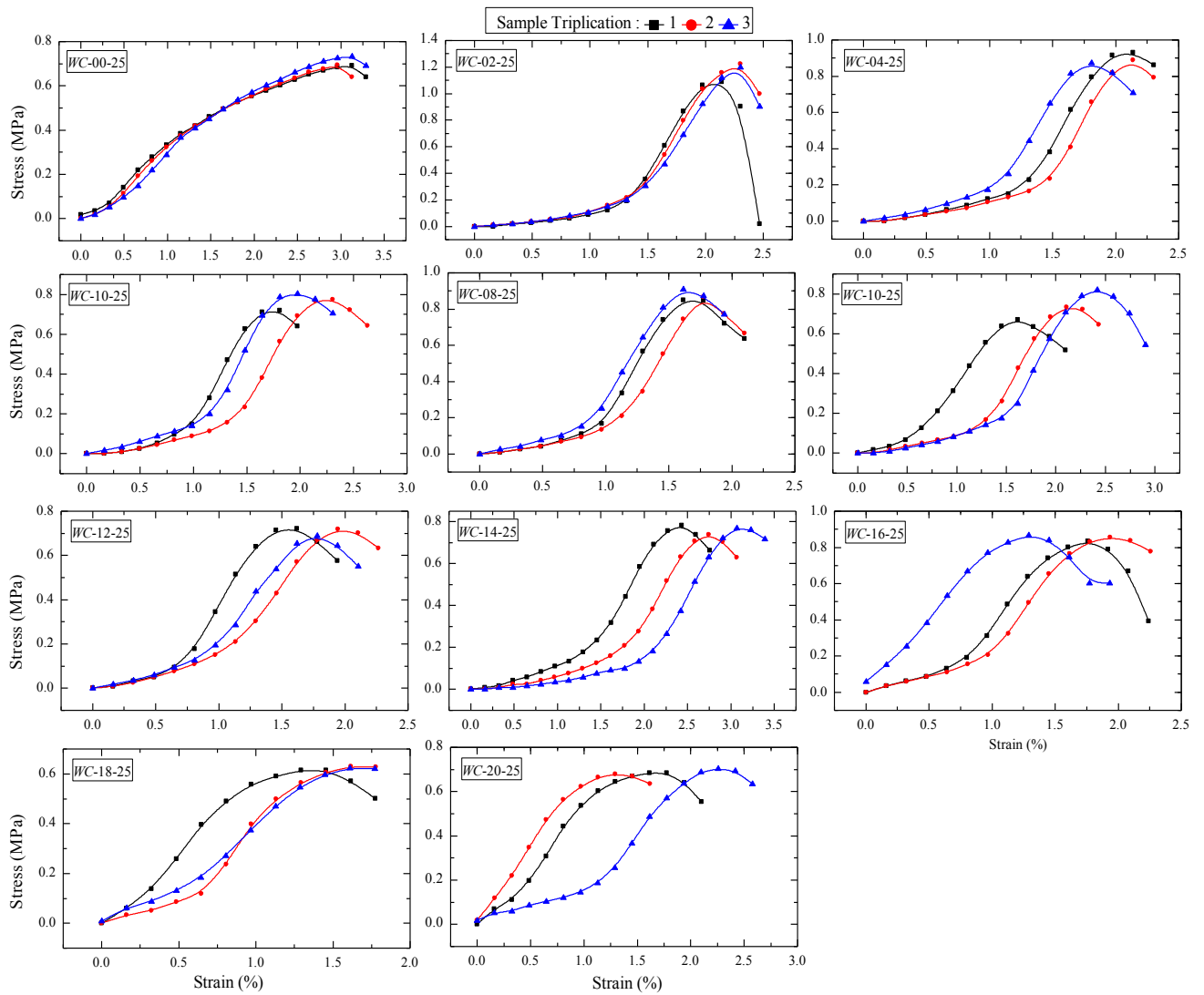


Figure A- 2 Stress-strain curves of lime-treated white clay cured at 25 °C for 28 days

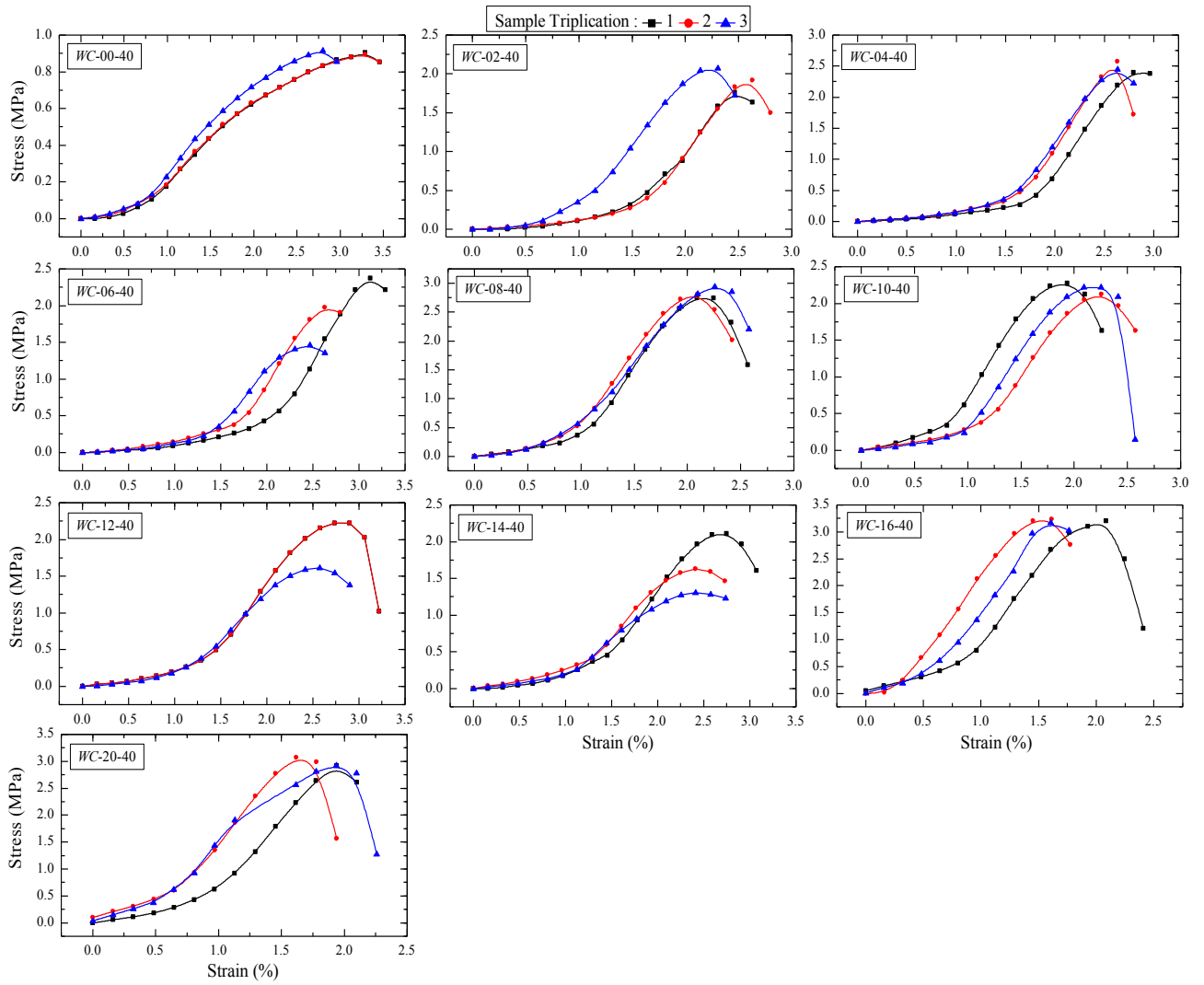


Figure A- 3 Stress-strain curves of lime-treated white clay cured at 40 °C for 28 days

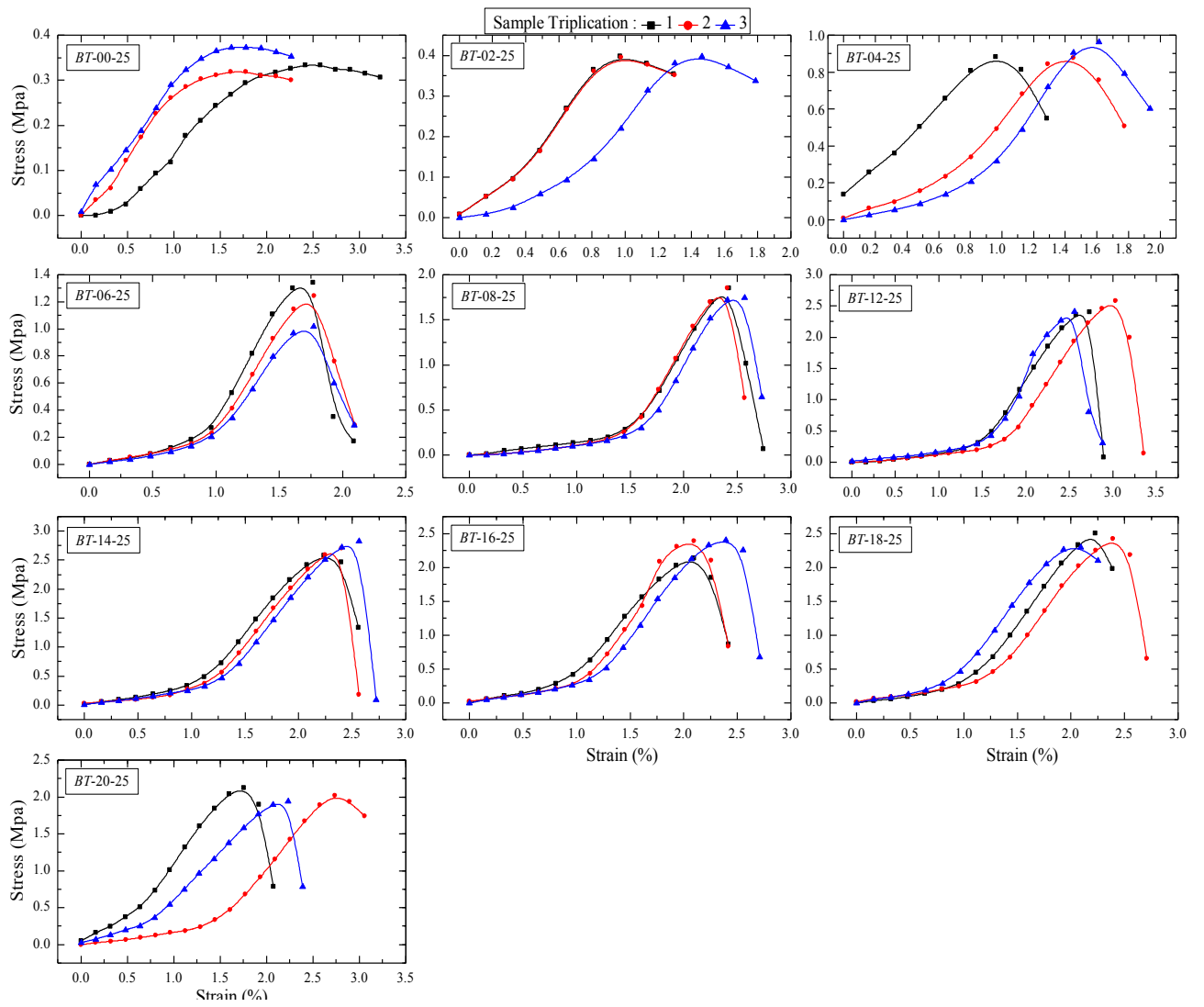


Figure A- 4 Stress-strain curves of lime-treated sodium bentonite cured at 25 °C for 28 days

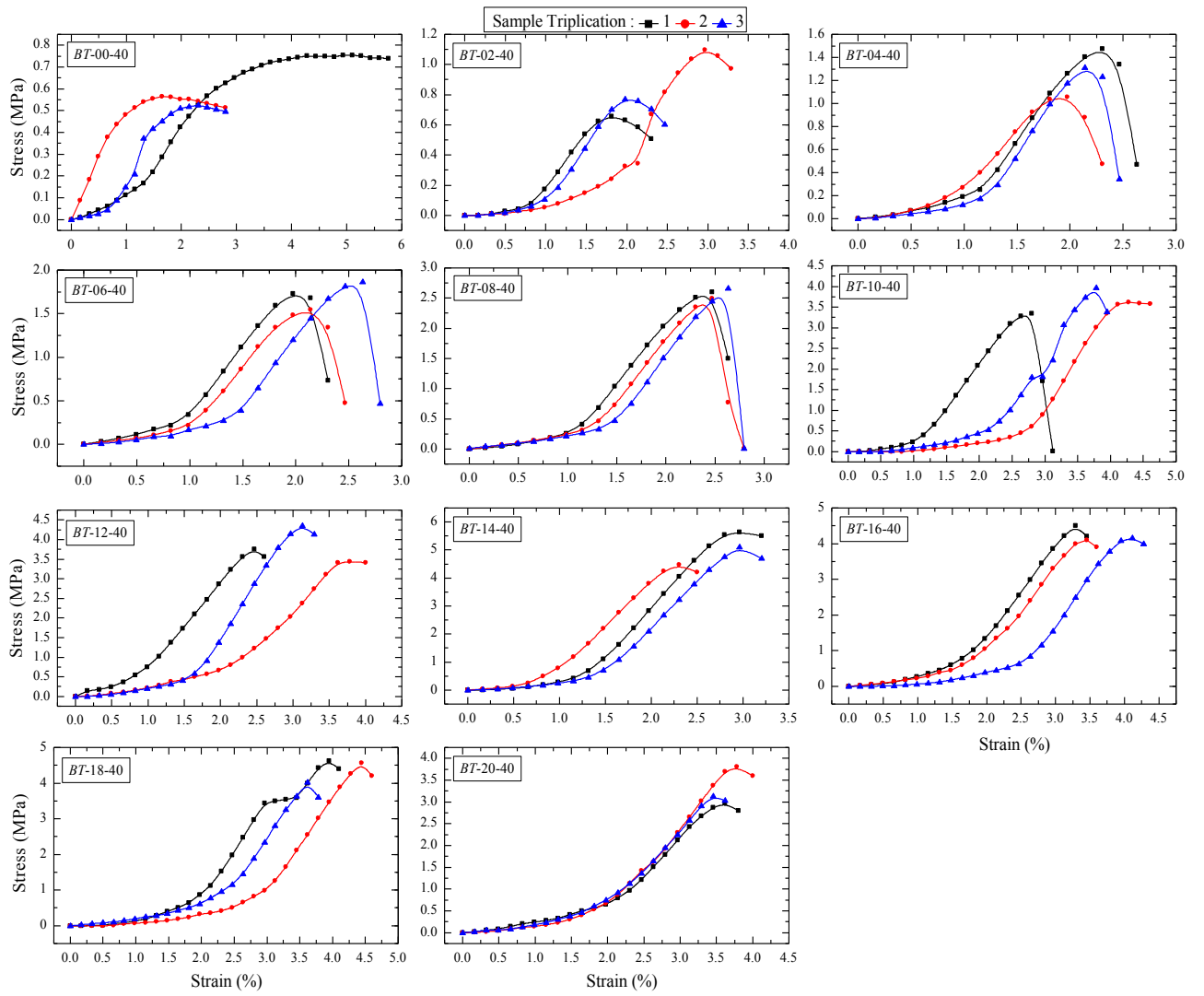
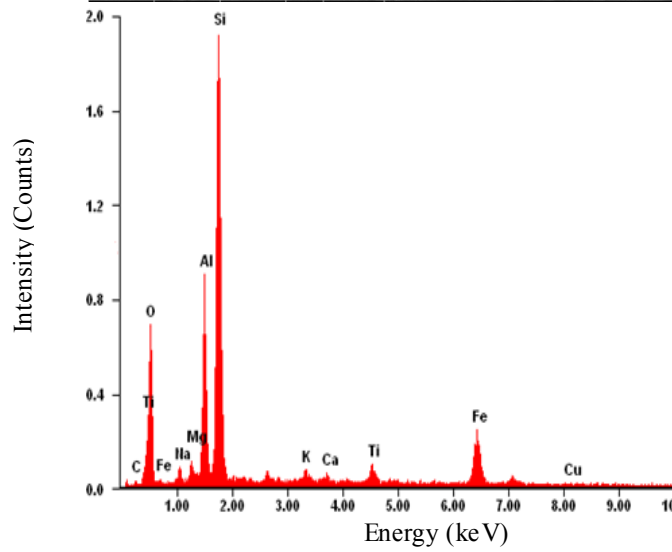
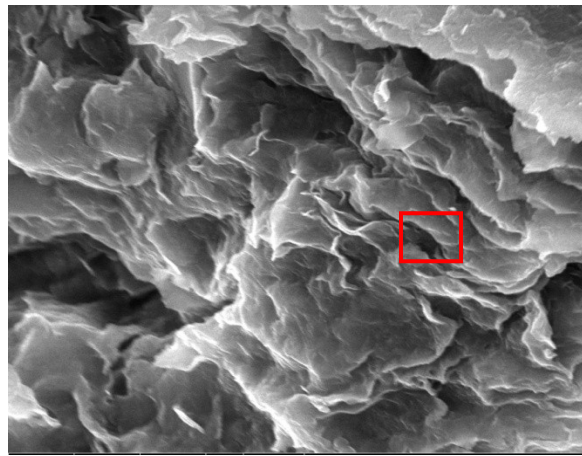


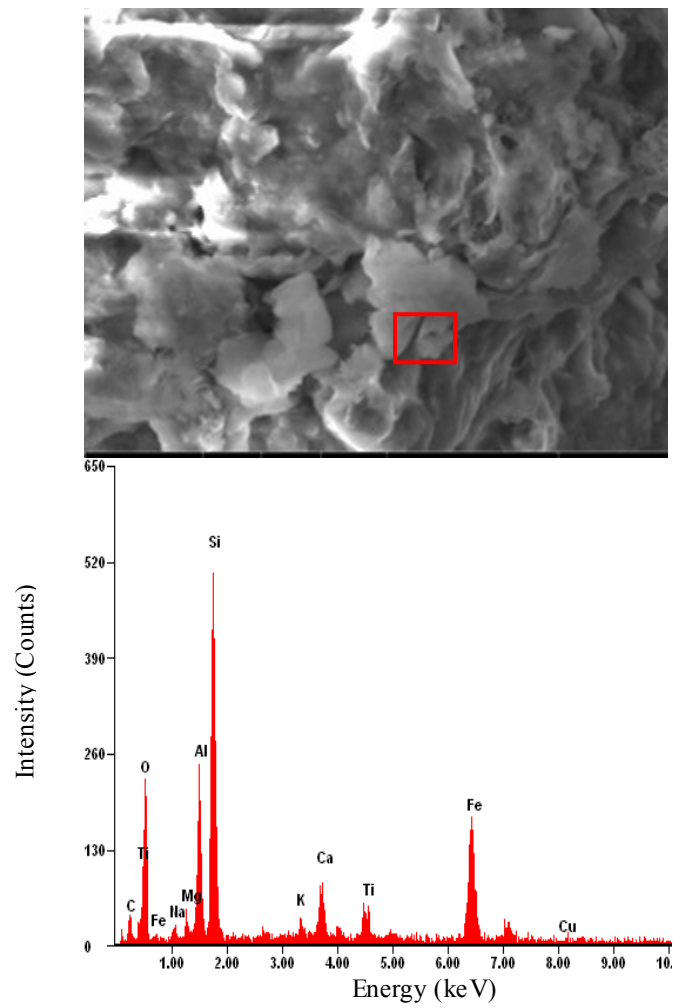
Figure A- 5 Stress-strain curves of lime-treated sodium bentonite cured at 40 °C for 28 days





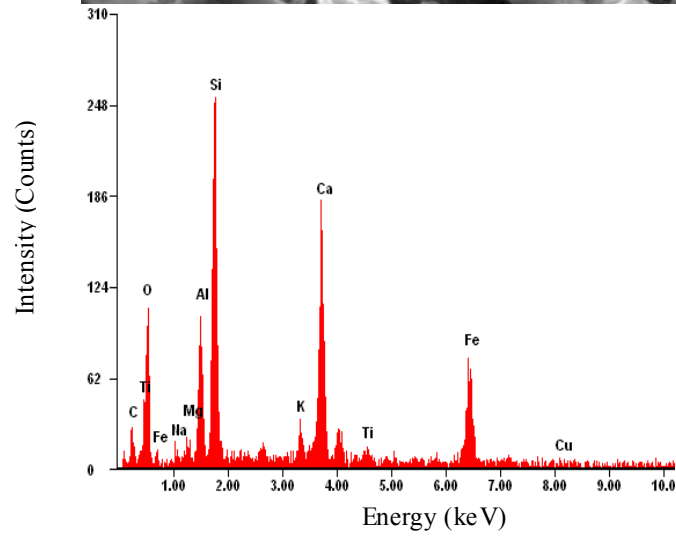
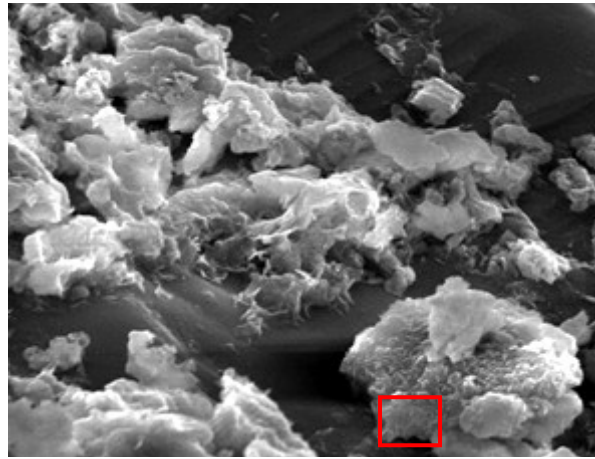
Element	Wt %	At %
C	8.205	14.318
O	35.308	46.997
Na	1.498	1.403
Mg	1.342	1.182
Al	11.056	8.798
Si	27.681	21.022
K	1.007	0.547
Ca	0.805	0.437
Ti	1.261	0.568
Fe	11.447	4.595
Cu	0.381	0.131

Figure A- 6 Energy dispersive spectroscopy of untreated sodium bentonite cured for 28- days at 25 °C



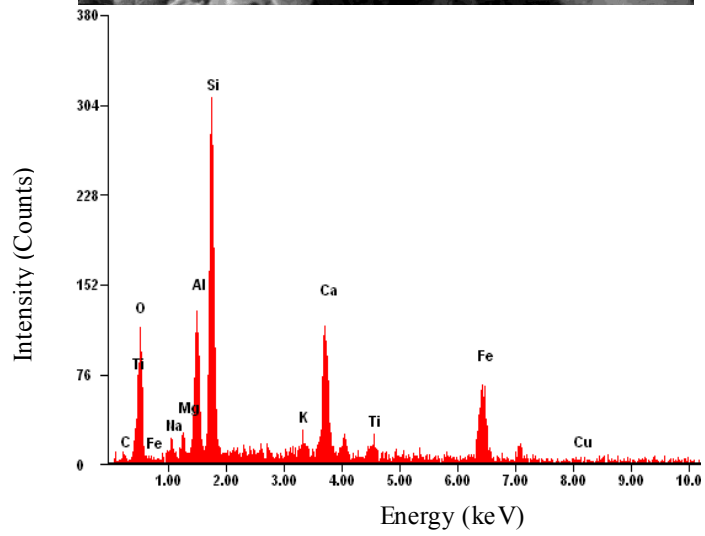
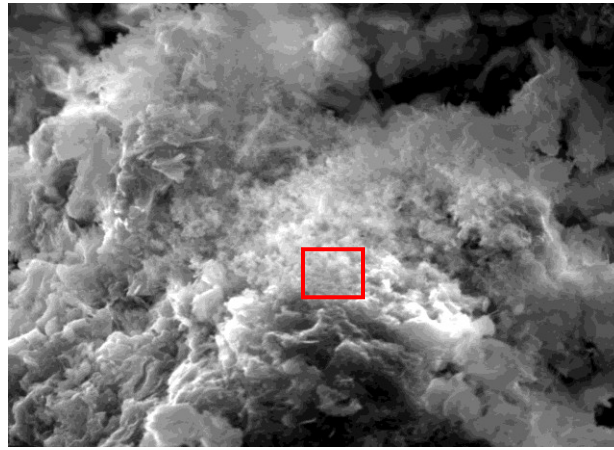
Element	Wt %	At %
C	10.646	18.256
O	32.488	43.152
Na	1.612	1.499
Mg	1.438	1.272
Al	10.855	8.658
Si	24.653	18.815
K	1.221	0.665
Ca	4.321	2.402
Ti	1.711	0.794
Fe	10.655	4.343
Cu	0.398	0.14

Figure A- 7 Energy dispersive spectroscopy of sodium bentonite treated with 6 % lime and cured for 28-days at 25 °C



Element	Wt %	At %
C	14.608	23.805
O	32.445	43.808
Na	1.56	1.423
Mg	1.325	1.133
Al	8.52	6.63
Si	21.945	14.226
K	1.073	0.57
Ca	9.588	4.99
Ti	1.45	0.638
Fe	6.968	2.605
Cu	0.513	0.168

Figure A- 8 Energy dispersive spectroscopy of sodium bentonite treated with 12 % lime and cured for 28-days at 25 °C



Element	Wt %	At %
C	5.931	10.832
O	34.335	47.681
Na	1.672	1.622
Mg	1.66	1.522
Al	10.437	8.63
Si	23.368	18.54
K	1.128	0.645
Ca	12.13	6.688
Ti	1.772	0.824
Fe	7.134	2.867
Cu	0.425	0.148

Figure A- 9 Energy dispersive spectroscopy of sodium bentonite treated with 20 % lime and cured for 28-days at 25 °C

## REFERENCES

---

- 1). **Alkan, M., Demirbaş, O. and Dogan, M.** (2005). Electrokinetic properties of kaolinite in mono and multivalent electrolyte solutions, *Microporous and Mesoporous Materials*, **83**, 51-59.
- 2). **Al-Kiki, I. M., Al-Atalla, M. A. and Al-Zubaydi, A. H.** (2011). Long term strength and durability of clayey soil stabilized with lime, *Journal of Engineering & Technology*, **29(4)**, 725-735.
- 3). **Al-Mukhtar, M., Khattab, S. and Alcover, J. F.** (2012). Microstructure and geotechnical properties of lime-treated expansive clayey soil, *Engineering Geology*, **139-140**, 17-27.
- 4). **Al-Mukhtar, M., Lasledj, A. and Alcover, J. F.** (2010). Behaviour and mineralogy changes in lime-treated expansive soil at 50°C, *Applied Clay Science*, **50**, 199-203.
- 5). **Arabani, M. and Karami, M. V.** (2007). Geomechanical properties of lime stabilized clayey sands, *Arabian Journal for Science and Engineering*, **32(1B)**, 11-25.
- 6). **Arnepalli, D. N., Shanthakumar, S., Rao, B. H. and Singh, D. N.** (2007). Comparison of methods for determining specific-surface area of fine-grained soils, *Geotechnical and Geological Engineering*, **26**, 121-132.
- 7). **Arvind, K. J. and Sivapullaiah, P.V.** (2016). Volume change behavior of lime treated gypseous soil-influence of mineralogy and microstructure, *Applied Clay Science*, **119**, 202-212.
- 8). **ASTM D2166** (2016). Standard test method for unconfined compressive strength of cohesive soil, *ASTM International*, West Conshohocken, PA, USA.
- 9). **ASTM D2487** (2011). Standard practice for classification of soils for engineering purposes (Unified Soil Classification System), *ASTM International*, West Conshohocken, PA, USA.
- 10). **ASTM D422** (2007). Standard test method for particle-size analysis of soils, *ASTM International*, West Conshohocken, PA, USA.

- 11). **ASTM D4318** (2010). Standard Test Methods for liquid limit, plastic limit, and plasticity index of soils, *ASTM International*, West Conshohocken, PA, USA.
- 12). **ASTM D5550** (2006). Standard test method for specific gravity of soil solids by gas pycnometer, *ASTM International*, West Conshohocken, PA, USA.
- 13). **ASTM D6276** (2006). Standard test method for using pH to estimate the soil–lime proportion requirement for soil stabilization, *ASTM International*, West Conshohocken, PA, USA.
- 14). **ASTM D698** (2012). Standard test methods for laboratory compaction characteristics of soil using standard effort, *ASTM International*, West Conshohocken, PA, USA.
- 15). **ASTM D7503** (2010). Standard test method for measuring the exchange complex and cation exchange capacity of inorganic fine-grained soils, *ASTM International*, West Conshohocken, PA, USA.
- 16). **Barker, J. E., Rogers, C. D. F. and Boardman, D. I.** (2006). Physico-chemical changes in clay caused by ion migration from lime piles, *Journal of Materials in Civil Engineering*, **18**, 182-189.
- 17). **Beetham, P., Dijkstra, T., Dixon, N., Fleming, P., Hutchison, E. I. R. and Bateman, J.** (2014). Lime stabilization for earth works: a UK perspective, *Proceedings of the ICE - Ground Improvement*, **168 (2)**, 81-95.
- 18). **Bekki, H., Djilaili, Z., Tlidji, Y. and Daouadji, T. H.** (2015). Durability of treated silty soil using lime and cement in road construction - a comparative study, *The Online Journal of Science and Technology*, **5(2)**, 23-31.
- 19). **Bozbey, I. and Garaisayev, S.** (2010). Effect of soil pulverization quality on lime stabilization of an expansive soil, *Environmental Earth Science*, **60**, 1137-1151.
- 20). **Bray, H. T. and Redfern, S. A. T.** (1999). Kinetics of dehydration of Ca-montmorillonite, *Physics and Chemistry of Minerals*, **26**, 591-600.
- 21). **Cerato, A. B. and Lutenecker, A. J.** (2002). Determination of surface area of fine-grained Soils by the ethylene glycol monoethyl ether (EGME) method, *Geotechnical Testing Journal*, **25(3)**, 1-7.

- 22). **Cherian, C. and Arnepalli, D. N.** (2015). A critical appraisal of the role of clay mineralogy in lime stabilization, *International Journal of Geosynthetics and Ground Engineering*, **1(8)**, 1-20.
- 23). **Chew, S. H., Kamruzzaman, A. H. M. and Lee, F. H.** (2004). Physico-chemical and engineering behaviour of cement treated clays, *Journal of Geotechnical and Geo-environmental Engineering*, **130(7)**, 696-706.
- 24). **Chorom, M. and Rengasamy, P.** (1995). Dispersion and zeta potential of pure clays as related to net particle charge under varying pH, electrode concentration and cation type, *European Journal of Soil Science*, **46**, 657-665.
- 25). **Croft, J. B.** (1968). The problem in predicting the suitability of soils for cementitious stabilization, *Engineering Geology*, **2(6)**, 397-424.
- 26). **Dellisanti, F., Minguzzi, V. and Valdre, G.** (2006). Thermal and structural properties of Ca-rich montmorillonite mechanically deformed by compaction and shear, *Applied Clay Science*, **31**, 282-289.
- 27). **Drits, V. A., Derkowski, A. and McCarty, D. K.** (2012). Kinetics of partial dehydroxylation in dioctahedral 2:1 layer clay minerals, *American Mineralogist*, **97(5-6)**, 930-950.
- 28). **Eades, J. L. and Grim, R. E.** (1962). Reaction of hydrated lime with pure clay minerals in soil stabilization, *Highway Research Board, Bulletin*, **262**, 51-63.
- 29). **Eades, J. L. and Grim, R. E.** (1966). A quick test to determine lime requirements for lime stabilization, *Highway Research Board, Bulletin*, **139**, 61-72.
- 30). **Eisazadeh, A., Khairul, A. K. and Nur, H.** (2010). Molecular characteristics of phosphoric acid treated soils, *International Journal of Civil, Environmental, Structural, Construction and Architectural Engineering*, **4(3)**, 56-58.
- 31). **Eisazadeh, A., Khairul, A. K. and Nur, H.** (2010). Thermal characterization of lime stabilized soils, *19<sup>th</sup> World Congress of Soil Science, Soil Solutions for a Changing World*, 1-6 August, Brisbane, Australia, 20-23.

- 32). **Eisazadeh, A., Khairul, A. K. and Nur, H.** (2011). Characterization of phosphoric acid- and lime-stabilized tropical lateritic clay, *Environmental Earth Sciences*, **63**, 1057-1066.
- 33). **Eisazadeh, A., Khairul, A. K. and Nur, H.** (2012). Solid-state NMR and FTIR studies of lime stabilized montmorillonitic and lateritic clays, *Applied Clay Science*, **67-68**, 5-10.
- 34). **Federer, C. A. and Hornbeck, J. W.** (1985). The buffer capacity of forest soils in New England, *Water, Air and Soil Pollution*, **26**, 163-173.
- 35). **Gabrovsek, R., Vuk, T. and Kaucic, V.** (2006). Evaluation of the hydration of portland cement containing various carbonates, *Acta Chimica Slovenica*, **53**, 159-165.
- 36). **George, S. Z., Ponniah, D. A. and Little, J. A.** (1992). Effect of temperature on lime-soil stabilization, *Construction and Building Materials*, **6(4)**, 247-252.
- 37). **Ghods, P., Chini, M., Alizadeh, R. and Hoseini. M.** (2012). The effect of different exposure conditions on the chloride diffusion into concrete in the Persian Gulf region, *2<sup>nd</sup> International Conference on Microstructure Related Durability of Cementitious Composites*, 11-13 April, Amsterdam, The Netherlands.
- 38). **Ghosh, A. and Subbarao, C.** (2001). Microstructural development in fly ash modified with lime and gypsum, *Journal of Materials in Civil Engineering*, **13(1)**, 65-70.
- 39). **Gillot, J. E.** (1987). *Clay in Engineering Geology*, 2<sup>nd</sup> Edition, Elsevier Science. USA.
- 40). **Horpibulsuk, S., Rachan, R., Chinkulkijniwat, A., Raksachon, Y. and Suddeepong, A.** (2010). Analysis of strength development in cement-stabilized silty clay from microstructural considerations, *Construction and Building Materials*, **24**, 2011-2021.
- 41). **Huiming, S., Bin, G., Yuan, T., Xianqiang, Y., Congrong Yu., Yiquan, W. and Lena, Q.** (2010). Kaolinite and lead in saturated porous media: facilitated and impeded transport, *Journal of environmental engineering*, **136(11)**, 1305-1308.



- 42). **Hussain, M. and Dash, S.K.** (2009). Influence of lime on compaction behaviour of soils, *Indian Geotechnical Conference*, 17-19 December, Guntur, India, 15-17.
- 43). **Ingles, O. G. and Metcalf, J. B.** (1972). *Soil Stabilization: Principles and Practice*, Butterworths, Melbourne.
- 44). **IS 2720, Part XXIV** (1976). Methods of test for soils: determination of cation exchange capacity, *Bureau of Indian Standards*, New Delhi, India.
- 45). **Ismail, H. A. H.** (2006). Cement kiln dust chemical stabilization of expansive soil exposed at el-Kawther quarter, Sohag region, Egypt, *International Journal of Geosciences*, **4**, 1416-1424.
- 46). **Ismail, A. I. M.** (2004). Engineering and petrological characteristics of clayey silt soils to be used as road base and their improvement by lime and cement, *Doctoral Dissertation*. Technical University of Clausthal, Germany.
- 47). **James, B. A.** (2013). Physicochemical behaviour of artificial lime stabilised sulphate bearing cohesive soils. *Doctoral Dissertation*, University of Nottingham, England, U.K.
- 48). **Jawad, I. T., Taha, M. R., Majeed, Z. H. and Khan, T. A.** (2014). Soil stabilization using lime: advantages, disadvantages and proposing a potential alternative, *Research Journal of Applied Sciences, Engineering and Technology*, **8(4)**, 510-520.
- 49). **Jayakumar, M and Lau Chee Sing.** (2012). Experimental studies on treated subbase soil with fly ash and cement for sustainable design recommendations, *International Journal of Engineering and Applied Sciences*, **68**, 331-334.
- 50). **Jimenez, F., Palomo, A., Pastor, J. Y. and Martin, A.** (2008). New cementitious materials based on alkali-activated fly ash: performance at high temperatures, *Journal of the American Ceramic Society*, **91**, 3308-3314.
- 51). **Jung, C. and Bobet, A.** (2008). Post-construction evaluation of lime-treated soils, *Joint Transport Research Program Technical Reports*, School of Civil Engineering, Purdue University, USA.
- 52). **Kavak, A. and Baykal, G.** (2012). Long-term behaviour of lime-stabilized kaolinite clay, *Environmental Earth Sciences*, **66(7)**, 1943-1955.

- 53). **Kenneth, C. J. V. R., Edward, A. S., Rao, P. S. C. and Ramesh Reddy, K.** (1991). Evaluation of laboratory techniques for measuring diffusion coefficients in sediments, *Environmental Science Technology*, **25(9)**, 1605-1611.
- 54). **Kissel, D. E., Isaac, B., Hitchcock, R., Sonon, L. and Vendrell, P. F.** (2005). Lime requirement by measurement of the lime buffer capacity. <http://www.naptprogram.org/files/napt/publications/method-papers/2005-lime-requirement-by-the-measurment-of-the-lime-buffer-capacity.pdf>
- 55). **Kolias, S., Kasselouri-Rigopoulou, V. and Karahalios, A.** (2005). Stabilisation of clayey soils with high calcium fly ash and cement, *Cement & Concrete Composites*, **27**, 301-313.
- 56). **Kontori, E., Perraki, T., Tsvilis, S. and Kakali, G.** (2009). Zeolite blended cements: evaluation of their hydration rate by means of thermal analysis, *Journal of Thermal Analytical Calorimetry*, **96**, 993-998.
- 57). **Lasledj, A. and Al-mukhtar, M.** (2008). Effect of hydrated lime on the engineering behaviour and the microstructure of highly expansive clay, *The 12<sup>th</sup> International Conference of International Association for Computer Methods and Advances in Geomechanics (IACMAG)*, 1-6 October, Goa, India.
- 58). **Lav, M. A. and Lav, A. H.** (2000). Microstructural development of stabilized fly ash as Pavement base material, *Journal of Materials in Civil Engineering*, **12(2)**, 157-163.
- 59). **Lee, J., Fox, P. J. and Lenhart, J. J.** (2009). Investigation of consolidation-induced solute transport. I: Effect of consolidation on transport parameters, *Journal of Geotechnical and Geoenvironmental Engineering*, **135(9)**, 1228-1238.
- 60). **Leroy, P., Revil, A. and Coelho, D.** (2005). Diffusion of ionic species in bentonite, *Journal of Colloid and Interface Science*, **296**, 248-255.
- 61). **Little, D. L.** (1987). Fundamentals of the stabilization of soil with lime, *National Lime Association, Bulletin 332*, Arlington, Virginia.
- 62). **Mackenzie, R. C., Heller-Kallai, L., Rahman, A. A. and Moir, H. M.** (1988). Interaction of kaolinite with calcite on heating: III. effect of different kaolinites, *Clay Minerals*, **23**, 191-203.

- 63). **Madejova, J. and Komadel, P.** (2001). Baseline studies of the clay minerals society source clays: Infrared methods, *Clays and Clay Minerals*, **49(5)**, 410-432.
- 64). **Magdy, A. A. and Mostafa, A. A.** (2012). Measured effects on engineering properties of clayey subgrade using lime-Homra stabiliser, *International Journal of Pavement Engineering*, **14(4)**, 321-332.
- 65). **Marto, A., Hassan, M. A., Makhtar, A. M. and Othman, B. A.** (2013). Shear strength improvement of soft clay mixed with Tanjung bin coal ash, 4<sup>th</sup> *International Conference on Environmental Science and Development*, 19-20 January, Dubai, United Arab Emirates.
- 66). **Mitchell, J. K. and Soga, K.** (2005). *Fundamentals of Soil Behaviour*, 3<sup>rd</sup> Edition, Wiley, New York, USA.
- 67). **Mooney, M. A. and Toohey, N. M.** (2010). Accelerated curing and strength-modulus correlation for lime-stabilized soils, *The Colorado department of transportation (DTD), Applied Research and Innovation Branch, Report No. CDOT-2010-1*.
- 68). **Morsey, M. S. and Heikal, M.** (2004). Effect of curing temperature on the thermal expansion and phase composition of hydrated limestone-slag cement, *Ceramics - Silikaty*, **48 (3)**, 110-116.
- 69). **Muhmed, A. and Wanatowski, D.** (2013). Effect of lime stabilisation on the strength and microstructure of clay, *IOSR Journal of Mechanical and Civil Engineering*, **6(3)**, 87-94.
- 70). **Muntohar, A. S.** (2005). The influence of molding water content and lime content on the strength of stabilized soil with lime and rice husk ash, *Civil Engineering Dimension*, **7 (1)**, 1-5.
- 71). **Muntohar, A. S. and Jiun-Liao, H.** (2006). Strength distribution of soft clay surrounding lime-column. *Proceedings of the Fourth International Conference on Soft Soil Engineering*, 4-6 October, Vancouver, Canada, 315-320.
- 72). **Narmluk, M. and Nawa, T.** (2014). Effect of curing temperature on pozzolanic reaction of fly ash in blended cement paste, *International Journal of Chemical Engineering and Applications*, **5 (1)**, 31-35.

- 73). **Nasrizar, A. A., Muttharam, M. and Ilamparuthi, K.** (2010). Role of lime content on soil-lime reaction under thermal curing, *Indian Geotechnical Conference*, 16-18 December, Mumbai, India, 595-598.
- 74). **Nelson, J. D. and Miller, D. J.** (1992). *Expansive soils: Problem and Practice in Foundation and Pavement Engineering*, John Wiley, New York, USA.
- 75). **Nontananandh, S., Boonyong, S. and Yoobanpot, T.** (2005). Investigations on reaction products in soil cement, GTE 13-16, *In Proceeding of the 10<sup>th</sup> National Convention on Civil Engineering*, 2-4.
- 76). **Quang, N. D. and Chai, J. C.** (2015). Permeability of lime and cement-treated clayey soils, *Canadian Geotechnical Journal*, **52**, 1221-1227.
- 77). **Rajasekaran, G. and Rao, S. N.** (2002). Compressibility behaviour of lime-treated marine clay, *Ocean Engineering*, **29**, 545-559.
- 78). **Rajasekaran, G. and Rao, S. N.** (2004). Falling cone method to measure the strength of marine clays, *Ocean Engineering*, **31**, 1915-1927.
- 79). **Rao, N. S. and Mathew, P. K.** (1995). Effects of exchangeable cations on hydraulic conductivity of marine clay, *Clays and Clay Minerals*, **43(4)**, 433-437.
- 80). **Rao, N. S. and Rajasekaran, G.** (1994). Lime injection technique to improve the behaviour of soft marine clays, *Ocean Engineering*, **21(1)**, 29-43.
- 81). **Robin, V., Cuisinier, O., Masrouri, F. and Javadi, A. A.** (2014). A chemo-mechanical modeling of yield stress for lime treated soils, *Applied Clay Science*, **95**, 211-219.
- 82). **Rogers, C. D. F and Glendinning, S.** (1996). The role of lime migration in lime pile stabilization, *Quarterly Journal of Engineering Geology and Hydrogeology*, **29**, 273-284.
- 83). **Saeed, K. A. H., Kassim, K. A., Nur, H. and Yunus, N. Z. M.** (2013). Characterization of hydrated lime-stabilized brown kaolin clay, *International Journal of Engineering Research & Technology (IJERT)*, **2(11)**, 3722-3727.

- 84). **Saeed, K. A. H., Kassim, K. A., Nur, H. and Yunus, N. Z. M.** (2015). Physico-chemical characterization of lime stabilized tropical kaolin clay, *Jurnal Teknologi (Sciences & Engineering)*, **72(3)**, 83-90.
- 85). **Sakr, M. A., Shahin, M. A. and Metwally, Y. M.** (2009). Utilization of lime for stabilizing soft clay soil of high organic content, *Geotechnical and Geological Engineering*, **27**, 105-113.
- 86). **Sarkar, G., Islam, R., Alamgir, M. and Rokonuzzaman.** (2012). Study on the geotechnical properties of cement based composite fine-grained soil, *International Journal of Advanced Structures and Geotechnical Engineering*, **1(2)**, 42-49.
- 87). **Sasanian, S. and Newson, T. A.** (2013). Use of mercury intrusion porosimetry for microstructural investigation of reconstituted clays at high water contents, *Engineering Geology*, **158**, 15-22.
- 88). **Sato, H., Yui, M. and Yoshikawa, H.** (1996). Ionic diffusion coefficients of  $\text{Cs}^+$ ,  $\text{Pb}^{2+}$ ,  $\text{Sm}^{3+}$ ,  $\text{Ni}^{2+}$ ,  $\text{SeO}_4^{-2}$  and  $\text{TcO}_4^-$ , in free water determined from conductivity measurements, *Journal of Nuclear Science and Technology*, **33(12)**, 950-955.
- 89). **Schifano, V. and Hadlow, C. N.** (2007). Evaluation of quicklime mixing for the remediation of petroleum contaminated soils, *Journal of Hazardous Materials*, **141(2)**, 395-409.
- 90). **Shackelford, C. D. and Daniel, D. E.** (1991). Diffusion in saturated soil II: results for compacted clay, *Journal of Geotechnical Engineering*, **117(3)**, 485-506.
- 91). **Shah, P. and Singh, D.** (2006). Methodology for determination of hygroscopic moisture content of soils, *Journal of ASTM International*, **3(2)**, 1-14.
- 92). **Sharma, N. K., Swain. S. K. and Umesh Sahoo. C.** (2012). Stabilization of a clayey soil with fly ash and lime: a micro level investigation, *Geotechnical and Geological Engineering*, **30(5)**, 1197-1205.
- 93). **Shen, S., Huang, X., Ji du, S. and Jie Han.** (2010). Laboratory studies on property changes in surrounding clays due to installation of deep mixing columns, *Marine Georesources & Geotechnology*, **21(1)**, 15-35.

- 94). **Sridharan, A. and Sivapullaiah, P. V.** (2005). Mini compaction test apparatus for fine grained soils, *Geotechnical Testing Journal*, **28(3)**, 240-246.
- 95). **Stoltz, G., Cuisinier, O. and Masroui, F.** (2012). Multi-scale analysis of the swelling and shrinkage of a lime-treated expansive clayey soil, *Applied Clay Science*, **61**, 44-51.
- 96). **Thyagaraj, T., Rao, S. M., Suresh, P. S. and Salini, U.** (2012). Laboratory studies on stabilization of an expansive soil by lime precipitation technique, *Journal of Materials in Civil Engineering*, **24**, 1067-1075.
- 97). **Tran, T. D., Cui, Y., Tang, A. M., Audiguier, M. and Cojean, R.** (2014). Effects of lime treatment on the microstructure and hydraulic conductivity of Hericourt clay, *Journal of Rock Mechanics and Geotechnical Engineering*, **6**, 399-404.
- 98). **Tsai, S., Ouyang, S. and Hsu, C.** (2001) Sorption and diffusion behavior of Cs and Sr on Jih-Hsing bentonite, *Applied Radiation and Isotopes*, **54**, 209-215.
- 99). **Ukrainczyk, N., Ukrainczyk, M., Sipisic, J. and Matusinovic, T.** (2006). XRD and TGA investigation of hardened cement paste degradation, *International Conference on Materials, Processes, Friction and Wear MATRIB '06 Vela Luka Croatia*, 243-249.
- 100). **Van Olphen, H.** (1963). An introduction to clay colloid chemistry: for clay technologists, geologists, and soil chemists, *Interscience Publishers*, New York, London.
- 101). **Vazquez, E. V., Moreno, R. G., Tarquis, A. M., Requejo, A. S., Miras-Avalos, J. M. and Paz-Ferreiro.** (2010). Multifractal characterization of pore size distributions measured by mercury intrusion porosimetry, *19<sup>th</sup> World Congress of Soil Science, Soil Solutions for a Changing World*, 1-6 August, Brisbane, Australia.
- 102). **Vedalakshmi, R., Sundara Raj, A., Srinivasan, S. and Ganesh Babu, K.** (2003). Quantification of hydrated cement products of blended cements in low and medium strength concrete using TG and DTA technique, *Thermochimica Acta*, **407**, 49-60.
- 103). **Villain, G., Thiery, M. and Platret, G.** (2007). Measurement methods of carbonation profiles in concrete: thermogravimetry, chemical analysis and gammadensimetry, *Cement and Concrete Research*, **37**, 1182-1192.

- 104). **Vincent, C. and Craig, B. L.** (2013). Influence of water on diffusion and porosity parameters of soil-cement materials, *Canadian Geotechnical Journal*, **50**, 351-358.
- 105). **Vitale, E., Deneele, D. and Russo, G.** (2016). Multiscale analysis on the behaviour of a lime treated bentonite, *Procedia Engineering*, **158**, 87-91.
- 106). **Weaver, A. R., Kissel, D.E., Chen, F., West, L.T., Adkins, W., Rickman, D. and Luvall, J.C.** (2004). Mapping soil pH buffering capacity of selected fields in the coastal plain, *Soil Science Society of America Journal*, **68(2)**, 662-668.
- 107). **Wild, S., Abdi, M. R. and Leng-Ward, G.** (1993). Sulphate expansion of lime stabilized kaolinite: II. reaction products and expansion, *Clay minerals*, **28**, 569-583.
- 108). **Wilkinson, A., Haque, A., Kodikara, J., Adamson, J. and Christie, D.** (2010). Improvement of problematic soils by lime slurry pressure injection: case study, *Journal of Geotechnical and Geoenvironmental Engineering*, **136**, 1459-1468.
- 109). **William Powrie.** (1987). *Soil Mechanics: Concepts and applications*, CRC Press, Taylor and Francis group, London, Newyork.
- 110). **Winterkorn., Hans, F. and Fang, H. Y.** (1972). Effect of temperature and moisture on the strength of soil-pavement systems, *Fritz Laboratory Reports*. <http://preserve.lehigh.edu/engr-civil-environmental-fritz-lab-reports/1975>.
- 111). **Yong, R. N., Ouhadi, V. R. and Goodarzi, A. R.** (2009), Effect of  $\text{Cu}^{2+}$  ions and buffering capacity on smectites microstructure and performance, *Journal of Geotechnical and Geoenvironmental Engineering, ASCE*, **135**, 1981-1985.
- 112). **Yong, R. N., Warkentin, B. P., Phadungchewit, Y. and Galvez, R.** (1990), Buffer capacity and lead retention in some clay materials, *Water, Air and Soil Pollution*, **53**, 53-67.
- 113). **Yunus, N. Z. M., Wanatowski, D. and Stace, L. R.** (2012). Effectiveness of chloride salts on the behavior of lime-stabilised organic clay, *International Journal of GEOMATE*, **3(2)**, 401-412.

- 114). **Zawawi, N. A. B. A., Shafiq, N. and Nuruddin, F.** (2004). Chloride ion migration in normal and blended concrete by applying electrical field at different voltages, *29th Conference on our world in concrete & structures*, 25-26 August, Singapore, 381-386.
- 115). **Zhang, J. Z., McLoughlin, I. M. and Buenfeld, N. R.** (1998). Modelling of chloride diffusion into surface-treated concrete, *Cement and Concrete Composites*, **20**, 253-261.
- 116). **Zhang, Q. and Ye, G.** (2012). Dehydration kinetics of Portland cement paste at high temperature, *J Therm Anal Calorimetry*. **110**, 153-158.
- 117). **Zhang, T. and Gjorv, O. E.** (1996). Diffusion behavior of chloride ions in concrete, *Cement and Concrete Research*, **26(6)**, 907-917.



## PUBLICATIONS FROM THE STUDY

---

### Papers in Journals

- 1). **Bandipally. S**, Cherian. C, Arnepalli. D. N (2017). “Chemical characterization of lime treated sodium bentonite using thermogravimetry analysis for assessing short-term strength behaviour”, *Indian Geotechnical Journal* (communicated on 1<sup>st</sup> May, 2017).

### Papers in Conference Proceedings

- 1). **Bandipally, S.**, Cherian, C., Arnepalli, D. N. and Pooja, C. P. (2014). “Influence of *pH* on Long Term Performance of Lime Stabilized Fine-Grained Soils”, *Proceedings of Indian Geotechnical Conference (IGC-2014)*, 18-20 December, Kakinada, India, 1-10.
- 2). **Bandipally, S.**, Cherian, C., Anjana, R. K. and Arnepalli, D. N. (2016). “Sorptions and diffusion studies to evaluate the degree of lime stabilization”, *Proceedings of Indian Geotechnical Conference (IGC-2016)*, 15-17 December, Madras, India, 1-4.
- 3). Cherian, C., **Bandipally, S.**, Arnepalli, D. N., Dhulipala, V. R. and Korupolu, R. N. (2016). “Reappraisal of Optimum Lime Content Determination for Lime Stabilization of Fine-grained Soils”, *6<sup>th</sup> Asian Regional Conference on Geosynthetics*, 8-11 November, New Delhi, India, 260-275.
- 4). Cherian. C, **Bandipally. S**, Kollannur. N. J, Arnepalli. D.N (2017). “Study on calcium sorption mechanisms in clay-lime system”, *International Clay Conference (ICC-2017)*, 16-21 July, Granada, Spain.

## CURRICULUM VITAE

---

1. NAME : *Bandipally Sandeep*

2. DATE OF BIRTH : *13<sup>th</sup> August 1992*

3. EDUCATIONAL QUALIFICATIONS

**2013** : *Bachelor of Technology (B. Tech.)*

INSTITUTE : *Sree Dattha Institute of Engineering, Hyderabad, Telangana*

SPECIALIZATION : *Civil Engineering*

**2017** : *Master of Science (M. S.)*

INSTITUTE : *Indian Institute of Technology Madras, Chennai*

REGISTRATION DATE : *15<sup>th</sup> July 2013*

## GENERAL TEST COMMITTEE

---

- Chairman** : **Dr. K. Ramamurthy**  
Professor and Head  
Department of Civil Engineering  
Indian Institute of Technology Madras  
Chennai-600036, India.
- Supervisor** : **Dr. D. N. Arnepalli**  
Associate Professor  
Department of Civil Engineering  
Indian Institute of Technology Madras  
Chennai-600036, India.
- Member** : **Dr. Manu Santhanam**  
Professor  
Department of Civil Engineering  
Indian Institute of Technology Madras  
Chennai-600036, India.
- Member** : **Dr. S. Sankaran**  
Associate Professor  
Department of Metallurgical Engineering  
Indian Institute of Technology Madras  
Chennai-600036, India.